Ministry of Higher Education
and Scientific Research
University of Babylon
College of Science
Department of Applied Geology

Structural Analysis and Rock Slopes Stability and Determine Geological Hazards of Selected Areas of Zurbatiya-Eastern Iraq

A Thesis Submitted to the Council of the College of Science
University of Babylon
in Partial Fulfilment of the
Requirements for the Degree
of Master of Science in Geology

By
Mustafa Baqer Abdulwahab Fattah

B.Sc. in Geology, University of Baghdad, 2010

Supervised by

Prof. **Dr.**
Jaffar Hussain Ali Al-Zubaydi

Sen. Chief Geologist Dr.
Maher Tahseen Hatem Zainy

1445 A.H **2023 A.D**

بِسْمِ اللَّهِ الرَّحْمَنِ الرَّحِيمِ

((وَتَرَى الْجِبَالَ تَحْسَبُهَا جَامِدَةً وَهِيَ تَمُرُّ
مَرَّ السَّحَابِ ۚ صُنْعَ اللَّهِ الَّذِي أَتْقَنَ كُلَّ
شَيْءٍ ۚ إِنَّهُ خَبِيرٌ بِمَا تَفْعَلُونَ ﴿٨٨﴾))

صدق الله العلي العظيم

سورة النمل، الاية ٨٨

SUPERVISORS CERTIFICATION

We certified that this thesis (**Structural Analysis and Rock Slopes Stability and Determine Geological Hazard of Selected Areas of Zurbatiya-Eastern Iraq)** had been prepared under our supervision, in the Department of Applied Geology of Science – University of Babylon in Partial Fulfillment of the Requirements for the degree of Master in Geology.

Signature:

Name: Dr. Jaffar Hussain Ali Al-Zubaydi

Title: Professor.

Address: Department of Applied Geology – College of Science – University of Babylon.

Date: / / 2023

Signature:

Name: Dr. Maher Tahseen Hatem Zainy

Title: Senior Chief Geologist

Address: Iraqi Geological Survey (GEOSURV)

Date: / / 2023

APPROVED BY THE HEAD OF DEPARTEMENT OF APPLIED GEOLOGY

In view of the available recommendation, I forward this thesis for debate by the examining committee.

Signature:

Name: Dr. Mohanad Rasim Al- Owaidi

Title: Assist Professor.

Address: Head of Department of Applied Geology/ College of Science-University of Babylon.

Date: / / 2023

Certification of the Examining Committee

We the chairman and the members of the examining committee, certify that after reading this thesis entitled **" Structural Analysis and Rock Slopes Stability and Determine Geological Hazard of Selected Areas of Zurbatiya-Eastern Iraq "** submitted by the student (**Mustafa Baqer Abdulwahhab Fattah**) and as the examination committee examined the student in its content, we think in our opinion it is adequate for award of the degree of Master of Science in Geology.

Signature
Title: Professor
Muhsen O. Khalaf
College of Science/University of Babylon
Data: / / 2023
Chairman

Signature
Title: Professor
Dr. Abdul-Kareem Hussein Abd
College of Science/University of Basrah
Data: / / 2023
Member

Signature
Title: Assist Professor
Dr. Mohammed Ahmed Ali
College of Science/University of Babylon
Data: / / 2023
Member

Signature
Title: Professor
Dr. Jaffar Hussain Al-Zubaydi
College of Science/University of Babylon
Data: / / 2023
Member and Supervisor

Signature
Title: Professor
Dr. Maher Tahseen Zainy
College of Science/University of Babylon
Data: / / 2023
Member and Supervisor

Approved by the Dean of the College of Science

Signature/
Professor Dr. Mohammed Hadi Shinen Alshammeri
Dean
College of Science / University of Babylon

Dedication

To the honour of the faithful Prophet and his faithful household, peace be upon him and his family, and to the soul of my lady, Umm Al-Banin Peace be upon her

To the owner of good opinion, wisdom and dignity... my father

To the fountain of tenderness and the centre of safety...my mother

To the one who supported me and helped me in every step I took...my wife

To my smile and my joy in my life... my daughter

To those who removed the worry and fatigue from me...my sons

To those who are my support in this world… my brothers.

To those who submerged me with their kindness and prayers...my brothers and sisters

To the one whose prayers walk with me every step of the way... my grandmother

I dedicate this humble research

Mustafa

Acknowledgements

First and foremost, I would like to thank Allah infinitely and praise Him infinitely for what He has bestowed upon me and enabled me to do.

My appreciation and thanks to the Ministry of Higher Education and Scientific Research of Iraq and for University of Babylon, College of Science and Department of Applied Geology for giving me the chance to join Msc research.

I would like to extend my thanks to my supervisors, *Prof*. Dr. Jaffar Hussain Al-Zubaydi / Department of Applied Geology and Dr. Maher Tahseen Zainy (Senior Chief Geologist) / Iraqi Geological Survey (GEOSURV-IRAQ) for their notes that evaluate my work to what it has reached now, and for their time and effort to highlight this research in the best way.

My deepest thanks to Mr. Ameer A. Mahmoud (Senior Chief Geologist) for helping in the field works, to Dr. Talal H. Kadhim (Head of Remote sensing division in GEOSURV-IRAQ) Dr. Younis Ibrahim (Head of Information Department) and Mr. Alaa Shaqir Qanber for their bits of help with software installation.

I would like to extend my thanks to the staff of GWOSURV-IRAQ, especially to the staff of the Al-Najaf Branch, and most especially to Mr. Haydar Hadi Al-Ibrahemi and Mr Zaid Abdul Ameer Assal for supporting me through the study period.

I would like to thank my family for supporting me throughout the study period, especially my wife who helped me by using softwares.

Summary

The study includes a geometrical analysis for discontinuities to elicit their influence on the stability of rock slopes within Fatha (Middle Miocene), Injana (Late Miocene) and Mukdadiya (Late Miocene – Pliocene) formations in Zurbatiya which is one of the most important regions in Iraq. The study area is located between the latitudes (33° 28′ 03″ N and 33° 23′ 25″ N) and the longitudes (45° 56′ 07″ E and 46° 00′ 00″E) within the Himreen and Koolic1 anticlines, and Al- Faraa syncline.

Seventeen stations have been selected to operate the analysis; two stations were selected within Kolic1 anticline/Fatha Formation, one station within Al-Farae syncline/Fatha Formation, while all other stations were within Himreen anticline and distributed within all of the three exposed formations.

The field work involves field data collection, a tilt test to estimate the internal friction angle for measured discontinuities surfaces within the rock masses, and rock sampling for the point load test. The collected data of discontinuities have been plotted and analyzed using stereographic projection techniques/ lower hemisphere/ equal area by using stereonet v.11 software, the maps used in this study were modified using Arc map GIS v.10.2 software, and all layouts were carried out using Adobe illustrator, Corel Draw.22, and Photo filter software.

Joints of measured stations were analyzed and classified according to the relation between their planes and principal tectonic axes of the geological structure that contains them, The maximum principal stress σ1 was estimated according to the intersection of the system of conjugate joints; accordingly, two trajectories of the paleo tectonic movements were found, the first direction is NW-SE in the

East and south parts of the study area, while the second trend is NE-SW at the western parts.

Field observation and data analysis showed that all of the studied stations were unstable with different types of failures and different grades of hazard; the various types of present or potential rock failures are rock fall, Toppling, and sliding. The hazard grade for each station was estimated according to the Landslide Possibility Index (LPI) which is based on ten parameters. The hazards in the study area were classified into four grades (moderately hazardous, highly hazardous, and very highly hazardous) areas. A geological hazard map was created, based on the (LPI) categories.

List of content

List of Tables

List of Figures

List of Plates

List of Abbreviations

Abbreviation	Term
LFZ	Low Folded Zone
a, b and c	Principal tectonic axes
σ_1	Maximum principal tectonic stress
Ψ	General dip of the failure plane
Ψ_p	Dip angle of the sliding plane
Ψ_f	Inclination angle of the slope face
Ψ_i	Dip angle of the the intersection line
Φ	Frition angle
B.R.S.	Back release surface
L.R.S.	Lateral release surface
U.R.S.	Upper release surface
B.S.	Basal surface
Estmat.	Estimated value

Chapter One
Introduction

1-1preface

Structural geology is the discipline that deals with the study of deformation structures in the solid part of the earth and the understanding of their geometry, allocation, and forming processes (Ramsay & Huber, 1987; and Fossen 2010 & 2016). A most important structures are discontinuities are weakness planes that exist in rock masses and are created by fracturing processes. The existence of discontinuities can have an extreme influence on the total strength of the rock masses and can be very effective in term of the stability of the rock slopes (Lisle & Leyshon, 2004). Unstable rock slopes may cause hazards and create risks to the roads, the infrastructures, surrounding economies, as well as generally to the environment (Sissakian *et. al.*, 2017). Accordingly, the study and assessment for slope stability and instability take place in modern geology in an attempt to losses caused by the masse movement around our planet.

This study has estimated the stability of rock slopes in 17 stations and determined the types of past slope failures and also the potential to occur in the future by analyzing the data collected from the field by general geological, structural, and engineering surveys.

1-2 The importance of the study

Zurbatiyah region is one of the most encouraging areas for tourism and geological parks. Because of its stunning views and undulating areas, many tourists and hunters visit these areas despite their geological dangers. For this reason; in this study, a structural (geometrical) analysis of discontinuities was performed to assess their effect on the rock slope stability.

1-3 Location of the study area

The study area is situated approximately 30 km north of Badra district near the border between Iraq and Iran within Wasit governorate as shown in

(Figures 1.1, 1.2 and 1.3). The study area represents part of the southern Himrin anticline. The study area is limited by the latitudes of (33º 28′ 03″ N and 33º 23′ 25″ N) and longitude of (45º 56′ 07″ E and 46º 00′ 00″ E).

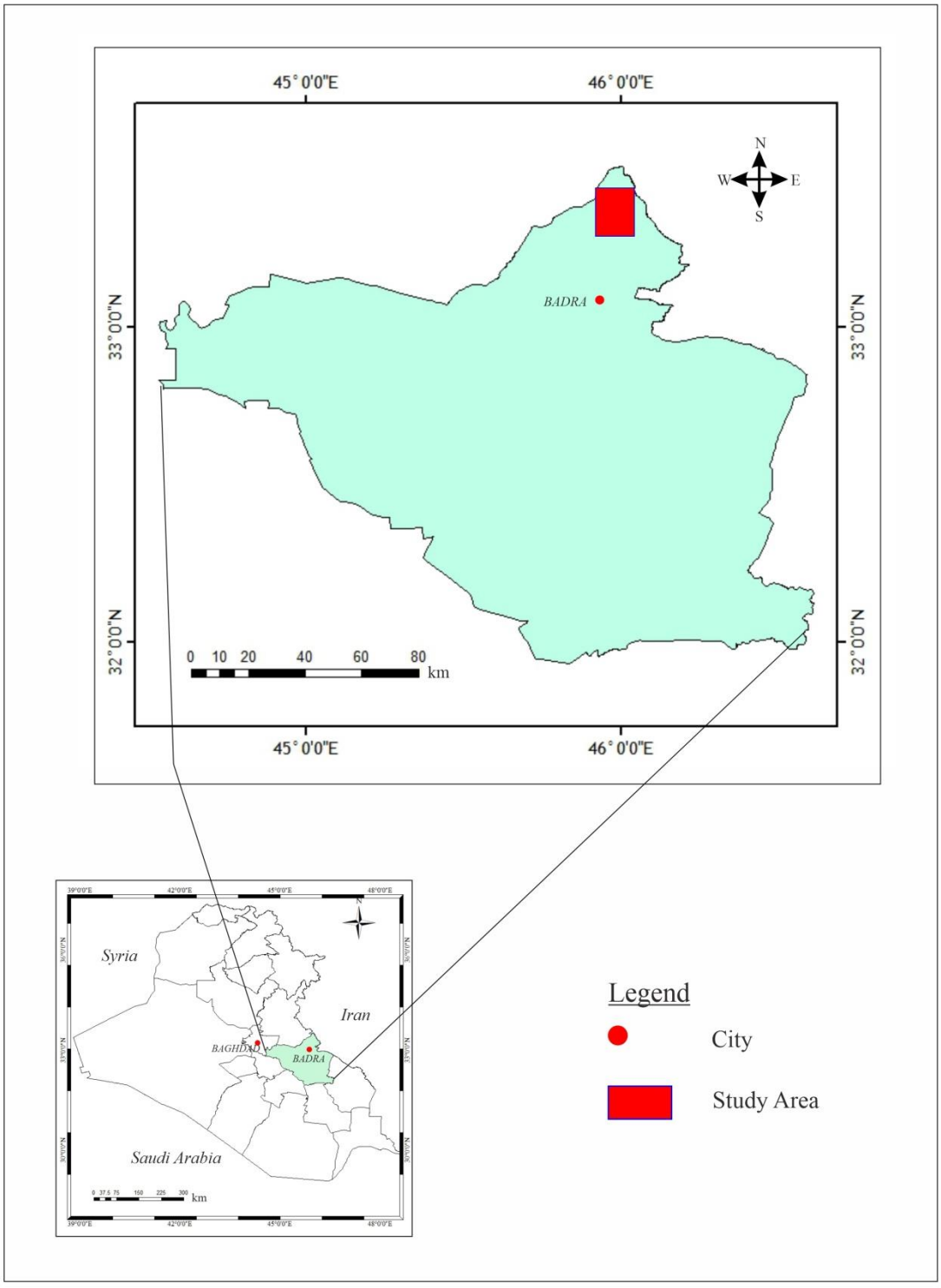

Figure 1.1: Location of the study area

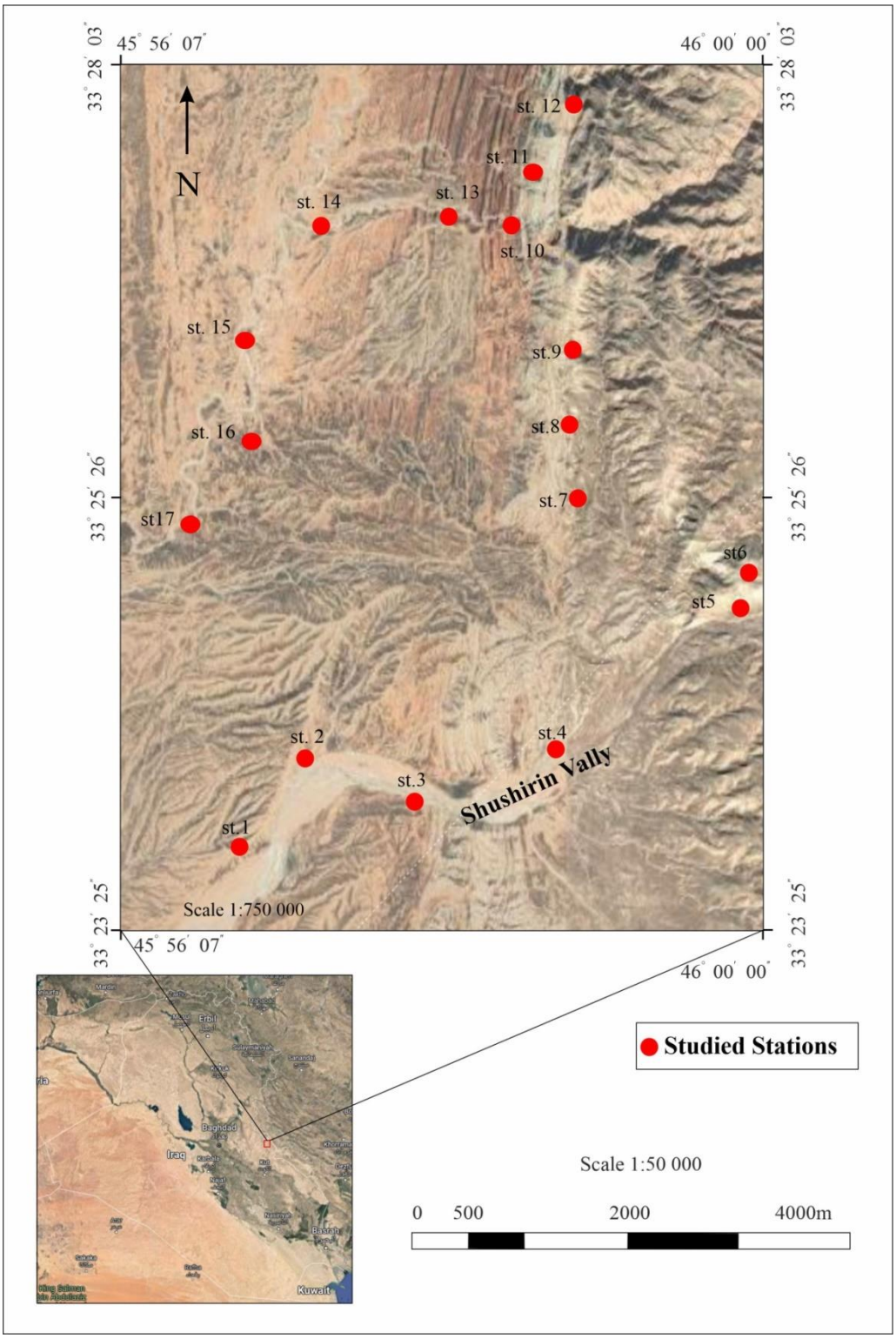

Figure 1.2: Satellite image illustrates the location of the study area and the distribution of the studied stations

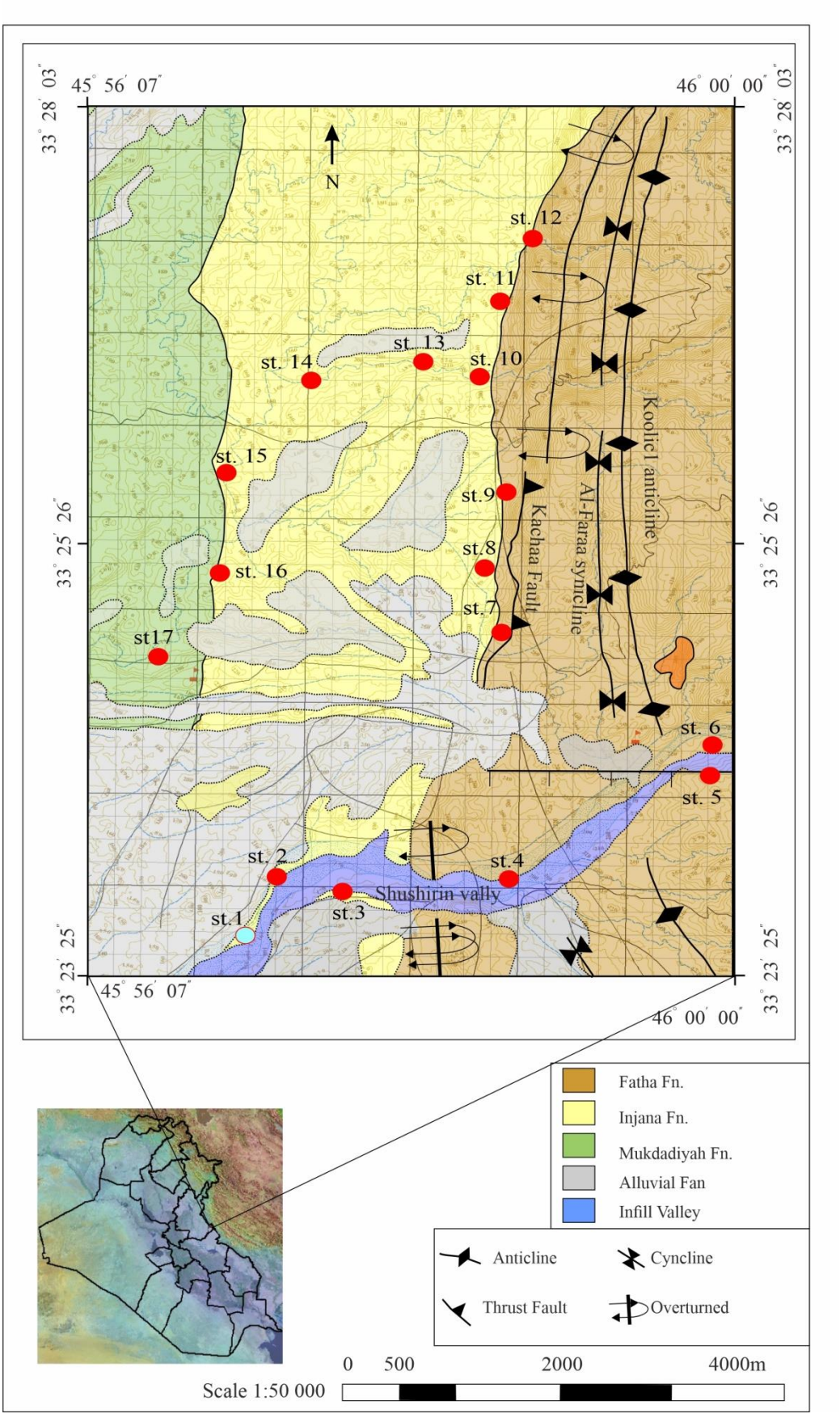

Figure 1.3: Geological map showing the location of the study area and the distribution of the studied stations (modified after Mouhmuod *et. al.*, 2018)

1-4 Aims of the study

The main purposes of this study will be listed briefly hereinafter:

1- Structural analysis of joints and classification according to the tectonic axes to determine their influence on the stability of rock slopes in the study area.
2- Investigating the instability of slopes in the study area in order to determine the different types of past failures and those potentially occurring in the future and their relationship with the discontinuities that exist in the rock masses.
3- Determining the hazard degree for the study area.
4- Preparing a failure hazard map of the study area.

1-5 Tectonic and Structural setting

1-5-1 Tectonic setting

According to the tectonic map (Figure 1.4), (Fouad, 2015), the study area is located in the Low Folded Zone of the Zagros Fold–Thrust belt. The sedimentary column in the study area has been affected by the late regional heavy tectonic movements that caused the uplifting of the Himreen Structure (Alavi, 2004; and Fouad, 2012).

The Zagros Fold – Thrust Belt is considered as the deformational result of the tectonic movement (Convergence) of the Arabian – Iranian (Eurasian) plates (Cretaceous–present day movement); the belt extends over than 1800 km from southern Turkey to the strait of Hormuz passing through north, northeast, and east of Iraq, the Low Folded Zone extends about 700km long, and about 100km wide belt (Fouad, 2012).

The Low Folded Zone contains a considerable number of folds that vary in size and geometries both along and across this zone (Fouad, 2012; and Jassim & Goff, 2006). The Makhul-Hemrin fault zone has a great surface expression by one of the longest chains of anticlines in the Middle East which involves Makhul in the northwest, Hemrin North and Hemrin South in the

midst, and Pesht-i-Kuh (in Iran) in the southeast along the Iraq-Iran borders (Jassim & Goff, 2006).

1-5-2 Structural setting

The study area is located within the Himreen Structure. Which is characterized by narrow and long anticlines and synclines these folds have an Nw-SE trend, and the trends of these anticlines and synclines are changing to N-S in the study area (Mouhmuod *et. al.,* 2018). The studied stations in this study are distributed within three folds: Himreen anticline, Al-Farae syncline and Kolic anticline which will be explained hereinafter:

- Himreen Anticline: generally, it is one of the largest structures in Zurbatiya region, its trend is NWN-SES, and the length is about (33) km, while the width differs from one place to another (Mouhmuod *et. al.,* 2018). In the study area, the width is about (7) km.

The dips increase towards the anticline core and reach up to 90° and turn towards the northeastern flank with a dipping range from 23° to 55° (Mouhmuod *et. al.,* 2018).

The exposed formations rocks in the study area within this fold are Fatha, Injana and Mukdadiya formations.

- Al-Farae Syncline: the trend of this fold is NW-SE. this syncline is affected by uncertain thrust fault as indicated by the disappearance of the Limestone-Marl unit of Fathe Formation in the northeastern limb and its appearance in the other limb. The fold axis is covered by slope sediments; thus, the thrust fault is not so clear (Mouhmuod *et. al.,* 2018).
- Koolic1 Anticline: It is a high-lying asymmetrical anticline, the trend is NW-SE and it is changes to N-S north of Shurshirin Valley, The length is about (33) km and the width is (1.5)km. this anticline affected and truncated by three strike-slip faults: Shurshirin fault, Al Hashima fault and Sheraw fault (Mouhmuod *et. al.,* 2018).

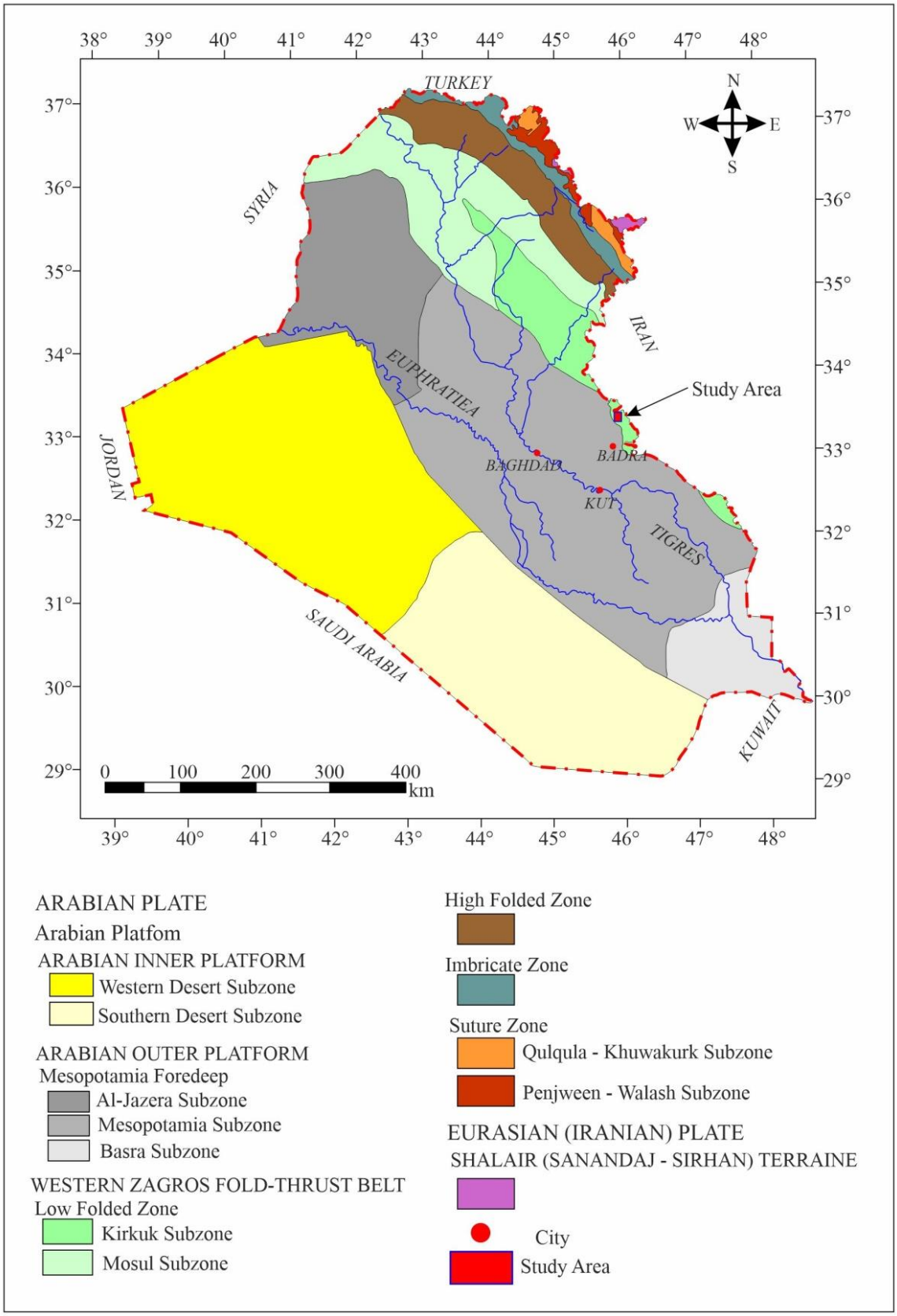

Figure 1-4: Tectonic map of Iraq (after Fouad, 2015)

1-6 Geology of the study area

1-6-1 Stratigraphy (Tertiary Formations)

Formations exposed within the study area will be explained briefly hereinafter (from oldest to youngest):

1-6-1-1 Fatha Formation (Middle Miocene)

The Fatha formation is one of the most widespread aerially and economically important formations present in Iraq (Bellen *et. al*., 1959; Buday, 1980; and Jassim & Goff, 2006). The formation consists of a cyclic alternation of calcareous claystone, Limestone, and Gypsum, it has been divided by many authors into two members (e.g. Lateef, 1975; Al-Mubarak and Youkhana, 1976 and Ma'ala *et al*., 1987). In the study area, (Mouhmuod *et. al.*, 2018) divided the formation into two members too, these members from bottom to top:

A- The Lower member: it was subdivided into four units which are (from bottom to top):

1- Gypsum, red claystone, limestone, and marl Unit, repeated in a cyclic manner.
2- Limestone Unit.
3- Red Claystone, Marl, and Gypsum Unit, in a cyclic manner too.
4- Sandstone and gypsum Unit, in a cyclic manner.

The maximum exposed thickness is (257) m (Mouhmuod *et. al.*, 2018).

The upper part of this member shows indications of a transitional zone, which indicates the beginning of the main change in the depositional environment from a sea lagoon to a continental environment (Sissakian, 1994).

B- The Upper member consists mainly of incompleted cycles, which are alternations of marl and gypsum, lacking limestone. The maximum exposed thickness of this member is 73.15m (Jassim and Goff, 2006).

The lower contact of the Fatha Formation is the last gypsum bed, whereas the upper contact with the Injana Formation is gradational (Buday, 1980; and Jassim & Goff, 2006).

1-6-1-2 Injana Formation (Late Miocene)

Injana formation consists of fine grained and pre-molasse sediments, deposited firstly in a coastal area, and finally in a fluvio lacustrine system (Bellen et. al., 1959; and Jassim & Goff, 2006). This formation comprises an alternation of claystone and Sandstone, Claystone beds prevail over thick Sandstone beds at the lower and upper parts of the formation, while in the middle parts, the thick Sandstone prevails over the Claystone beds and becomes recurrent (Jassim & Goff, 2006). The uppermost part is characterized by very thick (reaching up to 30m) Claystone with thin Sandstone. The total thickness of the formation is 350m (Mouhmuod *et. al.*, 2018).

Lower contact is gradational with the Fatha Formation; the contact is based on the top of the last gypsum horizon of the Fatha Formation which is always overlain by thick red claystone (Buday, 1980; and Jassim & Goff, 2006). The upper contact with the Mukdadiya Formation is gradational marked by the appearance of pebbly sandstone (Mouhmuod *et. al.*, 2018).

1-6-1-3 Mukdadiya formation (Late Miocene-Pliocene)

The Mukdadiya formation consists of about 2000m of fining-upward cycles of Gravely Sandstone, Sandstone, and red Mudstone, the Sandstone is predominantly strongly cross–bedded and associated with clay balls and channel lags (Bellen et. al., 1959; and Jassim & Goff, 2006). The alternation of Sandstone and Claystone is lenticular in order to deposition mod, with many lateral changes to each other, the total thickness is 110m (Mouhmuod *et. al.*, 2018).

The upper contact of the formation is taken at the first appearance of a thick, and coarse conglomerate, which returns to the BiHassan Formation (Mouhmuod *et. al.*, 2018).

1-6-2 Quaternary Sediments

1-6-2-1 Alluvial fans

The Alluvial fans in the study area according to (Mouhmuod *et. al.*, 2018 and Al-Musawi *et. al*., 2020) consists mainly of Conglomerate, the gravels are composed generally of Limestone fragments with a lesser quantity of Chert, Igneous rock fragments, and also Metamorphic rock fragments. The quantities of the Limestone fragments occupied 75% on average of the bulk size and reached 95% in some sites, cemented by calcareous sand, and are sometimes moderately compact (Mouhmuod *et. al.*, 2018).

1-6-2-2 Valley Fill Sediments (Holocene)

The Valley fill sediments in the study area represent the ephemeral stream sediments, which fill the gullies and are usually active during the rainy seasons. These sediments comprise -in the study area- gravels and lesser sizes of grains, and the size decreases downward the streams. Aeolian processes are associated usually with the ephemeral valley fill sediments in the dry seasons. The total thickness does not surpass a few meters (Mouhmuod *et. al.*, 2018; and Al-Musawi, 2020).

1-6-3 Geomorphological units

The main types of geomorphological units that exist in the study area will be explained briefly hereinafter:

1-6-3-1 Units of Structural–Denudational Origin

- **Structural Ridges Escarpments**

Scarp forming by erosional and tectonic processes, The scarps are affected by many factors, the most effectence of these are lithology, type of structures and topography (Davis, 1903; Stein *et. al*., 1988; and Quinn, 1997). These geomorphological features attributed in the study area to the tectonic activities by thrusting of the NE fold limb of Himreen structure that ranges in height between 50 to 820m a.s.l., and has a strike trending NW-SE, with variable dip toward NE and cropping out of rocks extend from Oligocene to Pliocene (Mouhmuod *et. al.*, 2018; and Al-Musawi, 2020).

- **Hogbacks and Questas**

Hogback is a sharply-crested ridge of hard rocks with steep dipping (more than 20°) strata, it is a result of slow differential erosion of alternating of soft and hard strata, while the Questa is an asymmetrical ridge built of dipping sedimentary rocks of alternating resistance versus erosion and weathering, elongated along the strike of strata (Ward & Roberts, 1997; and Singh, 2007). These types of geomorphological units are low-lying and have much-denuded characteristics; the questa type is created by the unit of sandstone and gypsum of the upper member of Fatha Fn., Injana and Mukdadiya formations, hogback is usually formed on the higher tilted resistance rocks (Gypsum and Limestone) belonging to the Fatha Formation (Mouhmuod *et. al.,* 2018).

1-6-3-2 Units of Denudational Origin

- **Badlands**

This geomorphological unit was as regions covered by sedimentary rocks and these are extensively eroded by numerous rills and channels which are occasionally developed due to rainstorms (Singh, 2007). Badlands are well developed in the SW limb of the Himreen structure because of the influence of rainwater on the relatively soft clastic of the Injana, Mukdadiya, and Bi Hassan formations which are segmented by a dense net of valleys (Mouhmuod *et. al.,* 2018).

- **Flat Iron**

This geomorphological feature is present in the study area and formed within the upper member of the Fatha Formation due to the alternation of hard rocks (Gypsum) and softer rocks (Claystone) (Mouhmuod *et. al.,* 2018 and Gzar, 2020).

1-6-3-3 Units of Fluvial Origin

- **Alluvial fan**

The Alluvial fan in the study area is well-developed north of Shorshreen Valley and extends for approximately 15km in length and reaches 8km in width, this alluvial fan has a thickness of more than 25m, the fan sediment deposited above the Pre-Quaternary formation and makes angular unconformity with them (Mouhmuod *et. al.*, 2018; and Al-Musawi, 2020).

- **Infilled valleys**

These features are present generally in the main valley in the study area (Shurshirin Valley) and some sites in the other minor valleys.

In low relief within the alluvial fan, valleys are filled by finer materials (such as Sand, Silt, and clayey materials), While in high relief areas within the alluvial fan, the valleys are filled by sandy gravels and pebbly sands with minor amounts of fine classics (Mouhmuod *et. al.*, 2018).

1-7 Climate

General parameters of the climate of the study area have been obtained from data recorded at Badra meteorological station, which is considered the nearest station with available data from 1994 to 2017 (Table 1.1). The data recorded in this station indicates that the climate of the study area is arid.

1-7-1 Rainfall

The rains initiate in October and end in May in general, while the rainfall in the other months may absent or very rare. Rainfall intensity shows high fluctuation among the seasons; so within every season (Figure 1.5).

Table (1.1): Monthly mean values of climatic parameters in Badra meteorological station during the period (1994 – 2017)

Month	Rainfall (mm)	Temp. (C°)		Relative humidity (%)	Evaporation (mm)	Wind speed (m/sec)
		Max.	Min.			
January	40.83	16	6.06	70.9	72.4	2.2
February	23.82	19.56	7.85	59.4	101.9	1.7
March	29.61	24.8	12	47.51	175.3	2.4
April	16.42	31.1	17.5	40.25	232	2.3
May	10.33	37.7	23.1	28.19	326	2.5
June	0.37	43	26.7	21.2	425.1	2.7
July	0.033	45.7	29	19.9	462	2.5
August	0.0	45	28	20.53	432.2	2.4
September	0.026	41.7	24	24.8	339.5	2.0
October	19.07	35	19.3	33.88	227.8	2.2
November	35.29	26	11.7	55.64	112.8	2.2
December	30.96	19.12	7.2	66.23	74.1	2.4

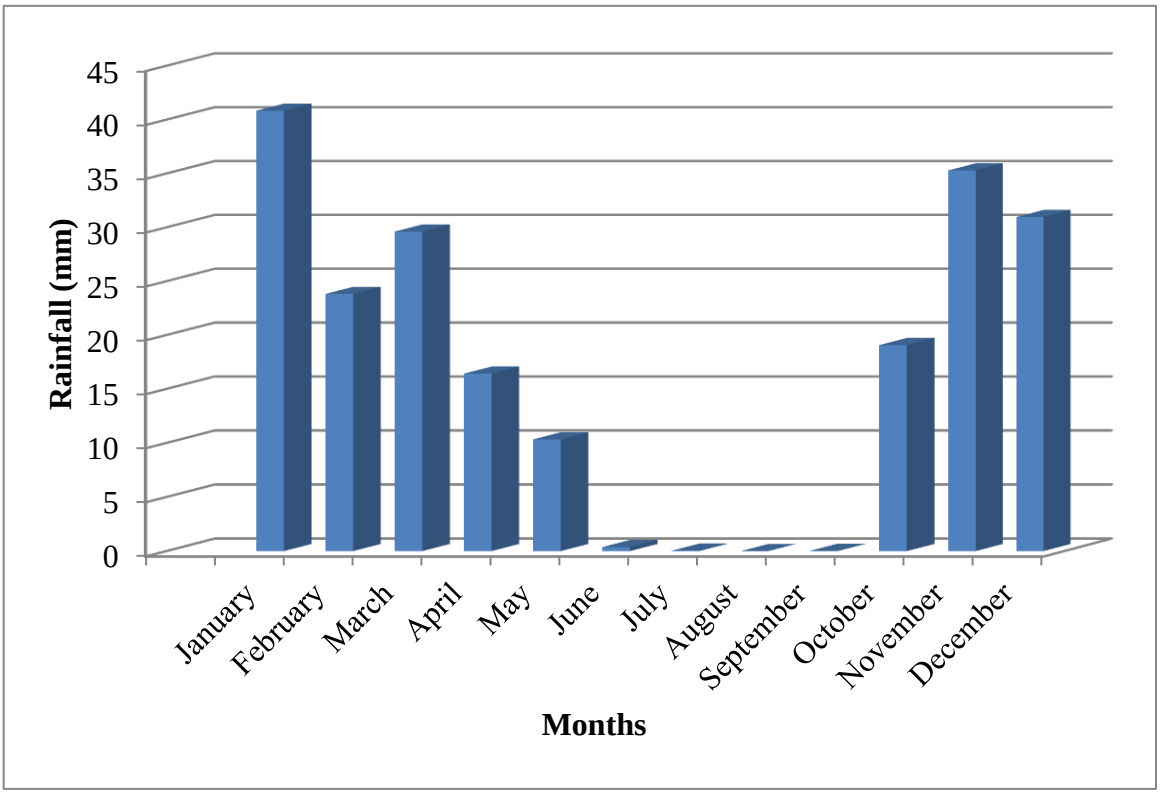

Figure 1-5: Mean monthly precipitation average in Badra meteorological station during the period (1994 – 2017)

1-7-2 Temperature

The air temperature generally follows the continental climate and is characterized by ratable variation among the year, as well as the daily temperature variations are ratable too; thus the mean monthly temperature in the study area has been explained (Figure 1-6).

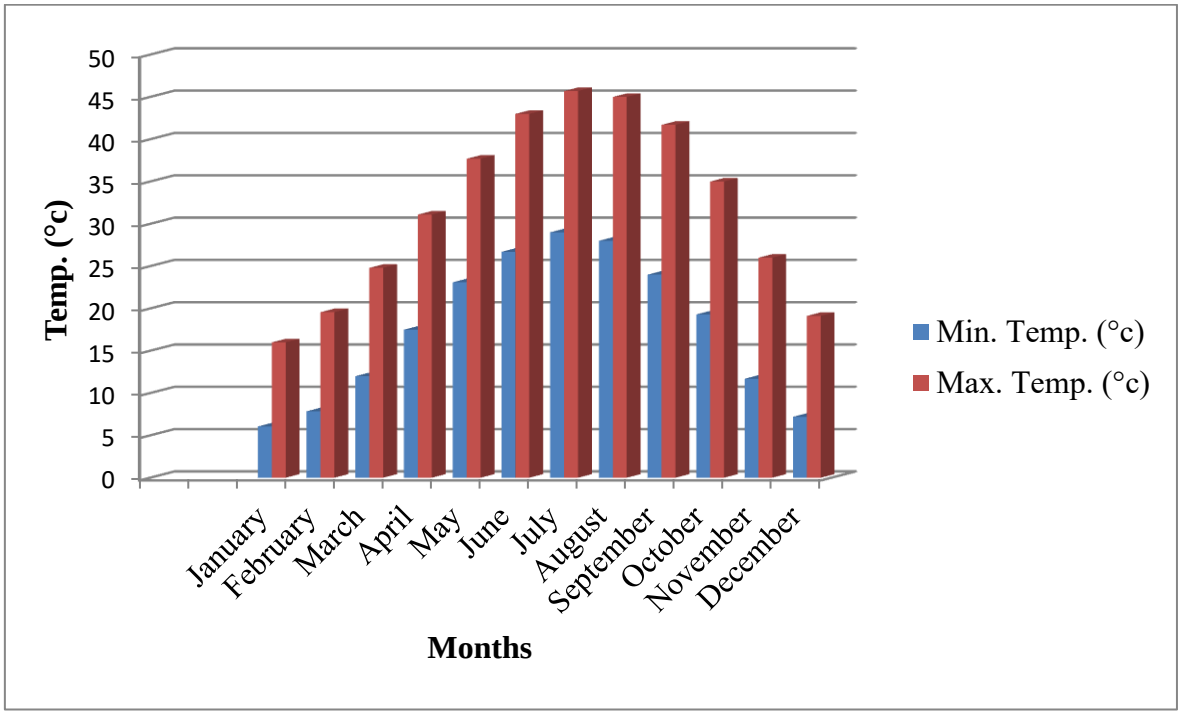

Figure 1-6: Mean of monthly temperature in Badra meteorological station during the period (1994 – 2017)

1-7-3 Relative humidity

Generally, the study area is influenced by an arid climate. The highest monthly value is in January whereas the lowest one was in July (Figure 1-7).

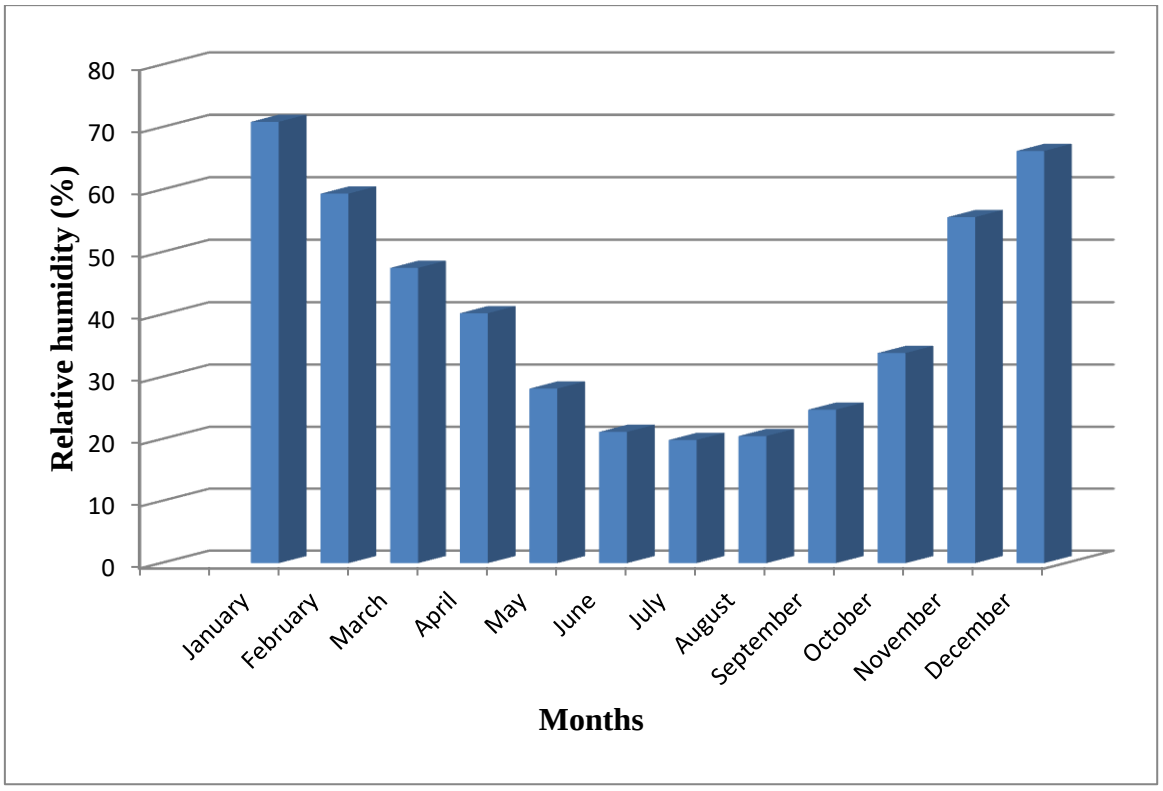

Figure 1-7: Mean of monthly relative humidity in Badra meteorological station during the period (1994 – 2017)

1-7-4 Evaporation

The summer months have the biggest share of the evaporation due to the rising in temperature, while in January, the lowest evaporation according to the fall in temperature in this month (Figure 1-8).

1-7-5 Wind speed

The wind speed fluctuation is not high as in order to the temperature fluctuation, generally, the highest wind speed is in the month (Feb. – Jul.) which exceeds 2m/sec (figure 1-9).

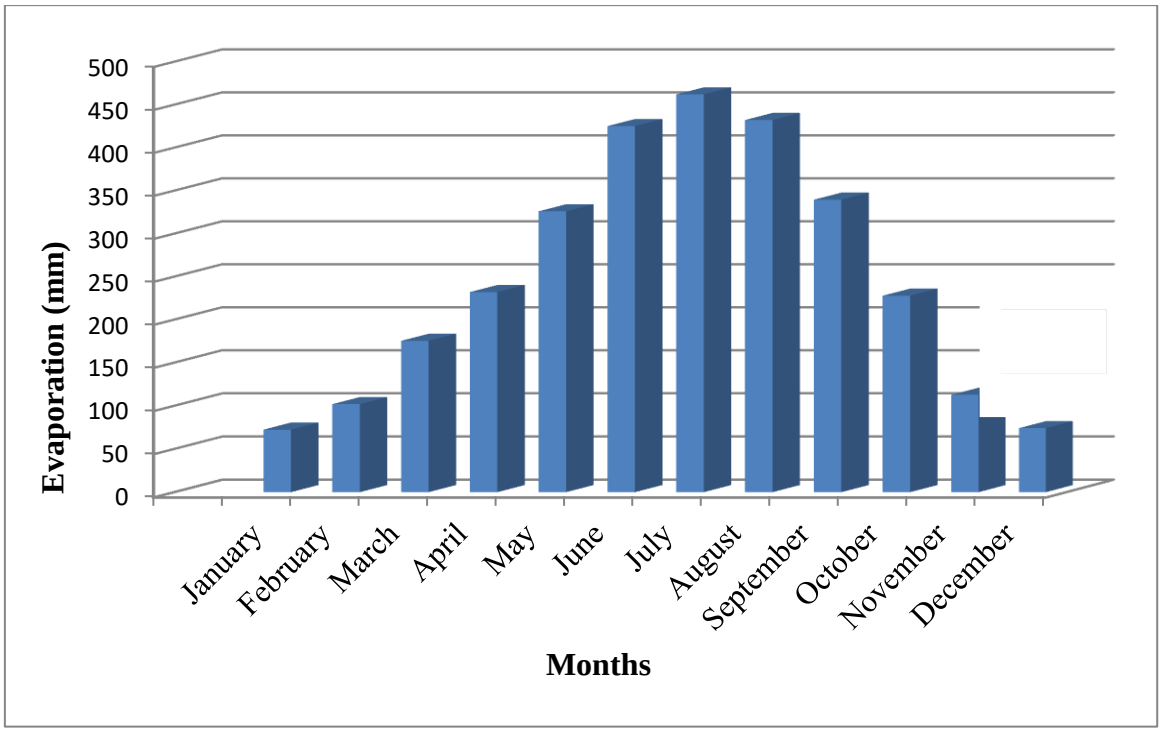

Figure 1-8: mean of monthly evaporation in Badra meteorological station during the period (1994 – 2017)

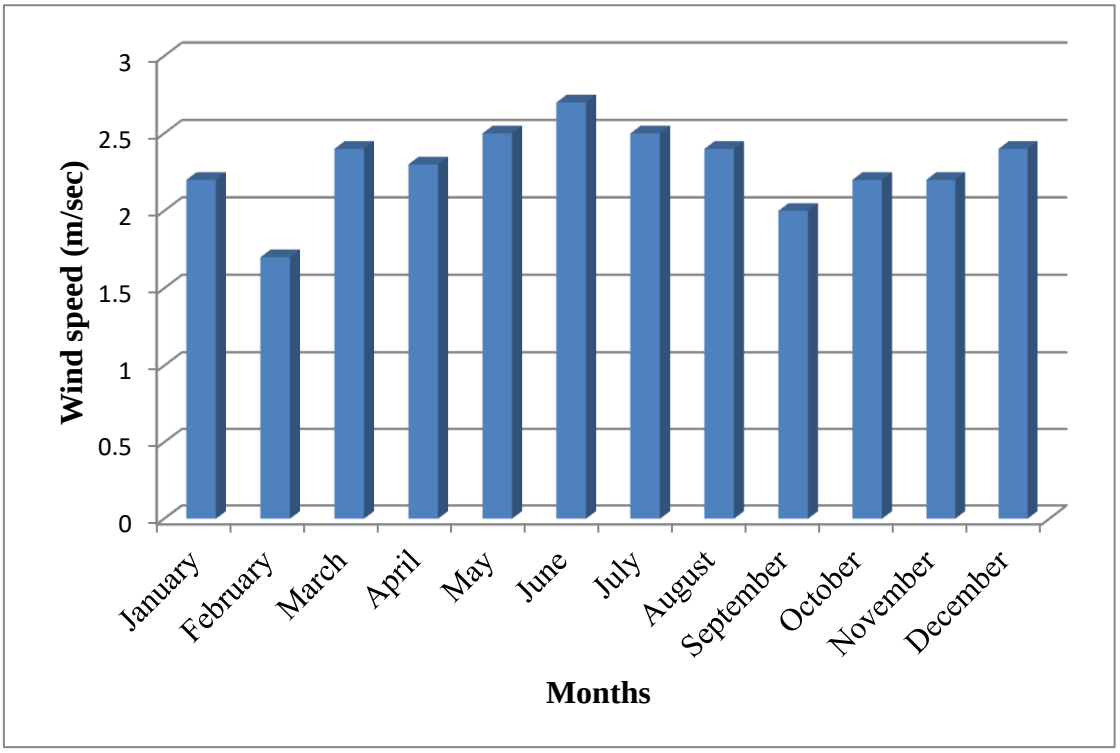

Figure 1-9: Mean of monthly wind speed in Badra meteorological station during the period (1994 – 2017)

1-8 Seismic activity

In any study about slope stability, on of the most important pieces of information that must be known is the seismic activity, the seismic hazard map (Figure 1.10) showed five regions of hazard in Iraq; the study area is located within the high-hazard grade region. The study area is located within the region Suffering from strong earthquakes with magnitudes ranging from (6-6.9) according to the Richter scale (WHO, 2010)

1-9 previous studies

1-9-1 Studies deal with structural geology

- **Al-Saadi (1981):** A method for mapping unstable slopes and classification of rock slopes were suggested by the author.
- **Hancock (1985):** This study suggested a method for discontinuities analysis and for classification relative to the tectonic axes.
- **Zaini (2005)**: This study was dialled with structural and geological studies applied in an area located north of Zakho, joint analysis has been performed according to the principal tectonic axes.
- **Emami *et. al.* (2010):** this study aimed to determine the probable geometry of the Anaran anticline at depth and its relationship to the Mountain front flexure by using both field geology and analog modelling to help to comprehend the interaction of the basement and the cover structures.

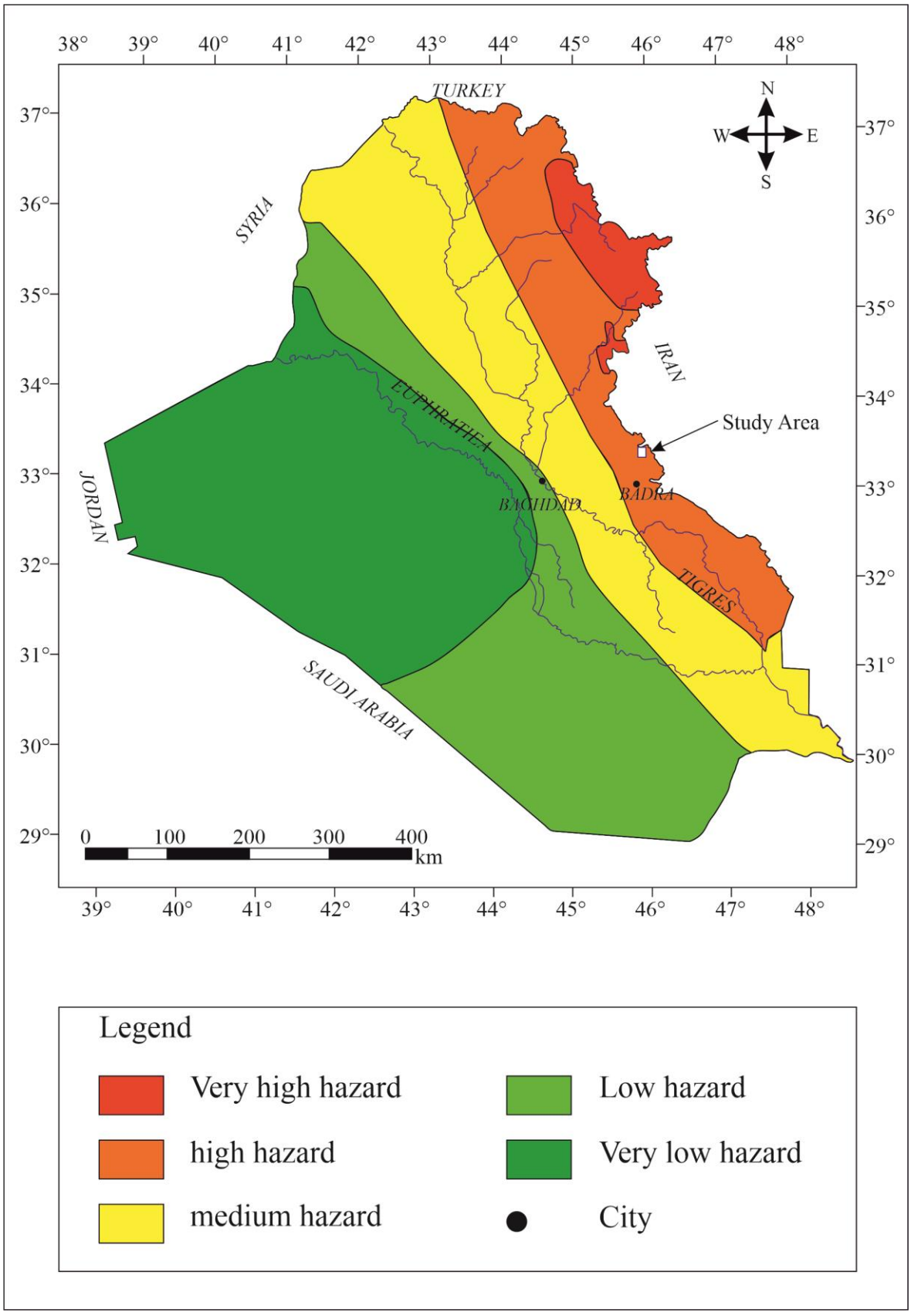

Figure 1-10: Seismic hazard map of Iraq. Modified after (WHO, 2010)

- **Peacock *et. al* (2017):** Focused on the description of some field examples, They were the aim of their studies to prepare a scheme for characterizing the relation between any two fractures, any type they have, in term of their topology and geometry, kinematic and time relation, thereby providing a notable framework for the analyzing of any interaction within fracture networks. And they provide a detailed analysis of the fracture interaction mechanics.

1-9-2 studies deal with slope stability

Hereinafter are some studies about slope stability in many sites in Iraq and some countries:

- **Al-Zubaydi (1998)** conducted an engineering geological study for rock slope stability in many stations in Tar Al- Najaf area. This study recorded many types of rock failures.

- **Al-Obaidi (2005)** conducted an engineering-geological study of many formations around the Shaqlawa area by using field measuring and laboratory tests. Failure hazard maps were performed for the studied area

- **Samarawickrama *et. al.* (2016)** in Sri Lanka; this study was done to identify the factors related to slope stability in open-cast rock quarries, which must be considered before designing and planning the quarries.

- **Hameed (2019)** Carried out a structural and geometrical analysis for discontinuities within the Bammo anticline to assess the rock slope stability.

- **Sissakian et. al. (2021)** carried out an analysis of slope stability of unstable rock slopes along a part of Haibat Sultan mountain, crossing the

road exists in the area by using the field (qualitative) method which was progressed by Bejerman (1994).

- **Ogila et. al. (2022)** this study carried out in Egypt to analyze and assess the various slope failures along the N- Galala plateau and prophesying the types of failures by their kinematic deterministic, then followed by a suggestion of reduction and supporting measures for each unstable zone.

1-9-3 studies about the study area

- **Barwary *et. al.* (1993)** compiled a geological map for Mandali Quadrangle at a scale of 1:250 000, they mentioned that there are some thrust faults in the study area (faults within the eastern part of Zurbatiyah area).

- **Hamza (1997)** compiled the geomorphological map of Iraq at a scale of 1:1 000 000, many geomorphological units were fixed within this study area.

- **Yacoub *et. al*., (2011)** conducted a study of the geomorphology of the Low Folded Zone (LFZ), they aforesaid that the geomorphologic evaluation of the LFZ is highly affected by the last phase of intensive orogenic processes which took place during the Late Miocene – Pliocene and continued during the Quaternary period; in which the geomorphological features that exist in the study area are well developed.

- **Sissakian and Ibrahim (2005)** compiled a geological hazard map of the Mandali Quadrangle at a scale of 1:250 000; as a part of a series of geological hazard maps of Iraq.

- **Sissakian and Al-Jiboury (2012)** conducted a study of the stratigraphy of the LFZ. Accordingly, the oldest exposed rocks in the study area are

belonging to the Fatha Formation, whereas the youngest belongs to the Mukdadiya Formation.

- **Fouad (2015)** compiled the Tectonic map of Iraq at a scale of 1:1000 000. Accordingly, the study area is located within the LFZ of the Zagros Thrust–Fold belt.

- **Mahmoud *et. al*., (2018)** carried out a detailed geological mapping of Zurbatiyah region, they aforesaid that the study area is greatly affected by the regional thrust faults. They measured eight joint stations in an area adjacent to the study area.

- **AL-MUSAWI (2020)** carried out a quantitative analysis of geomorphologic indices to make an understanding of the impact of tectonic processes on the geomorphological fluctuation of drainage basins as well as the alluvial fans.

1-10 Methodology

1-10-1 Data collection

This stage included obtaining available information about the study area from: 1) geological and topographical maps, 2) thesis and 3) research and reports about the study area as well as about similar subjects of this study that were carried out in other areas.

1-10-2 Fieldwork

This stage continued for 10 days (28^{th} Nov. – 7^{th} Dec. 2022). Seventeen stations have been selected to analyze slope stability and slope failure. The studied stations were distributed within three folds that exist in the study area as follows: two stations were within Koolic1 anticline, one station was within Al-Farae syncline and all other stations were within Himreen anticline.

Failures that exist and those that potentially occur have been determined and structural data were measured according to the following steps:

1- Determining the location and altitude for each station using GPS Garmin Oregon 650.

2- Measuring the height, extent and inclination of slopes and lateral slopes if exist.

3- Rock description and sampling.

4- Measuring the Dip direction /Dip of the bedding planes using Breithaupt Kassel compass.

5- Execution of a detailed survey for existing discontinuities in terms of their grade, Dip direction / Dip, extend, spacing, and aperture.

6- Determining the type of each failure.

7- Capturing directional photos.

8- A point load test for the collected rock samples has been operated to determine the indirect compression strength of the jointed beds using a portable device (Plate1.1)

The test method was based on (Broch & Franklin,1972). A sample (irregular lump) must be put across the diameter between two conical platens under pressure applied by a hydraulic jack until the sample breaks (Broch & Franklin,1972; and Willey & Mah, 2004), hereinafter a procedure for point-load Index test for irregular lumps of rock samples according to (Broch & Franklin,1972).

The point-load strength Index (I_s) for regular rock samples is defined as the ratio (P/D^2), while for irregular lumps it is defined as (P/De^2); for standard classification, the I_s (50) must be used, it can be obtained by correction the I_s

value to a reference diameter (50mm) using correction chart. (Figures 1.11 and 1.12). The median value can be obtained from a group of test results, the lowest and highest values must be deleted. The index (I_s) for each sample test must be obtained firstly and corrected for size (I_s 50), then the median value of these corrected values can be computed. The unconfined compressive strength from the point load test (UCS) of rocks can obtained by multiplying the results of this test (after correcting) by 24 (Broch & Franklin, 1972).

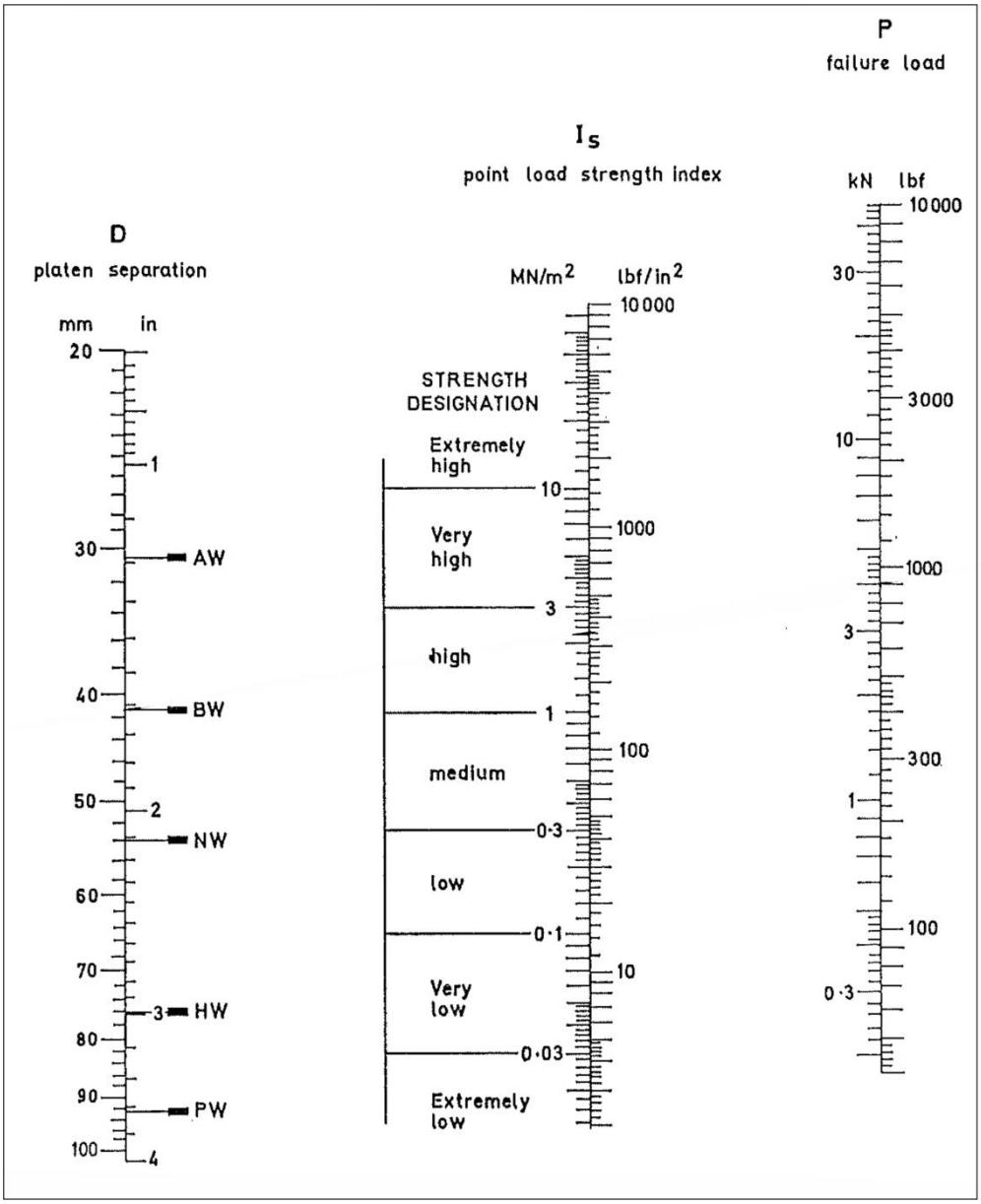

Figure 1.11: Nanogram for computing point load strength indes $I_s=P/D_e^2$. Modified after (Broch & Franklin,1972)

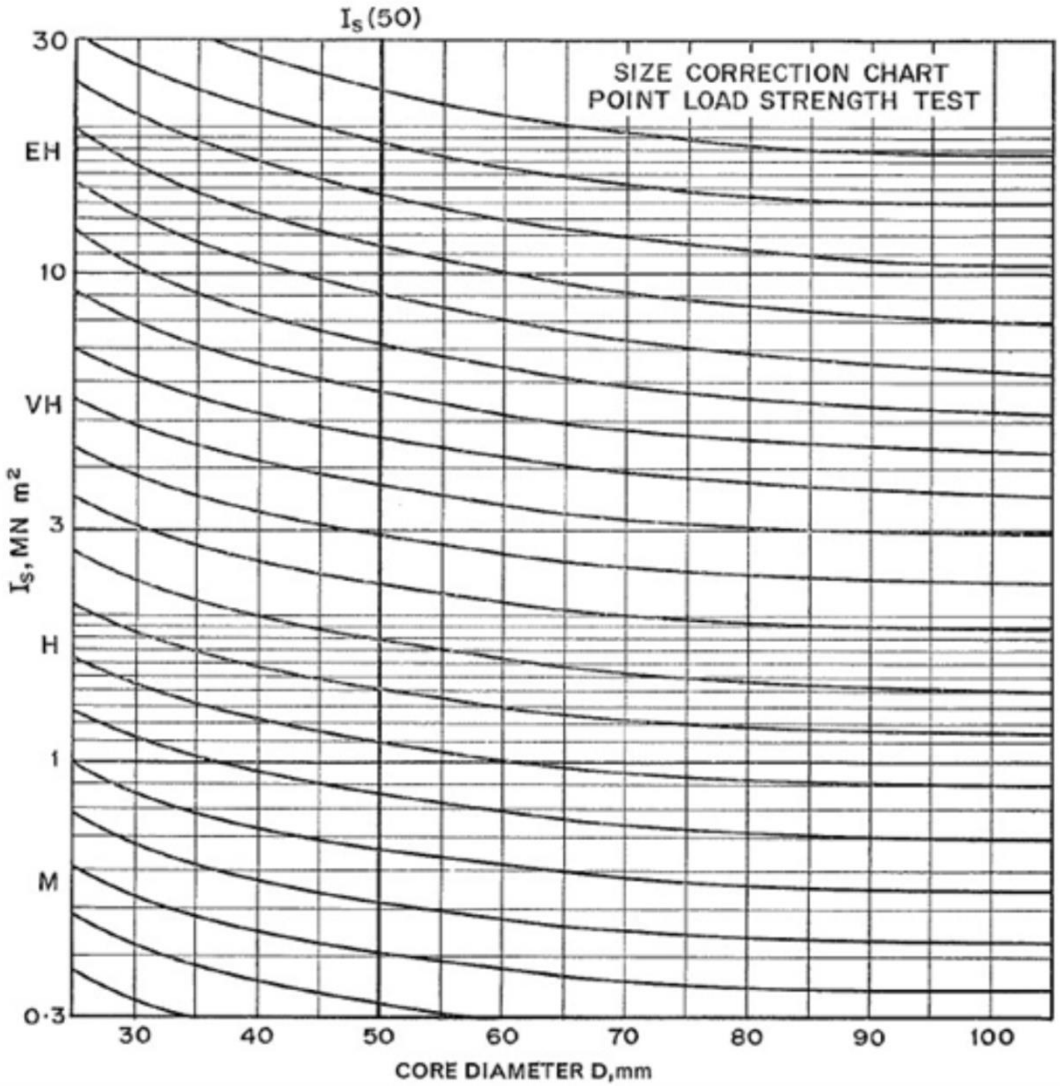

Figure (1.12): Size correction chart for point load test after (Broch & Franklin,1972).

9- The friction angle of the discontinuity surfaces was estimated using the tilt test according to (Freitas, 2009). Two pieces of rock involving the discontinuity must tilt while the angle of the discontinuity with the horizontal is measured, the angle measured at the moment when the top block moves downward is the tilt-angle which is the friction angle of the discontinuity surface when the discontinuity roughness is completely non-fitting (Freitas, 2009), (figure 1.13).

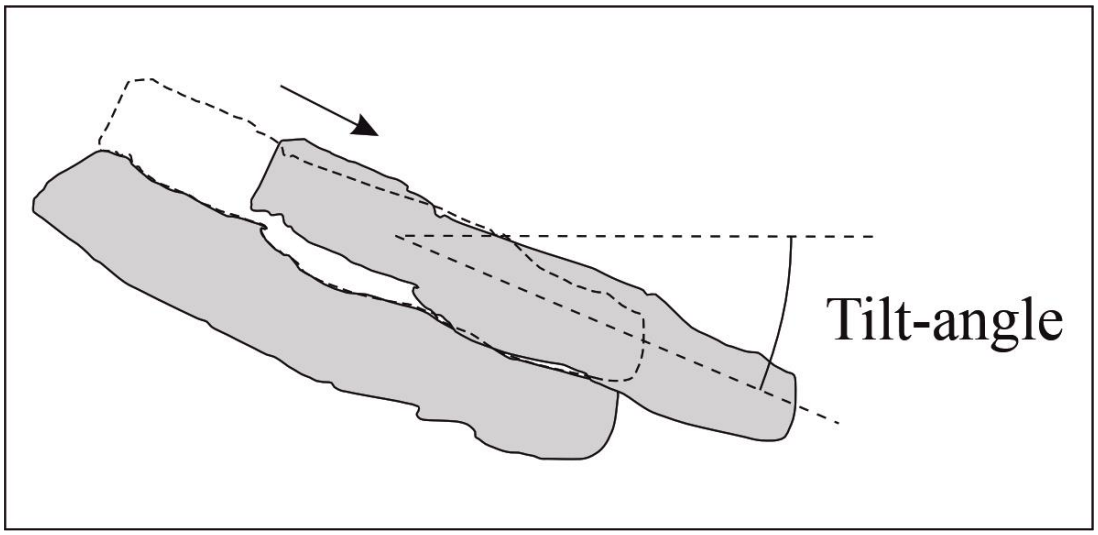

Figure (1.13): Tilt test. after (Freitas, 2009).

Plate (1.1): Point load test

1-10-3 Office work

This stage is presented by analyzing the field measurements and point load test results in order to find the effect of each on the stability of the studied slopes according to the following steps:

1- Presenting the attitude of each bedding plane, discontinuities, and slope for each station using Stereographic projection by using Schmidt net and then by using stereonet V.11 software for Windows Then the discontinuities have been classified according to the tectonic axes to assess their relation with the stability of the slopes containing them.

2- A complete analysis (depending on the field observations and measurements, compressive strength, and stereographic projection) was carried out and some treatments were suggested to stabilize the unstable slopes in the study area.

Softwares used in this study will be explained briefly hereinafter:

- ArcMap GIS: this software is used to clip and digitize the maps and present the location of the studied stations, the input was the files have an extension of jpg, img and tif. The selected output is jpg.
- Stereonet V.11: this software is used to present the bedding planes, joints and slopes for each station. The great circles have been drawn and then used to estimate the general direction of the maximum principal tectonic stress. The poles of the joints are plotted and then used in the classification of the joints according to the tectonic axes. The measurement digits were the input and the output was a pdf file.
- CorelDraw V.24: the not so clear figures were cleared by using this software, as well as the modification of the plates inserted in the subsequent chapters and the stereograms of the studied stations, all of

which were operated using this software. The input was files that have an extension of pdf, tif and jpg, while the output was usually jpg.

- Adobe Illustrator: this software is used to redraw the figures that were inserted within the text of this study, the input was files which have an extension of jpg and the output was jpg too.
- Photo filter: this software is too easy to compare with the above softwares but it has fewer utilities than them, thus this software is used less than CorelDraw and AdobIllustrator, and it is used to modify the figures used in the studyArcMap GIS: this software is used to clip and digitize the maps and present the location of the studied stations, the input was the files have an extension of jpg, img and tif. The selected output is jpg.

1-11 Work Obstacles

The spread of mines and unexploded shells remaining (Plate1.2) from wars was an obstacle to making some sites as study stations. Also, the lack of open roads in the study area made field work difficult.

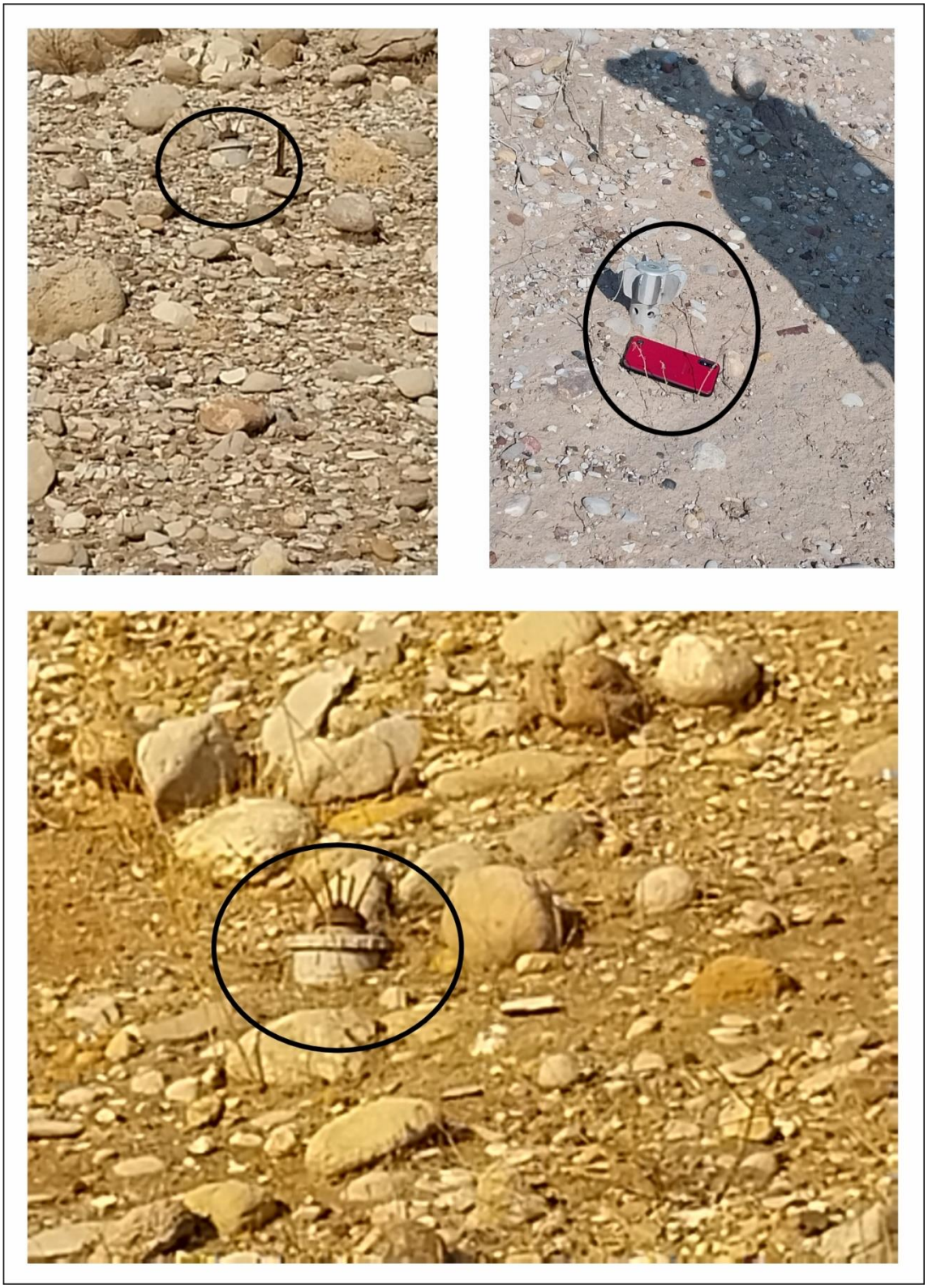

Plate (1.2): Mines and unexploded shell

Chapter two

Basic Concepts About Structures and Slope Stability

2-1 Basic Concepts about Structures

2-1-1 Preface

A kinematic and geometrical analysis has been carried out to the discontinuities within the slopes in the study area. The analysis included field measurements and office work in order to analyze and interpret the data; depending on the tectonic axes.

2-1-2 Folds

2-1-2-1 General Description of Folds

One of the most interesting geological features of the layered rocks which have been deformed among orogenies is that with a curved surface called Folds (Ramsay, 1967 and Fossen, 2016). A fold is a structure formed by folding (ductile deformation) of a planner surface responding to the tectonic activities (stresses) into a curved surface. The folding of pre-folded surfaces is called refolding (Fossen, 2016). And it occurs by transforming and shortening the flat layers into curved shapes (Ragan, 2009; and Davis *et. al*., 2011).

The size of folds varies from that fit into the hand palm to the regional folds with huge size which is best determined by satellites (Davis *et. al*., 2011). Most of the mountain chains around the world consist of large groups of folds accumulated in one area; the most famous of these is the Alps mountain chain which involves the Himalayas, Alps, Zagros, and Taurus (Ghazi, 2009: Zainy, 2020).

2-1-2-2 Geometry of the Folds

The first step before describing the fold, some terms must be understood, according to some authors (e.g. Ramsay & Huber 1987; Van der

Pluijm & Marshak, 2004; Davis *et. al.* 2011; and Fossen 2016) these terms are explained briefly in (Table 2.1) and (Figure 2.1).

Table 2.1: Terms used to describe the folds

Term	Description
Anticline	A dome-shaped fold where the folded rock layers get younger from the axial plain to the end of the flanks of the fold.
Syncline	A tub-shaped fold where the youngest rocks exist in the axial plane of the fold.
Limb	A flake of a fold, two limbs of a fold joining together at a hinge point. i.e. the two limbs separated by the max. curvature.
Hinge point	A point of the maximum curvature of a folded layer where two limbs join together.
Hinge line	A line that is defined by successive hinge points on a folded layer, it called a fold axis for a cylindrical fold. The plunge and direction of the hinge line are important in determining the orientation of the fold, some folds have more than one hinge line as the Box Fold.
Hinge zone	A zone of the maximum curvature in a gradual curvature fold

Axial surface	A theoretical surface joins the huge lines of successive layers in a fold. When it is a plane it is called (an axial plane) and can be described by dip and strike.
Axial trace	An imaginary line that joins the hinge point in a fold.
Fold axis	The straight line of a fold represents the orientation of the cylindrical fold.
Inflection points	Points at the fold limb where the curvature changes from anticlinal to synclinal, and vice versa.
Inflection line	A line connecting the inflection points at a fold limb.
Interlimb angle	The angle which surrounded by two limbs of a fold.
Wavelength	The distance between two hinges that have the same orientation
Amplitude	The distance between the envelope surface and the inflection points in a fold limb.
Envelope surface	The surface that tangents to individual hinges along a folded layer.

2-1-3 Discontinuities

Discontinuities take a wide range of attention in many geological studies because of their effect on the strength of rocks and the stability of the slopes(Kliche, 1999). Discontinuity is a term that points out to many different types of breaks in the rock fabric (Kliche, 1999; and Wyllie & Mah. 2004). Discontinuities represent weakness planes in the rock masses controlling the engineering properties of the rock by splitting the rock mass into many blocks

which are separated by these weakness planes such as bedding, joints, faults, and so on (e.g. Kliche, 1999; Abramson *et. al*.; 2002, Bell, 2007; and Wyllie, 2018).

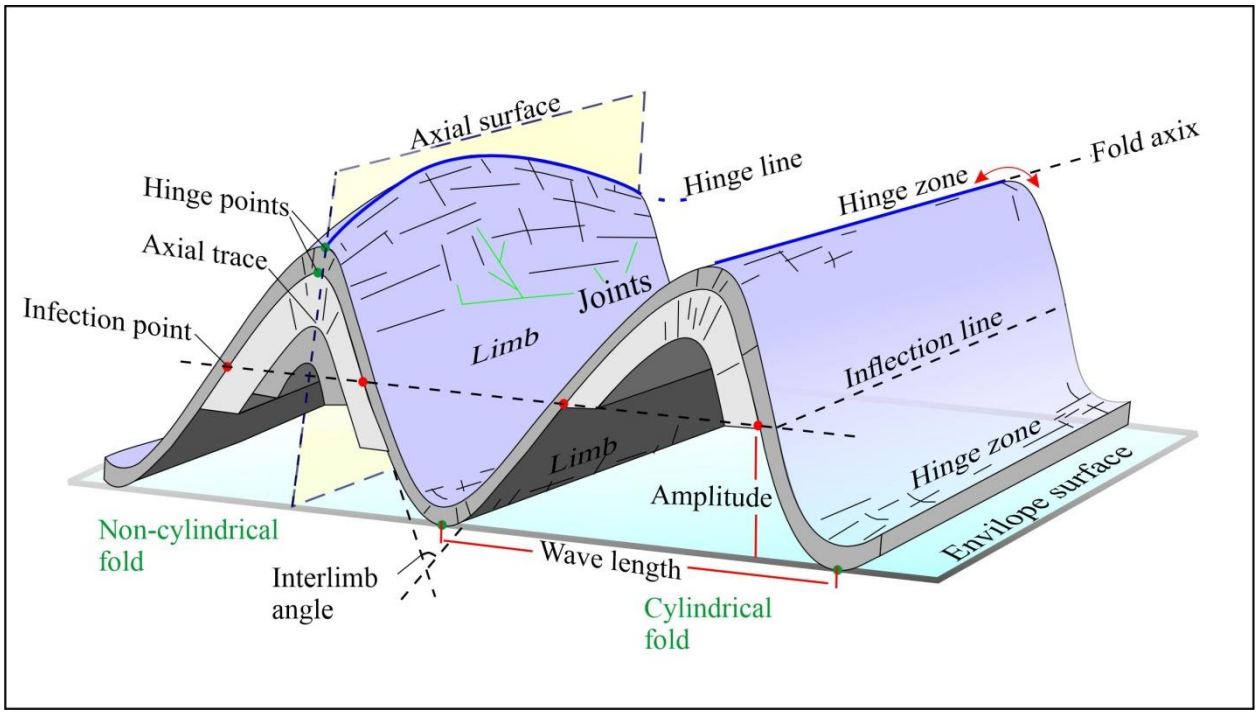

Figure 2.1: Basic geometric aspect of folds. (modified after Fossen, 2010 and 2016)

Discontinuities reduce the strength of the rock mass by presenting weakness planes in the rock mass, while sedimentation of stronger materials at the discontinuity plain such as Quartz can increase the strength (e.g. Priest & Hudson, 1976 and EdyTonnizam et. al., 2005).

The discontinuities are divided into two types: the first one is the integral discontinuities- that discontinuities have yet to be opened by weathering or tectonic movements, they have tensile strength and true cohesion (Bell, 2007 and Freitas, 2009). The other type is the mechanical discontinuities- they have been opened as a result of stresses or weathering; have no or little tensile strength and they do create shear strength. Intact bedding planes, strongly cemented joints, and foliation planes are integral

discontinuities, while faults and other joints are mechanical discontinuities (Freitas, 2009; and Gudmundsson, 2011).

2-1-4 Parameters of Discontinuities

There are many parameters of discontinuities: orientation, spacing, persistence, roughness, filling, aperture, and intensity (e.g. Pollard & Aydin, 1988; Wyllie & Mah. 2004; Bell, 2007 and Freitas, 2009), (Figure 2.2). The most important category in order to slope failures is the orientation (Kliche, 1999).

1- **Orientation:** The discontinuity is a plane, it has an attitude and this attitude is called the orientation of this plane (discontinuity), the orientation can be represented by the dip and dip direction or by the dip and strike of the surface. The dip of a plane is the angle of the plane inclination from the horizontal (angle ψ) which is on record in degrees between 0^o to 90^o. The dip direction is the horizontal trace of the dip of a plane, measured clockwise (angle α) from the true north (e.g. Davis & Reynolds, 1996 and Kliche, 1999), (Figure 2.3).

2- **Spacing:** one of the most important parameters of discontinuities in order to structural analysis and slope stability assessment is the spacing of the discontinuities which exist in a geologic structure, The spacing means the perpendicular distance between two adjacent discontinuities (ISRM, 1978 and Zhang, 2016).

3- **Density:** (e.g. Hoek & Bray, 1981; Davis & Reynolds, 1996; Zhang, 2016) defined the discontinuity density as the cumulative trace length of discontinuities in a given area, regardless of its orientation.

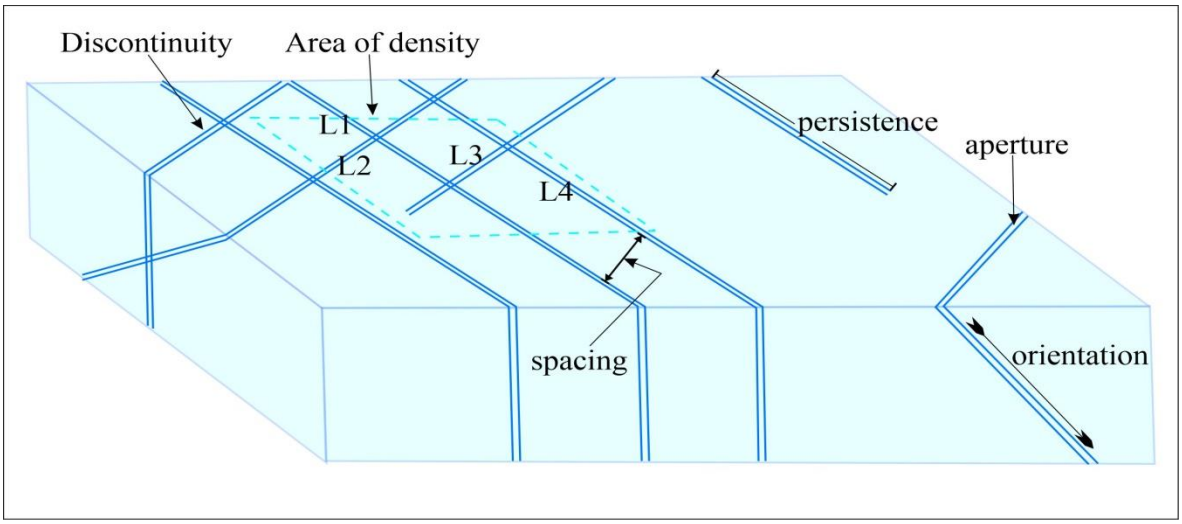

Figure 2.2: Illustrating the discontinuity parameters (modified after ISRM, 1978 and (Davis & Reynolds, 1996)

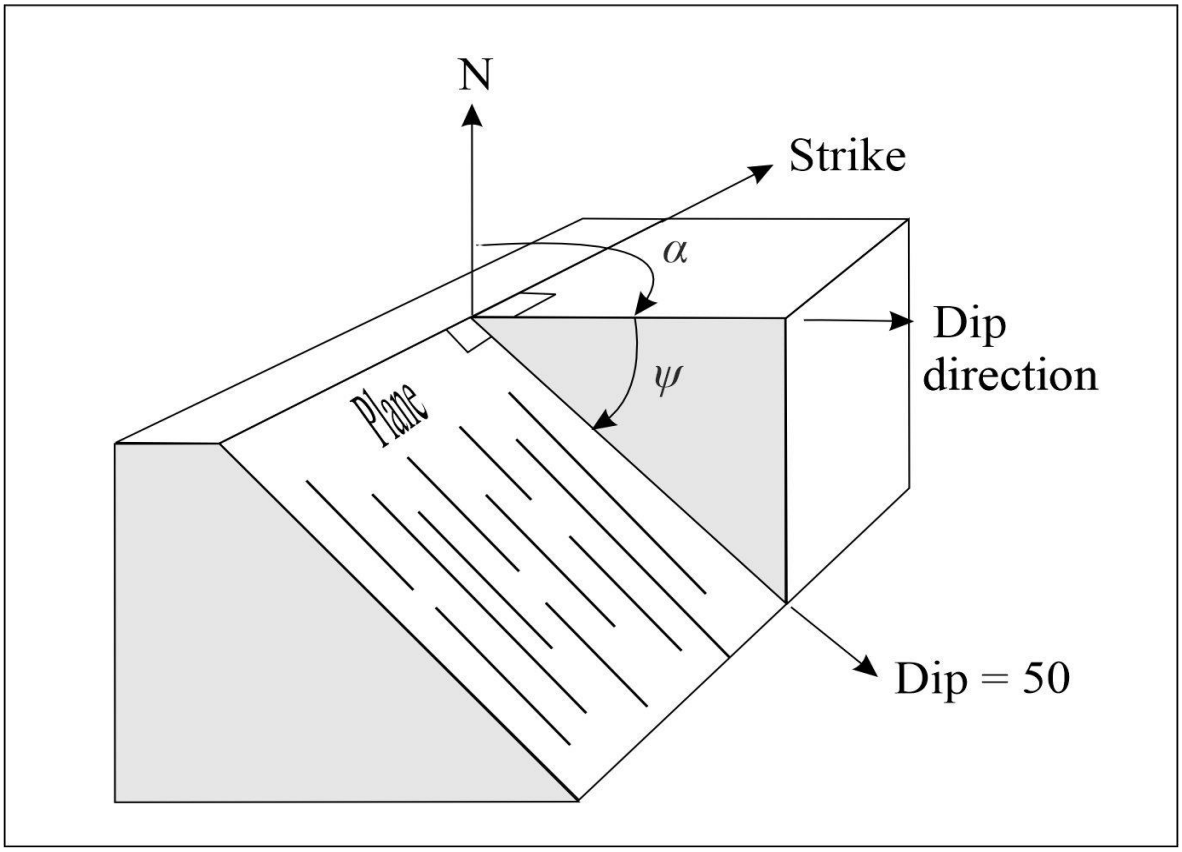

Figure 2.3: Illustrating the attitude of a plane (after Wyllie & Mah, 2004).

4- **Persistence:** The discontinuities may persist for a long distance (e.g. bedding planes), or they may end with other discontinuities like the joints (Freitas, 2009). The persistence is the trace length of a discontinuity as found in an exposure surfaces (ISRM, 1978; and Zhang, 2005).

5- **Aperture:** It was defined as the perpendicular distance between the two walls of a discontinuity; the intervening space should have been filled by air or water (e.g. Zhang, 2005 and Gudmundsson, 2011).

6- **Filling:** This important parameter has been defined by (e.g. ISRM, 1978, Giani, 1992; and Zhang, 2016) as the materials that are deposited within the space between the two walls of a discontinuity. These materials are usually weaker than the host rock, the filling materials are sand, silt, clay, breccia, …etc. (e.g. Zhang, 2016).

7- **Block size**: The dimension of block size is limited by the spacing between two discontinuities, the combined orientation and the spacing of discontinuity sets affect the size and shape of the individual blocks (e.g. Davis *et. al.* 2011 and Zhang, 2016).

2-1-5 Types of Discontinuities

A discontinuity is a general expression that includes a large range of mechanical defects or weakness planes in rock masses Regardless of their origin (Wyllie & mah, 2004; Kliche, 1999 and Wyllie, 2018). This term includes bedding planes and ether fractures such as joints, faults, etc., and other planer surfaces (Schultz, 2009). Discontinuity types range from tension joints of limited length reach to faults that extend to many kilometres in length (Fossen, 2010). Hereinafter brief explanation of the most important types of discontinuities:

1- **Bedding planes:** These are planes that divide the sedimentary rocks into beds or strata and they represent gaps in the course of deposition of the

rock materials (Gudmundsson, 2011 and Wyllie, 2018). Bedding planes are, in general, highly persistent features (e.g. Schultz, 2009 and Zhang, 2016). Bedding planes are surfaces parallel to the original surface of deposition (e.g. Wylli & Mah, 2004).

2- **Fractures**: Generally, the fractures have been divided into extension and shear fractures (Gudmundsson, 2011; and Fossen, 2016). Ideally, the extension fractures develop perpendicularly to the minimum stress and contain both of the intermediate and the largest (maximum) principal stresses; joints are the most wide-speared type of the extension fractures near or at the Earth's surface and they involve a very small strain. While the shear fractures are fracture-parallel slip and develop typically at 20°-30° to maximum principal stress (σ 1). Shear fractures are developed under conditions of confining pressure and temperature that correspond to the upper crust, and can be generated near the brittle-plastic transition too (e.g. Fossen 2010).

a- Joints: These are the most common and the most geotechnically worthy discontinuities in rock masses (Zhang, 2005). This type of discontinuities can be recognizable as a joint where no observable relative displacement occurs (e.g. Wylli & Mah, 2004, Zhang, 2016; and Shakir & Brano, 2020). A group of parallel or sub-parallel oriented joints is called a joint set, whereas intersected joint sets form a joint system (e.g. Hancock, 1985 and Zhang, 2016). There is no visible displacement parallel with, but there is a small normal to, the joint plane. Accordingly, the joint is a primarily extension fracture (Fossen, 2010), when there is clear movement parallel to the fracture plane, the fracture is regarded as a shear fracture and is called a Fault (Fossen, 2010 and Gudmundsson, 2011). A single joint conceder as a continuous fracture that has a planar or curviplanar geometry; the

planar type is referred to as regular joints and the non-planar (curviplanar) joints as irregular joints (Fossen, 2016). In this study, a geometrical analysis of Joints will be classified according to the tectonic axes (see Chapter 3). Joints are either sets or systems, joint planes which are perpendicular to one of the tectonic axes (a, b, and c) and containing the other two are called ab, ac, or bc according to the axes they contain. Whereas the planes that contain one axis and are oblique to the others are classified as okl, hol, or hko. Sometimes, there are planes oblique to all three axes; in this case, the plane will be called hkl, accordingly, o indicates the parallelism of a plane to an axis, whereas h, k, and l refer to the axes a, b, and c respectively; many hko, hol, and okl surfaces belong to conjugate fracture systems, these systems enclosing an acute angle about a, b, and c axes according to the orientation of these planes (Hancock, 1985). If joints are parallel or sub-parallel and planar, these joints will be described as systematic joints, whereas irregularly oriented joints are called nonsystematic (Bell, 2007).

b- Faults: Discontinuities can be recognised by the relative movement of the rock mass on one or both sides of the fault plane (e.g. Wylli & Mah, 2004; Gudmundsson, 2011; Zhang, 2016). Faults transect and displace the lithological layers; and the intersection between the fault plane and the transection surface is called the cut-off line of the markered horizon (Ramsay & Huber, 1987). Some faults extend only for a few centimetres, while others have extensions that reach up to hundreds of kilometres (Rowland et. al., 2007). Three essential types of faults will be explained briefly in the following:

- **Normal fault:** This type is one of the inclined fault types, usually, with a dip reaching 50º (Ramsay & Huber, 1987). In this type, the Dip-slip

component is large relative to the Strike-slip component, the hanging wall moves downward relative to the footwall (Ramsay & Huber, 1987 and Rowland *et. al*., 2007).

- **Revers fault:** As the normal fault, the reverse fault is a dip-slip fault too, when the hanging wall has been moved upward relative to the footwall (Ragan, 2009). When the dip angle on the fault plan is low; typically less than 30º, the fault is called the Thrust fault (Rowland et. al., 2007). While (Ramsay & Huber, 1987) mentioned that the reverse faults with a dip angle of less than 45º are called Thrust faults.

- **Strike-slip faults:** The movement in this type of faults is parallel to the strike of the fault plane (Fossen, 2010 and Ragan, 2009). Sometimes, the strike-slip fault called tear faults, transcurrent faults, or wrench faults (Fossen, 2010). It is divided into Dextrul and Sinistral Strike-slip faults according to the movement of the two adjacent fault walls (Rowland et. al., 2007 and Ragan, 2009).

c- Veins: This type of fractures refers to those that are filled partly or completely with secondary minerals such as calcite and quartz, Some veins are shear fractures but many, and predominant, are extension fractures (Gudmundsson, 2011).

d- Fissures: Open extension fractures, wide separate fractures that are filled with air, water, or hydrocarbon; Although the aperture of the fissure is wider than of that of joints, the borderline between them is not sharply defined (Fossen, 2016).

2-2 Basic Concepts about Slope Stability

2-2-1 Preface

Slope failure is one of the most important problems countered in the geology and engineering projects in the undulated and high-relief areas. Rock slope failure can be caused by many factors (e.g. Hoek & Bray, 1981, Small & Clarck, 1982 and Wyllie, 2018) that will be explained hereinafter:

2-2-2 The influence of the principal factors on slope stability

Slope stability analysis often depends on many natural and non-natural factors that influence the stability of slopes and the failures that may occur (e.g. Hoek & Bray, 1981; Wyllie, & Mah, 2004 and Wyllie, 2018), hereinafter an explanation of these factors:

1- Geological structure: discontinuities have an extreme influence on rock slope stability in terms of their orientation, persistence, and spacing (Blyth & Freitas, 1984; and Wyllie, 2018). The orientation of discontinuities plays an important role in the stability of segmented blocks, while the spacing and persistence determine the size of these blocks (Wyllie, & Mah, 2004 and Wyllie, 2018). In addition to this, the presence of joints often reduces the strength of rocks (Blyth & Freitas, 1984).

2- Hydrology factor: The presence of water within a rock slope, has a negative impact on its stability (Bell, 2007 and Cheng & Lau, 2014). If the opened joints are filled with water, which thence flows under the base of the blocks, the stability of the blocks will be reduced by the uplifting force on the base of these blocks (Freitas, 2009). The effect of water on stability can be concluded in the following (Blyth & Freitas, 1984; Bell, 2007 and Cheng & Lau, 2014):

a- Groundwater is considered an agent of weathering and erosion causing caves created by the dissolution of the soluble rocks within the slope (Blyth & Freitas, 1984). The existence of groundwater can increase the pore water pressure (Zhang, 2005). In claystone beds, the presence of groundwater may swell the clay and create an additional pressure on critical beds (Zhang, 2005 and Bell, 2007). All that may be causing a lack of the stability of the rock slopes and failure may occurs.

b- Freezing and de-freezing of groundwater due to a drop and rise in temperature can change the water level within the disintegration in different sizes according to the spacing of the discontinuities, and the molten of pore ice producing an additional pore pressure affects the stability of rock blocks (Wyllie, & Mah, 2004 and Bell, 2007).

c- Freezing of the surface water of the rock cliffs can give rise to the drainage pathways and cause an accumulation of water pressure in the slopes (Wyllie, & Mah, 2004). The large accumulation of snow can increase the load on the supports of the slope (Kliche, 1999). Any of that can cause rock slope failures.

3- Seismic disturbances: Seismic activity is one of the major factors affecting landslide and rock slope failures, earthquakes affect the slope stability by reducing the frictional strength and/ or decreasing the cohesion of the substrata by shattering of rock mass or liquefaction the friable rocks and the soils (e.g. Bell, 2007; Meunier *et. al*., 2008 and Tiwari & Ajmera, 2017).

4- Human activity: Human obtrusion can have a major role in the stability of critical slopes by operating a variety of works (Kliche, 1999 and Bolt *et. al*., 1975), these influential are:

a- Load increasing by expansion buildings construction on the slope can threaten its stability (Bolt *et. al*., 1975; Wyllie & Mah, 2004; Bell, 2007 and Wyllie, 2018).

b- Road and Train networks constructions in unconsidered ways can reduce the stability of cut slopes and cause failures (Kliche, 1999 and Wyllie & Mah, 2004.

c- Forest scraping can destabilize the slopes; the soil cover of the slopes may be exposed to erosion after removing the vegetation cover and this influences the slope stability (Bolt *et. al*., 1975).

2-2-3 The Modes of Failures

Many researchers proposed classifications of failures on rock slopes according to numerous criteria, one of the most important is the classification proposed by (Ali, *et. al*., 1991):

1- According to the type of motion: in which the failure is rock fall, sliding, or rock flow.

2- According to the failure plane: Planar, Circular, or irregular.

3- Forming of failed rock blocks: rock fragments, rock fragments with soil, or clayey soil with/or sandy soil.

4- Motion speed: Fast and raped or slow.

2-2-3-1 Rock failure classification according to the motion type

The classification of (Hoek and Bray, 1981) has been generated in this study:

1- Sliding

2- Toppling

3- Rock fall

2-2-3-1-1 Sliding

The Sliding is a shear motion of a rock slope downward the slope along a plane surface (called a sliding surface) within the rock mass (Hoek & Bray, 1981). The sliding is divided according to the nature of motion and shape of the sliding surface into Translational sliding and Circular sliding.

1- Translational sliding

The motion of this type of failure is along a straight line, it is subdivided into two types: Plane sliding and wedge sliding (Hoek & Bray, 1981).

Plane sliding:

It has a comparative occurrence in rock slopes (Wyllie & Mah, 2004). It happens when the motion occurs on a planar surface (Figure 2.4) and some condition should be satisfied (according to: Hoek & Bray, 1981, Kliche, 1999, Watts. *et. al.*, 2003, Wyllie & Mah, 2004), these are:

a- The plane of sliding should be parallel or sub-parallel to the slope face inclination (approximately $\pm 20^{\circ}$).

b- The sliding plane should daylight in the slope face, in which the dip of the sliding plane (Ψ_p) must be less than the inclination angle (Ψ_f)of the slope face, i.e. $\Psi_p < \Psi_f$.

c- The dip of the sliding plane should be greater than the friction angle of this plane, i.e. $\Psi_p > \Phi$.

d- The upper end of the sliding surface must either terminate in a tension crack or intersect the upper slope.

e- Release surfaces must exist in the rock mass to free the sliding block from any negligible resistance against the sliding, that is not all discontinuities can be release surfaces, like small persistent joints and any rough discontinuities (Al-Saadi, 1981).

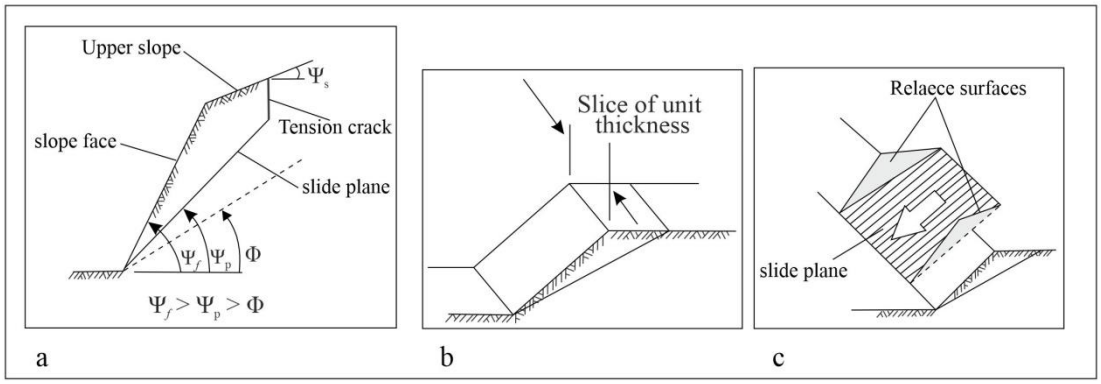

Figure 2.4: Illustrates the geometry of plane sliding. a) cross section showing parameters of plane sliding; b) thickness of slide block; c) release surfaces reach the upper slope, (after Wyllie and Mah,2004).

Wedge sliding:

It is one of the translational sliding types, it occurs when two sets of discontinuities intersect by an intersection line dipping with an angle less than the inclination angle of the slope face (Lisle & Leyshon, 2004 and Wyllie & Mah, 2004). Wedge sliding may occur much in a wider range of geologic and geometric conditions of the plane sliding (Wyllie & Mah, 2004). The wedge failure possibility exists where two discontinuities are strikes oblique across the slope face and their intersection line daylights in the slope face (Kliche, 1999), (Figure 2.5). Many conditions (according to Hoek & Bray, 1981; and Wyllie & Mah, 2004) are important for wedge sliding occurrence:

a- Two planes must intersect in a line; the dip of the intersection line (Ψ_i) must be less than the inclination angle of the slope face (Ψf) toward the downslope to form a daylight surface in the slope face.

b- The dip angle of the intersection line of the two planes (Ψ_i) should be equal to, or greater than the friction angle (Φ) of each one of the intersected planes, that is ($\Psi_f > \Psi_i > \Phi$).

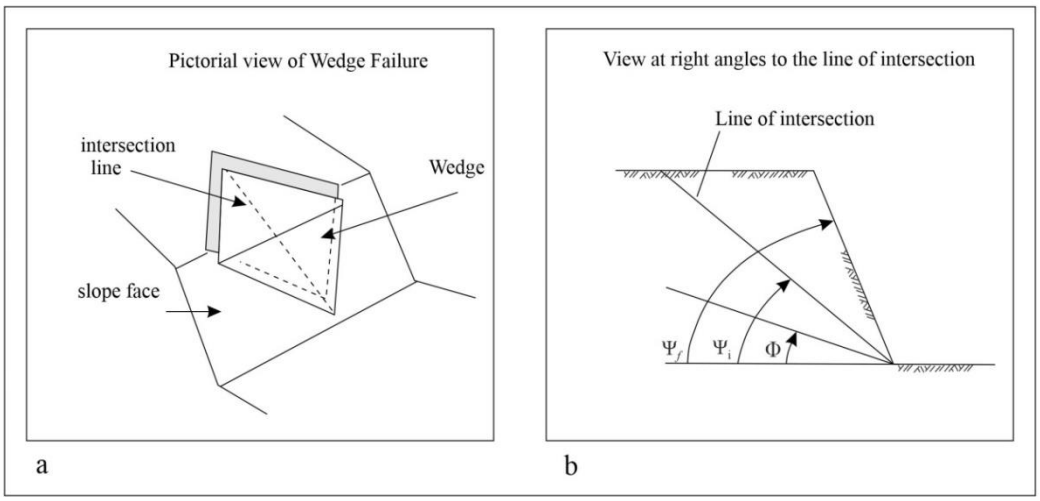

Figure 2.5: The geometry of Wedge sliding. a) Pictorial view of wedge failure; b) view of slope at right angles to the line of intersection, (after Wyllie & Mah,2004).

2- Rotational sliding (Circular sliding)

This type of failure often occurs as sliding along a circular plane in the highly segmented rocks by dense and randomly oriented discontinuities without specific structural orientation (Wyllie& Mah, 2004), (Figure 2.6). Before the failure occurrence, a tension crack can appear on the surface of the critical block; then a buckling in the downslope. After the failure, a spoon shape appears on the sliding surface (Kliche, 1999 and Wyllie & Mah, 2004). The number of discontinuities may be an important factor of rock slope stability in addition to the orientation with respect to the slope face inclination, a rock mass containing closely spaced joint sets perhaps changes the possible slope

failure mode from toppling or translational failure into rotational failure (Wyllie, 2018).

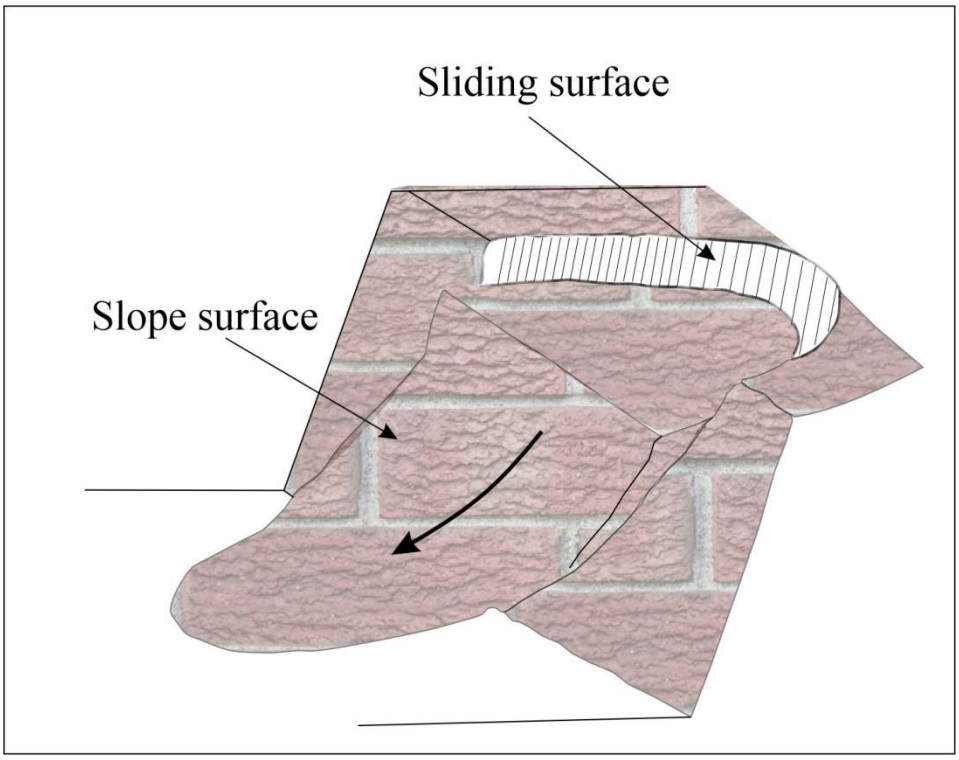

Figure 2.6: 3D sketch illustrating the rotational sliding (after Hoek & Bray, 1981).

2-2-3-1-2 Toppling

All types of sliding occur on a recognizable surface, while the toppling is done by rotation of geometrically dimensioned blocks at its base an axis, which is often parallel to the strike of the slope, and it topples downward the slope; the Weight vector must be out of the block base (De Freitas & Watters, 1973, Goodman & Bray, 1976, Al-Saadi, 1991 and Kliche, 1999). The most role conditions that should be present in order to toppling occurrence according to (De Freitas & Watters, 1973; Goodman & Bray, 1976 and Kliche, 1999) are:

1- The rock block must have an appropriate geometrical form (Figure 2.7), that is the ratio between the length of its base (perpendicular to the slope strike) to its height less than the tan of the dip angle of the plane in which the block rest above, accordingly the weight vector should lie out of the base through the block weight centre.

2- The rock columns should dip contrariwise to the slope direction and the support at the slope toe or rock block should be removed.

3- The dip angle of the plane (Ψ) must be equal to or greater than the friction angle (ø).

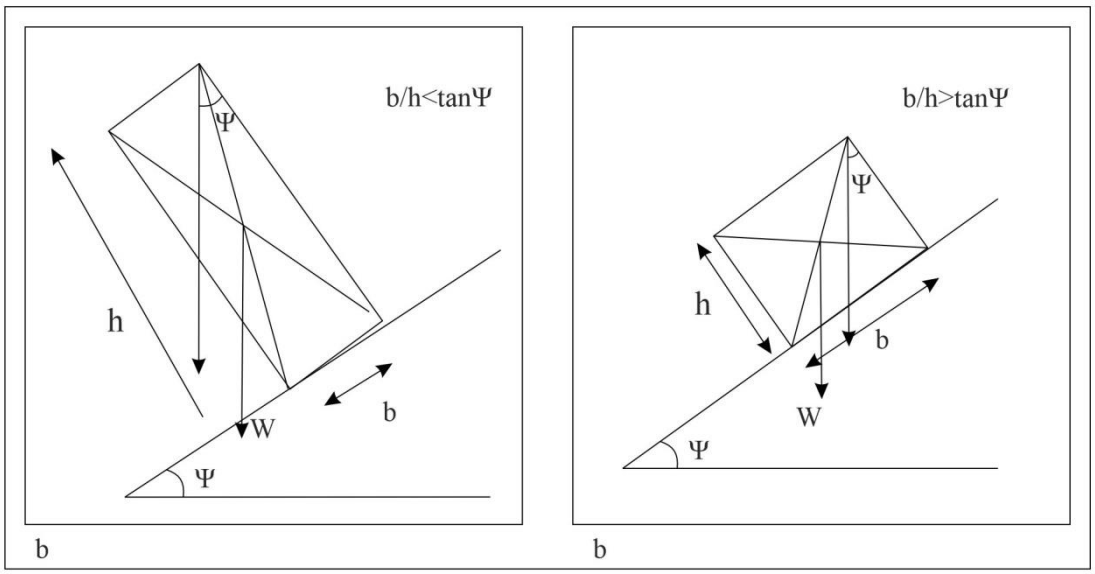

Figure 2.7: General scheme showing rock block resting on a plane inclined at (Ψ°). a) Possible toppling when (W) lies outside the block bas. b) No possible toppling when (W) lies inside the base. (after Al-Saadi, 1991).

Some rock slopes suffer from sliding and others may from toppling, (Hoek & Baray, 1981) proposed cases illustrating the relation between toppling and sliding (Figure 2.8), these are:

- Region 1: Ψ < ø and b/h > tan Ψ, the rock block is stable and will neither slide nor topple.
- Region 2: Ψ > ø and b/h > tan Ψ, the rock block will slide but it will not topple.
- Region 3: Ψ < ø and b/h< tan Ψ, the rock block will topple but it will not slide.
- Region 4: Ψ > ø and b/h < tan Ψ, the rock block can slide and topple.

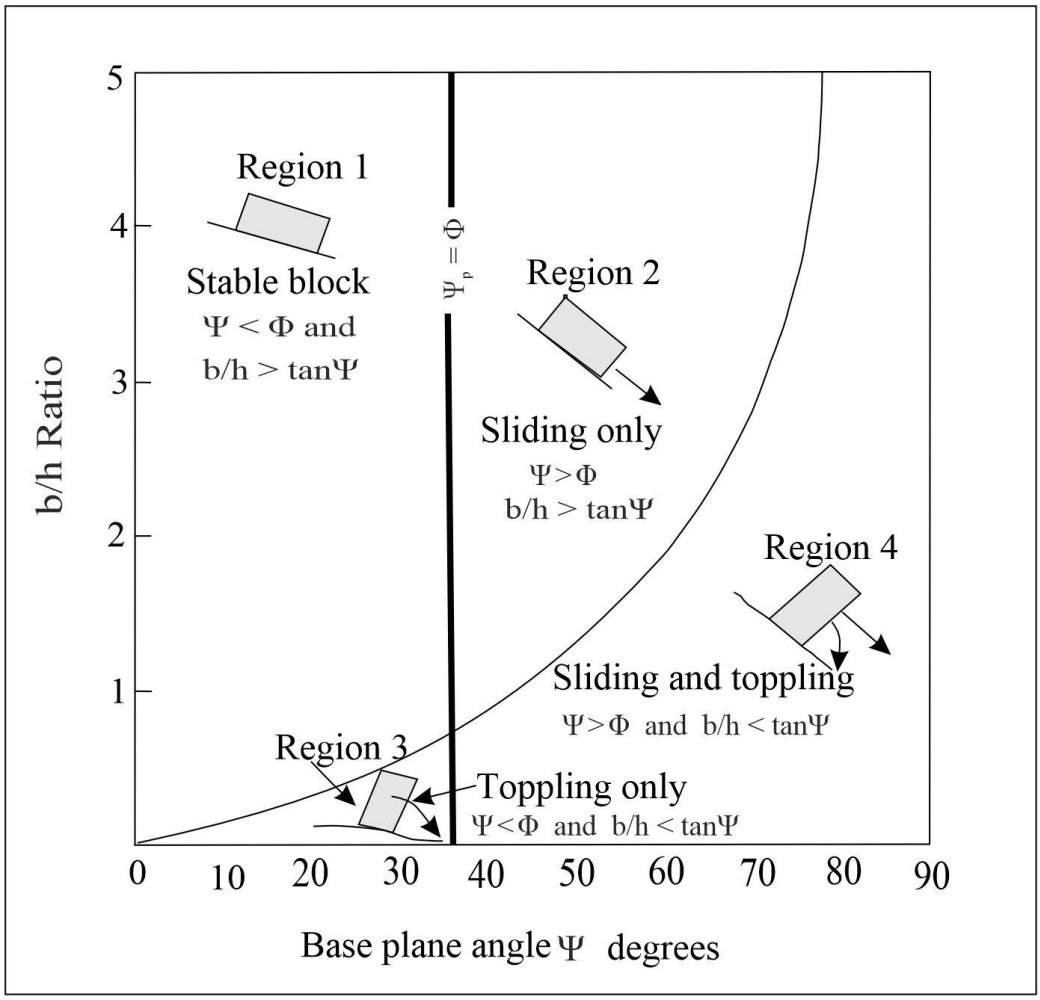

Figure 2.8: Condition of sliding and toppling of rock blocks set on an inclined plane with respect to the geometrical dimensions (after Hoek & Baray, 1981).

The toppling has been divided into three principal types (Goodman & Bray, 1976). Then it is subdivided into six secondary types by many researchers (Figure 2.9).

A- The main modes of toppling

1- **Block Toppling**: It occurs when a strong rock is segmented into individual columns by a set of joints dipping steeply contrariwise to the slope face (Goodman and Bray, 1976), (Figure 2.9 a) and widely spaced orthogonal joints set which defines the column's height (Al-Hussainy, 2010).

2- **Flexural toppling:** it occurs in continuous rock columns separated by well-developed steeply dipping discontinuities; breaking in flexure behaviour as they bound (Goodman and Bray, 1976), (Figure 2.9 b). Generally, the basal plane of flexural toppling is not as well-defined as the block toppling (Al-Hussainy, 2010).

3- **Block Flexure toppling**: It is depicted by pseudo–continuous flexure along long rock columns, that are segmented by many cross joints (Goodman and Bray, 1976), (Figure 2.9 c). In this type of failure, the toppling of rock columns can result by the accumulation of displacements on the cross joints (Al-Hussainy, 2010).

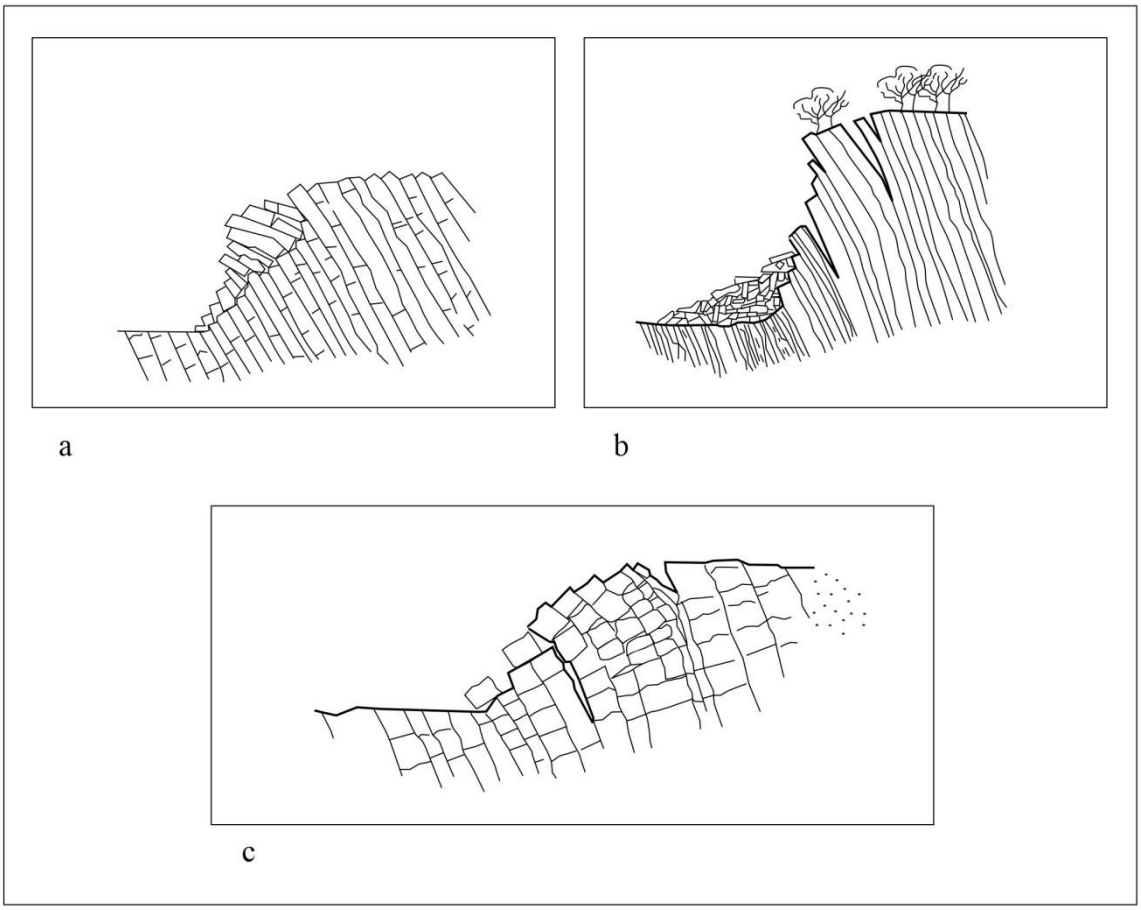

Figure 2.9: Main modes of toppling: a) block toppling of columns; b) flexural toppling; c) block flexure toppling. (Goodman and Bray, 1976).

B- Secondary modes of toppling

These types occur after natural or artificial (man-made) activities before the toppling occurrence, generally by undercutting the toe of the slope (Figure 2.10):

1- Slide Toe Toppling

It can occur at the slope toe as responding to the stress of the upper slope rock sliding (Goodman & Bray, 1976), (Figure 2.10a).

2- Slide Base Toppling

Where the upper part of the slope lies above a sami-vertical layered rock mass, if sliding occurs in the upper part; the underlain layerd will topple under the sliding plane (Goodman & Bray, 1976), (Figure 2.10b).

3- Slide Head Toppling

In this type, the sliding occurs at the toe of the slope and a void will remain behind the sliding block, and then a toppling will occur for the blocks behind the slide block (Goodman & Bray, 1976), (Figure 2.10c).

4- Toppling and Slumping:

It occurs in rock columns by wethering of the down parts of the slope (Goodman & Bray, 1976), (Figure 2.10d).

5- Tenson Crack Toppling

It is a toppling that occurs after a tension crack occurrence parallel to the slope strike (Hoek & Bray, 1981), (Figure 2.10e).

6- Differential Settlement Toppling

This type occurs for vertical rock columns by differential weathering of the bed which underlies the columns, where the maximum weathering at the slope surface decreases inside ward the rock mass (Evans, 1981), (Figure 2.10f).

2-2-3-1-3 Rock fall

A free and sudden fall of different sizes of rock masses from very steep vertical slopes as a result of undercutting, after initial detachment from the slope (Bromhead, 1992). The undercutting may result from differential erosion, an increase of pore water pressure by freezing and melting of the water in the joints, or by Human activity (Bromhead, 1992 and Giani, 1992).

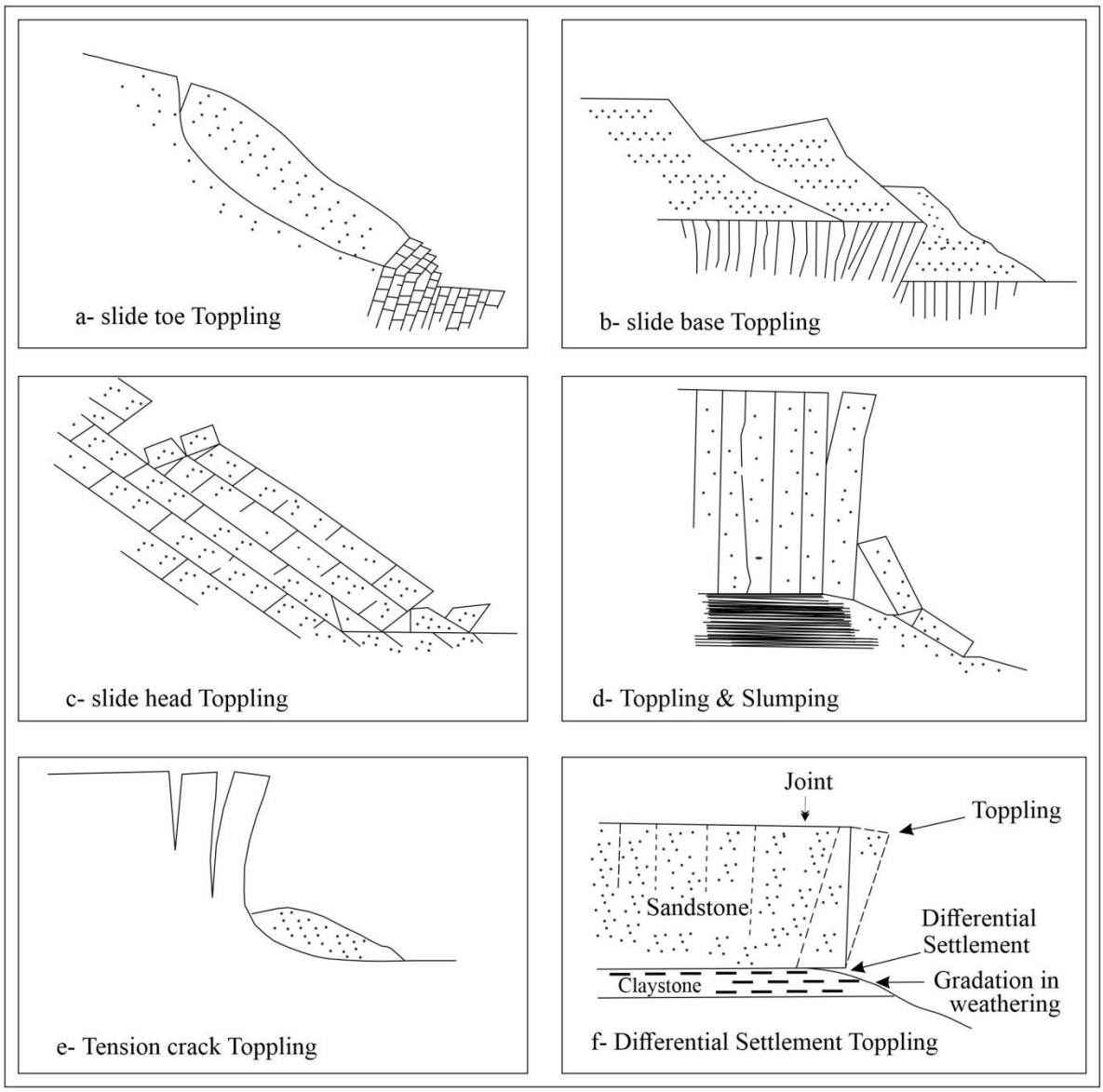

Figure 2.10: Secondary toppling modes (a-b-c-d) after (Goodman & Bray, 1976), (e) after (Hoek & Bray, 1981), and (f) after (Evans, 1981).

By assuming the rock mass is spherical, (Ritchie, 1963) suggested the following general cases for rock fall (Figure 2.11):

1- In the situation of not rough and regular gentle slopes, most rock masses remain stationary above the slope until a dip of less than (30°). While in the case of stepper slopes (40°-55°), the detached blocks will roll accusatory and still roll without relying on the slope inclination. Although

this case is not reliable for large rock fragments, it is most reliable for smaller fragments.

2- For slopes inclining between (55°-75°), fall-down rocks tend to bounce and spin and go far for a considerable distance from the base.

3- For steeper slopes of more than (75°), the fall-down rock blocks or fragments rarely touch the slope face again.

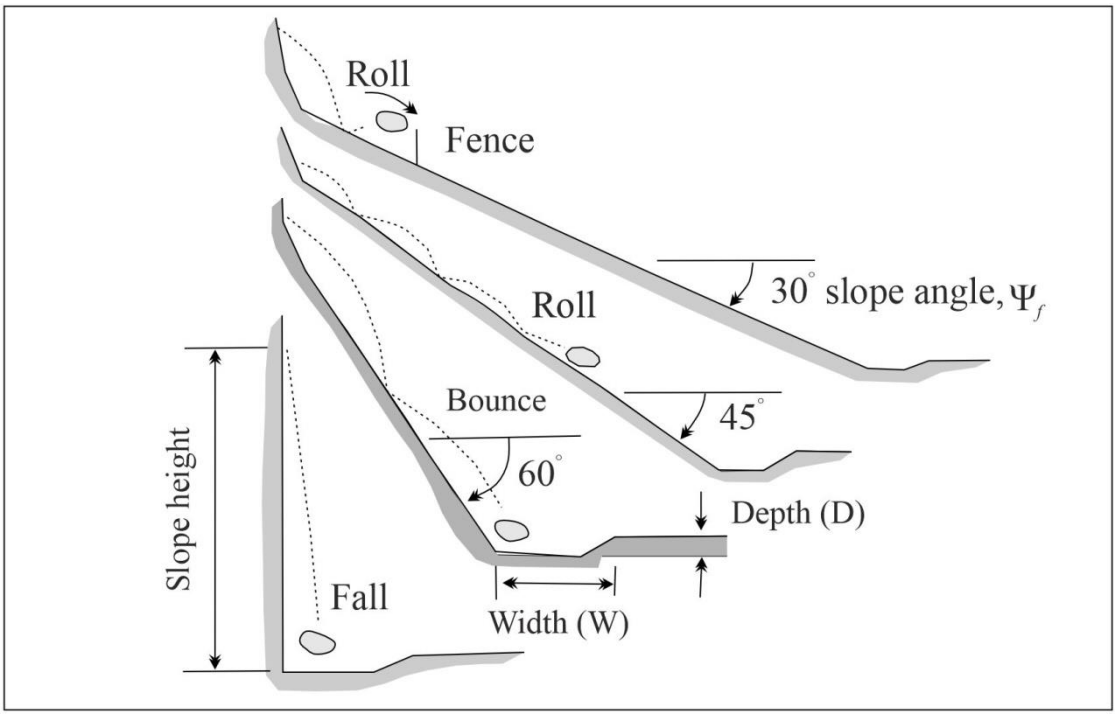

Figure 2.11: Types of rack fall according to the inclination angle (after Ritchie, 1963).

Chapter Three

Structural Analysis

3–1 Geometrical Classification of Joints

Joints are either sets or systems, because joints are kinematically inscrutable geologic structures, their interpretation has been performed controversially (Hancock, 1985).

The common method used for geometrical analysis refers to the geometry of a set or system to an orthogonal fabric cross; the three axes which are labelled (a, b, and c) without kinematic or dynamic application (Turner & Weiss, 1963), which are the base of the geometrical analysis of joints. These axes (Figur 3.1a) are related to the fold geometry (the hinge line and the bedding plane); these are (Turner & Weiss, 1963) :

- The (a) axis is parallel to the dip direction and normal to the fold hinge line.
- The (b) axis is parallel to the strike of beds and the hinge line.
- The (c) axis is normal to both (a and b) axes and the bedding plane.

The classification of joints in a geometric way will depend on the classification of (Hancock, 1985), which has been explained previously in (chapter 2), (Figure 3.1) illustrates the orthogonal tectonic axes and the types of joints. The joints were classified according to (Hancok and Atiya, 1979) by plotting the poles of the joints using a stereographic projection technique (figure 3.2).

3-2 Joints in the Study Area :

Seventeen stations with more than 200 measurements have been distributed in the study area (Figure 3.3).

The attitude of joints and bedding planes that contain these joints has been measured for each station. Then (Stereonet, ver.11) software was used to plot these attitudes using the stereographic projection Schmid net method to show the position of the pole and great circle of each joint concerning the great circle of the bedding plane. The classification was as described hereinafter :

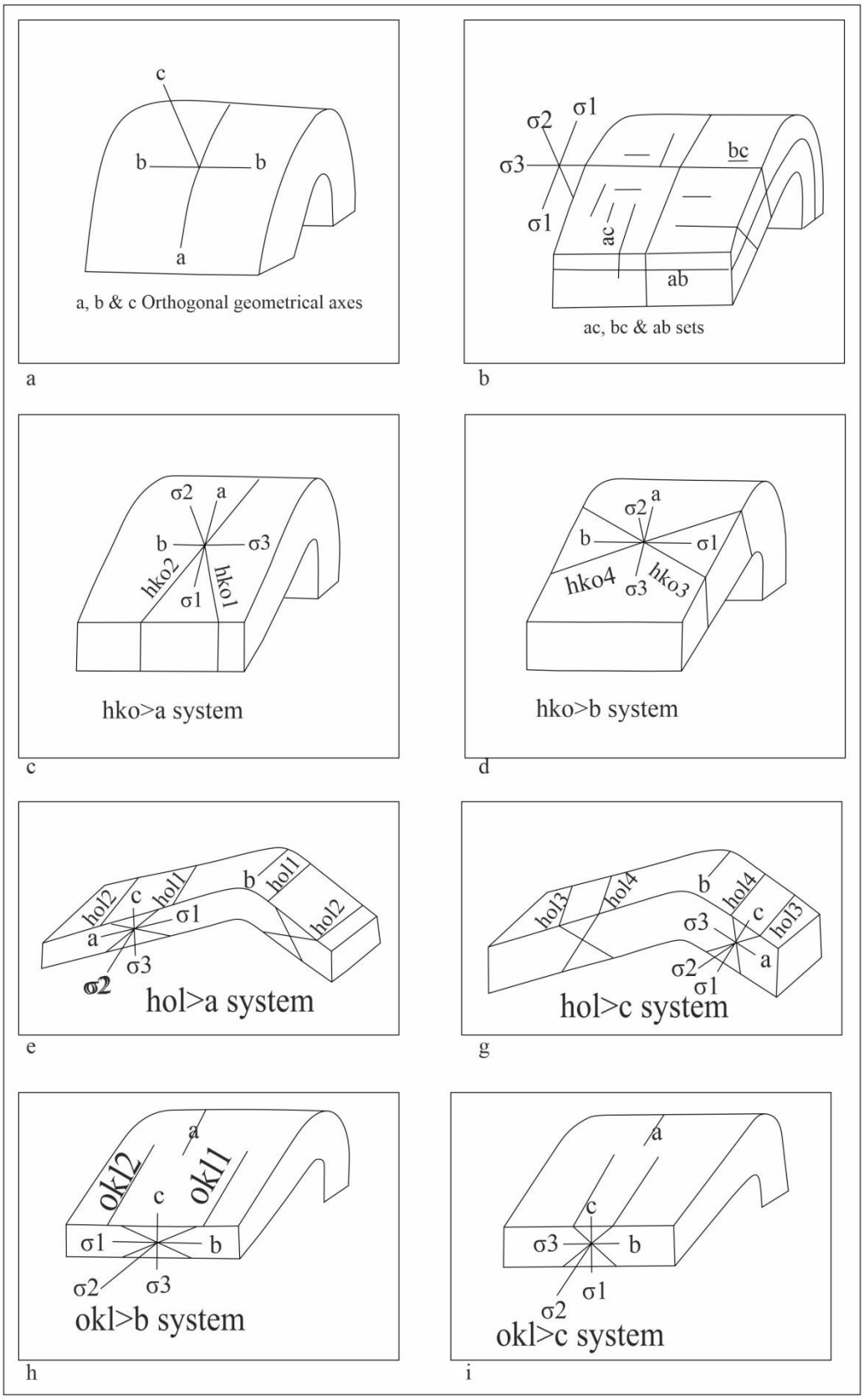

Figure 3.1: Geometrical classification of joints (after Hancock, 1985)

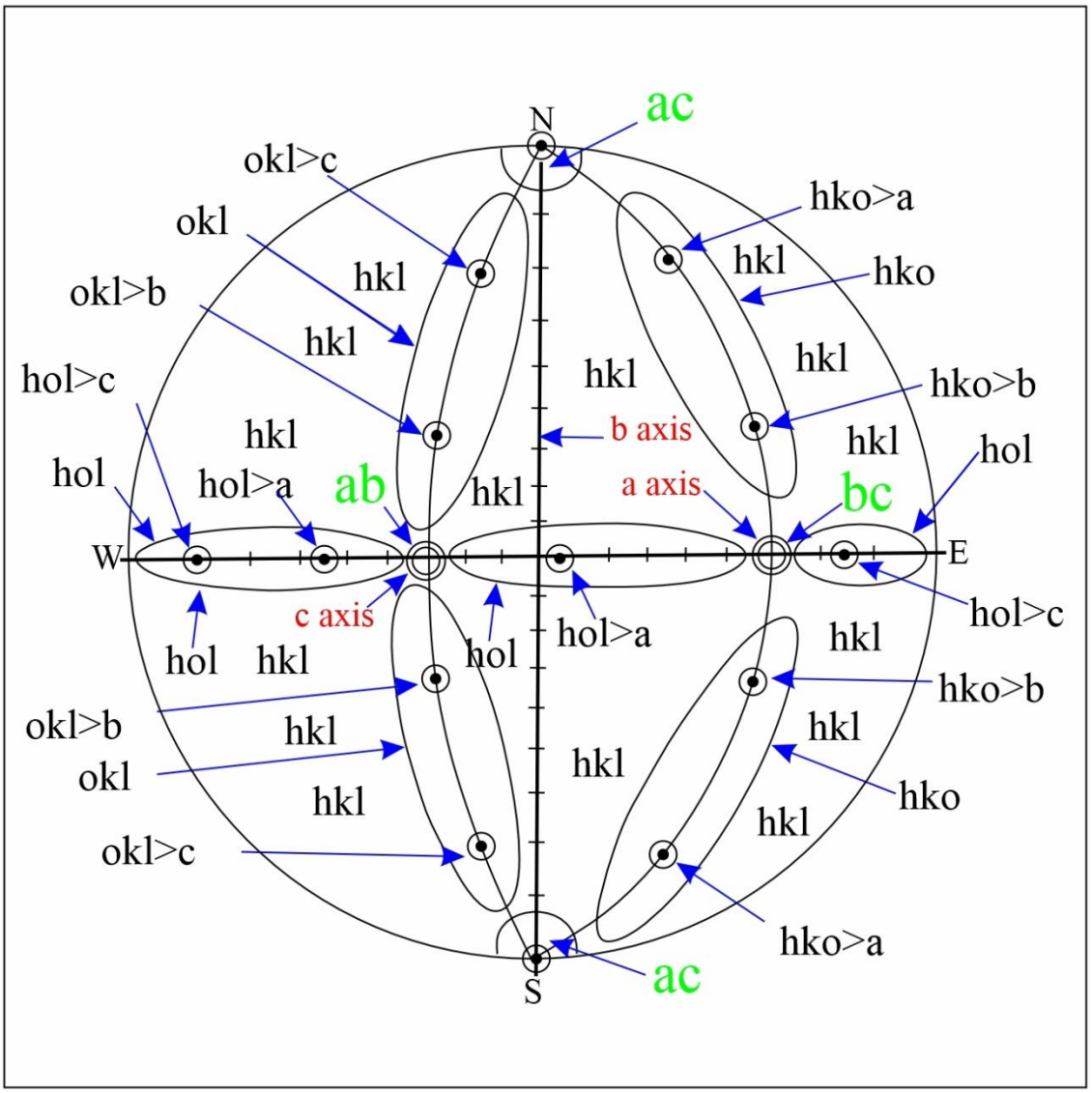

Figure 3.2: Joints analysis (after Hancock and Atiya, 1979)

1- ab joint set: The joint planes of this type are parallel to both (a and b) axes and perpendicular to the (c) axis, i.e. this set comprises all planes that parallel to the bedding plane and the bed strike. It is, generally, created by local unloading, not by tectonic processes (Hancock and Atiya, 1979). This joint plane was recorded in stations (5 and 13), (Plate 3.1).

Plate 3.1: ab joint set in station 13

2- (ac) joints set:

The planes of ac joints are parallel or sub-parallel to both (a and c) axes and perpendicular to the (b) axis, i.e. they are approximately normal to the fold hinge line. This set is recorded in stations (3, 4, 5, 7, 9, 10, 11, 13 and 14), (Plate 3.2).

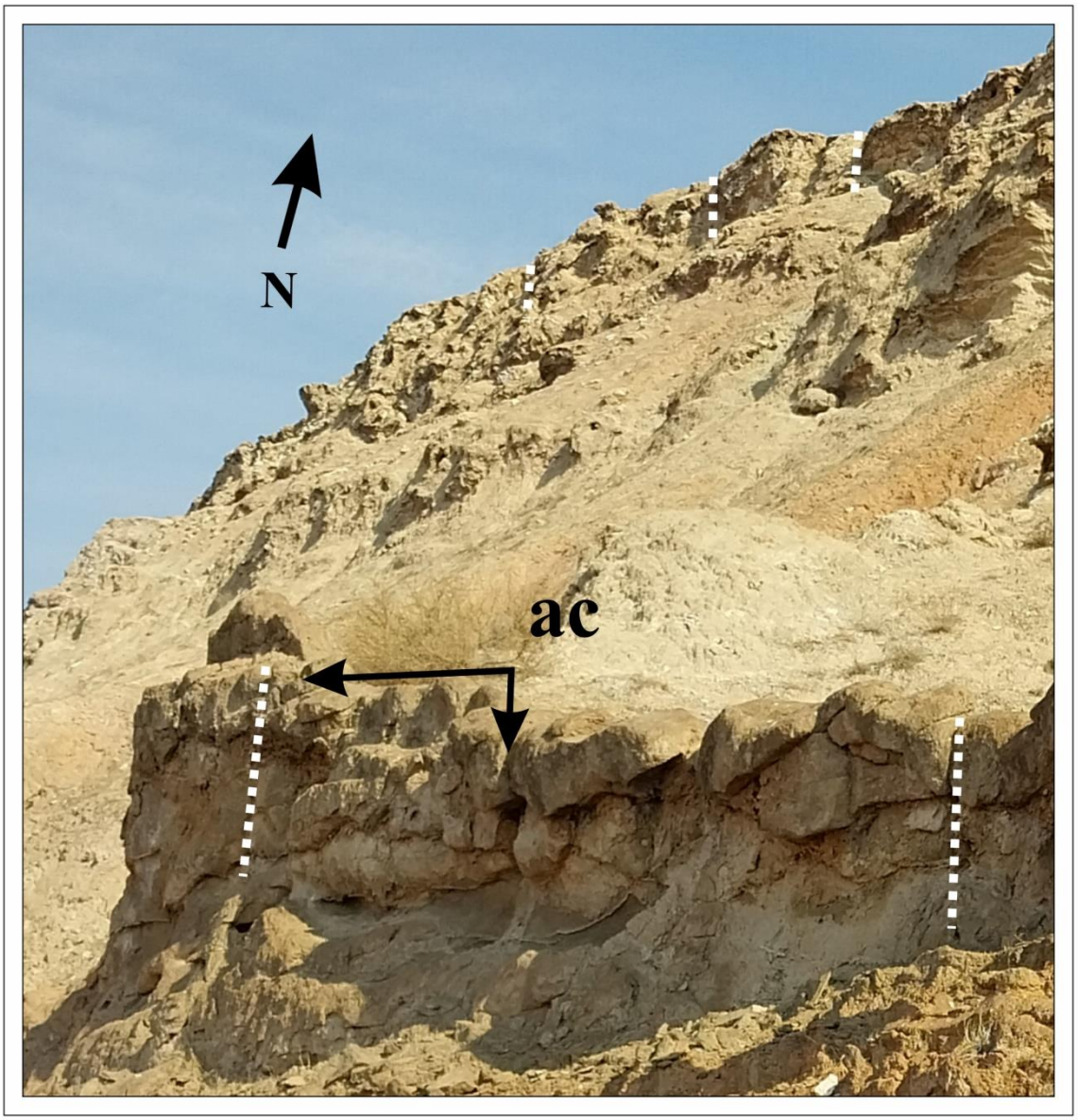

Plate 3.2: ac joint set in station 11

3- bc joints set:

The planes of ac joints are parallel to both (b and c) tectonic axes and perpendicular to the (a) axis,i.e. these planes are normal or sub-normal to the bedding plane dip direction, this type has been recorded in stations (1, 5, 9, 10, 13, 14, 15 and 17), (Plate 3.3).

Plate 3.3: bc joint set in station 17

4- hko joint system:

Joint planes of this system are parallel-subparallel to the (c) tectonic axis and intersect both (a and b) axes, these planes are approximately normal to the bedding plane. This system is subdivided into two subsystems.

A- hko > a subsystem:

Two conjugate joint sets form this subsystem, enclosing an acute angle about (a) axis and an obtuse angle about (b) axis. It was recorded in stations (2,8,12 and 16), plate. the maximum principal stress (σ1) is parallel to the (a) axis and the minimum principal stress (σ3) is parallel to the (b) axis, (Plate 3.4).

Plate 3.4: hko>a joint sestem in station 2

B- hko > b subsystem:

This subsystem can form by the intersection of two conjugate joints, these joint planes enclose an acute angle about (b) axis and an obtuse angle about (a) axis. (σ1) and (σ3) are parallel to (b and a) axes respectively. It is recorded in station No.11. (Plate 3.5).

Plate 3.5: hko>b joint sestem in station 11

5- okl joint system:

joint planes of this system are intersecting both (b and c) axes and parallel to (a) axis. Two subsystems are present under this system:

A- okl > b subsystem:

Two conjugate joint sets form this subsystem and enclose an acute angle about (b) axis and an obtuse angle about (c) axis. These planes are parallel-sub parallel to (a) axis; i.e. of the bedding planes. This subsystem dose not recorded in any one of the measured stations in the study area.

B- Okl > c subsystem:

The (c) axis bisects the acute angle which is enclosed by two conjugate intersected joints; while the (b) axis bisects the obtuse one. The maximum principal stress (σ1) is parallel to the (c) axis, whereas the minimum principal stress (σ3) is parallel to the (b) axis, this subsystem was recorded in stations (15) and (17), (Plate 3.6).

Plate 3.6: okl>c joint system in station 15

6- hkl joints:

Joint planes of this system intersect all tectonic axes;i.e. the planes of this system are oblique to the whole axes (a,b, and c), so there is no geometrical relation between the fold geometry and this system. It was recorded in stations (1,4,6 and 16), (Plate 3.7).

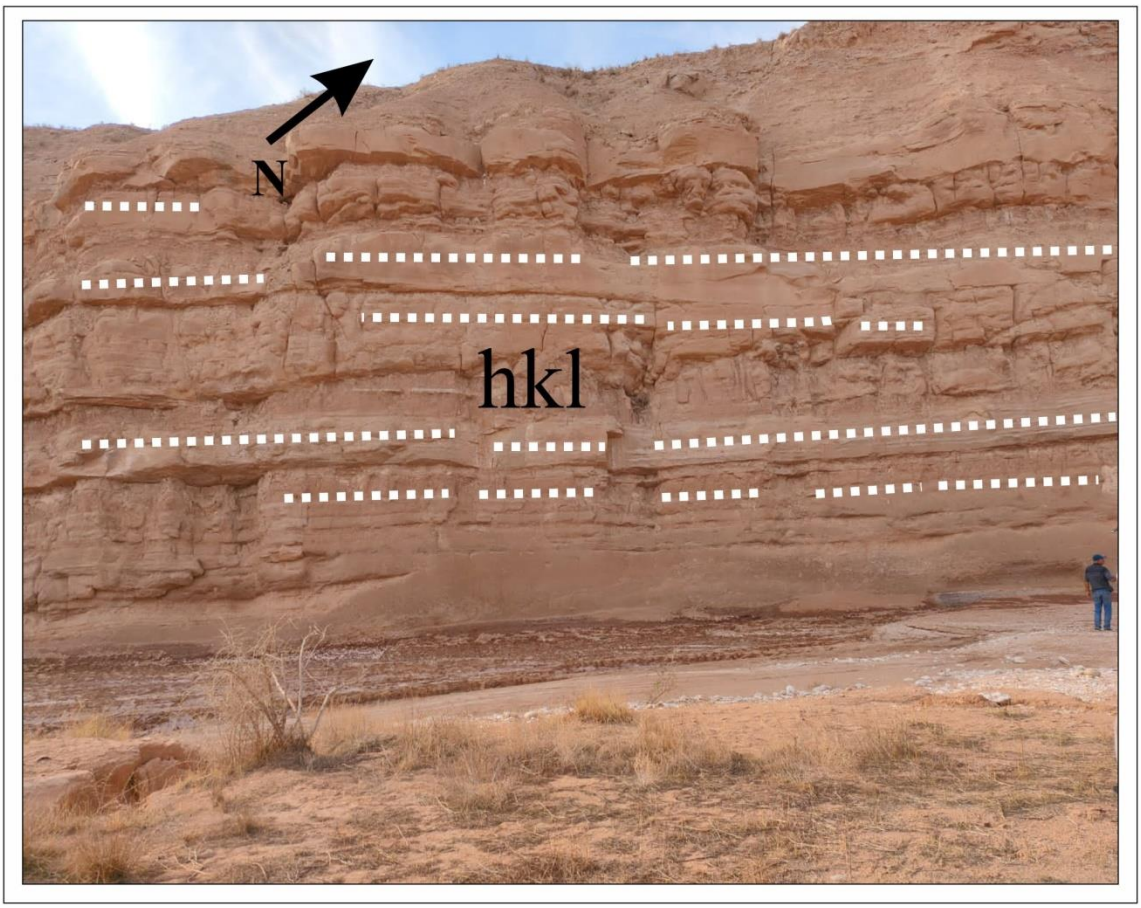

Plate 3.7: hkl joint sestem in station 15

3-3 Data Analysis:

The measurements of joints in the study area (Table 3.1) have been analyzed using stereographic techniques for each one, plotting was performed using (stereonet,v11) software, and they re-drawed by using (Coral Draw and Adobe Illustrator) softwares. The (ab) joint sets are distributed at a ratio of 7%, and the relatively dominant sets are (ac and bc) at percentages of 22% and 24% respectively. In order to the conjugate systems; hko > a present at a rate of 20%, hko > b 5%, and okl > c at a rate of 10%. (Figure 3.3). The maximum principal stress (σ1) was estimated from the stereogram of the conjugate systems, and two trajectories were found; the first orientation is NW-SE in the East and south parts of the study area, whereas it was NE-SW at the west stations, (Figure 3.4) illustrate the stereogram of the studied stations.

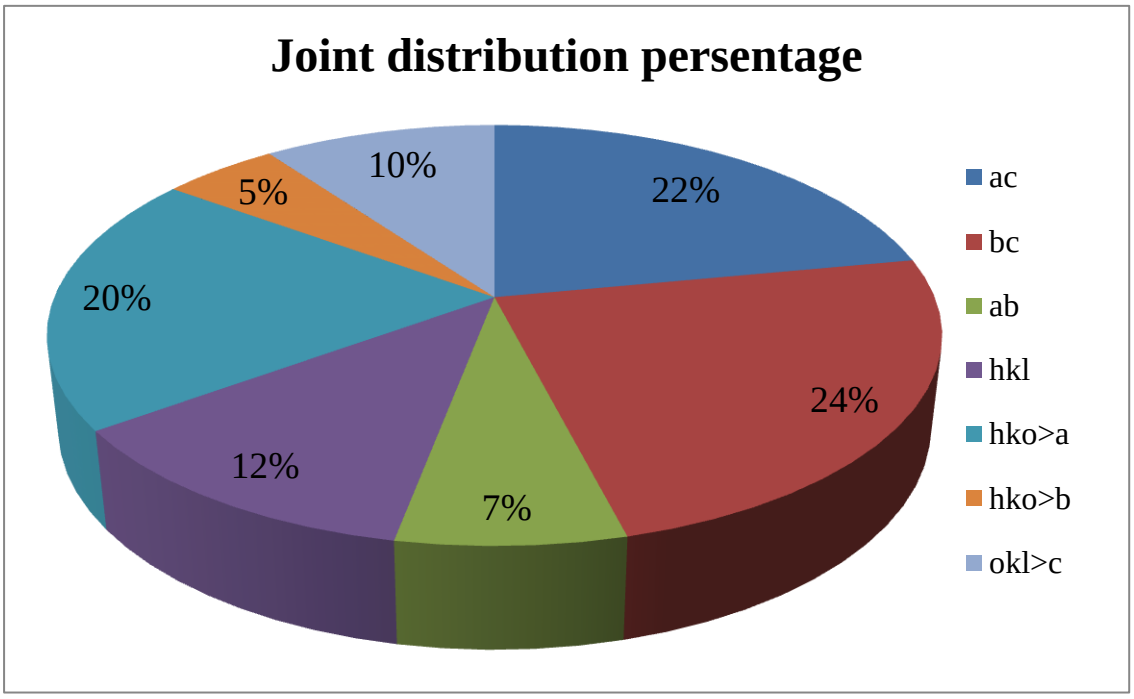

Figure 3.3: Distribution of joints in the study area

Table 3.1: Joints classification

Station No.	S1		S2		S3	
	Attitude	Type	Attitude	Type	Attitude	Type
St.1	060/78	hol	145/75	hkl	---	---
St.2	293/72	$hko_1>a$	181/74	$hko_2>a$	---	---
St.3	351/80	ac	082/47	hko	---	---
St.4	227/87	hkl	340/89	ac	---	---
St.5	344/55	bc	263/77	ac	173/42	ab
St.6	179/71	hkl_1	226/73	hkl_2	340/39	okl
St.7	011/80	ac	265/66	hko	---	---
St.8	013/47	$hko_1>a$	176/64	$hko_2>a$	---	---
St.9	358/86	ac	096/24	bc	---	---
St.10	168/86	ac	076/02	bc	---	---
St.11	193/84	ac	197/30	$hko_1>b$	005/44	$hko_2>b$
St.12	189/42	$hko_1>a$	012/55	$hko_2>a$	---	---
St.13	268/70	ab	090/24	bc	182/83	ac
St.14	357/75	ac	067/15	bc	---	---
St.15	012/62	$okl_1>c$	208/60	$okl_2>c$	113/71	bc
St.16	100/80	hkl	050/75	$hko_1>a$	170/80	$hko_2>a$
St.17	070/63	$okl_1>c$	163/75	bc	262/61	$okl_2>c$

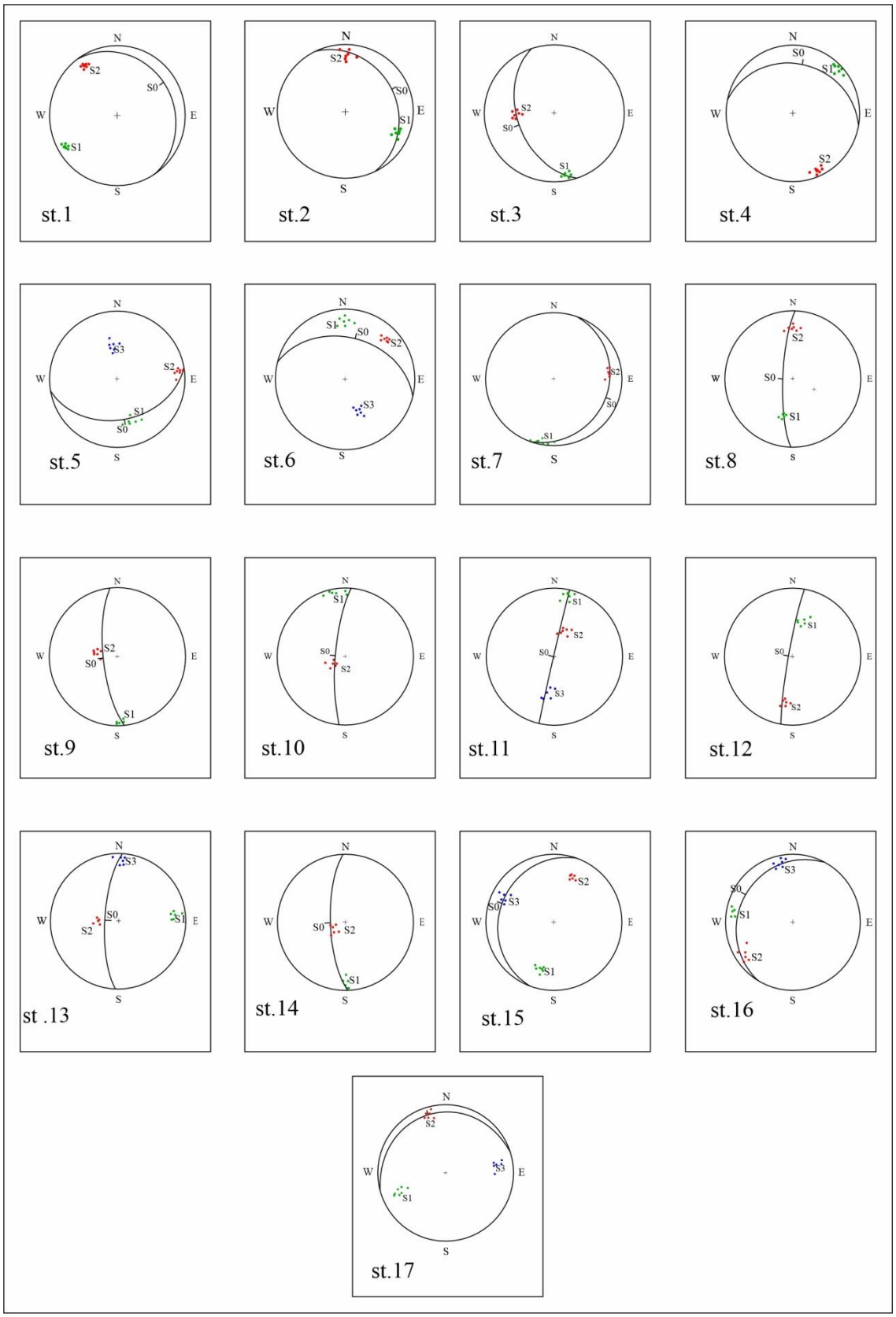

Figure 3.4: Lower-hemisphere, equal area stereographic projection of the studied station in the study area

Chapter Four
Slope Stability Analysis

4-1 Engineering geological description of rocks

The description of studied rock masses in the study area is based on a suggested report by the working party of the Engineering Group of the Geological Society / London (Anon,1972 and 1977). Eight properties are listed as prefixes and suffixes in Table (4.1).

Table 4.1: Engineering Geological Description of Rock (after Anon, 1972 & 1977).

Prefixes	**Suffixes**
Colour	Estimated mechanical strength of the rock material
Grain size	
Texture and structure	
Discontinuities within the mass	Estimate of mass permeability
Weathered state	
Alteration state	Other terms indicating special engineering characteristics
Minor lithologic characteristics	
ROCK NAME	

1- Rock color

The color of rocks can be expressed according to three parameters, hue which is the basic color of the rock, brilliance which is the intensity of color, and the value which is the lightness of color (Anon,1972), (Table 4.2).

Table 4.2: Description of rock colour (after Anon,1972).

VALUE	Brilliance	**HUE**
light	Pinkish	Pink
	Reddish	Red
	Yellowish	Yellow
	Brownish	Brown
	Olive	Olive
dark	Greenish	Green
	Bluish	Blue
	Grayish	White
		Grey
		Black

2- Grain size

The grain size ranges are used for rocks as well as for soil (Table 4.3).

Table 4.3: Rock grain size and descriptive terms (after Anon, 1972 & 1977).

Equivalent soil grade	**Term**	**Size of component particles**
Boulder & cobbles	Very coarse-grained	> 60 mm
Gravel	Coarse-grained	2 mm - 60mm
Sand	Medium grained	60 microns-2mm
Silt	Fine-grained	2 microns-60 microns (Grains larger than 10 microns visible using x 10 hand lens)
Clay	Very fine grained	< 2 microns

3- Texture and Fabric of rock mass

The texture term refers to the arrangement of the grains forming the rock mass, it reflects the rock fabric; the structure reflects the texture feature on a large scale (Anon, 1972). The description of sedimentary rock bedding spacing is illustrated in Table (4.4).

Table 4.4: Scales used to describe the bedding spacing of sedimentary rocks modified (after Anon, 1972 and 1977).

Term	**Spacing**
Very thickly bedded	>2m
Thickly bedded	600mm - 2m
Medium bedded	200mm - 600mm
Thinly bedded	60mm - 200mm
Very thinly bedded	20mm - 60mm
Laminated (sedimentary rocks)	6mm - 20mm
Thinly Laminated (sedimentary rocks)	> 6mm

4- Discontinuities within the Rock Mass

The most important parameters of discontinuities that affect slope stability are the orientation, persistence, and spacing between adjacent discontinuities (Wyllie & Mah, 2004). The spacing was described by (Anon,1972) and a modification of this description has been operated by (Anon,1977), (Table 4.5).

5- Weathering

The weathering decreases the compressive strength of the intact rocks (Wyllie & Mah, 2004). The weathering can be described relative to the distribution of the weathered materials (within the rock mass) and the effect on discontinuities (Anon,1977). Weathering grades are listed in (Table 4.6) based on (Anon, 1972).

Table 4.5: Discontinuity spacing (after Anon,1977).

Term	**Spacing**
Very widely spaced	> 2m
Widely spaced	600mm - 2m
Moderately widely spaced	200mm – 600mm
Closely spaced	60mm - 200mm
Very closely spaced	20mm - 60mm
Extremely closely spaced	< 20mm

6- Rock Name

The rock name may be preceded by suffixes including the compressive strength, spacing of discontinuities, grain size, and so on, it has to be written in capital letters (Anon,1972).

Table 4.6: Weathering grades (after Anon,1972 and Bejerman, 1994).

Term	**Grade symbol**	**Diagnostic features**
Fresh	W I	Parent rock shows no discoloration, loss of strength, or any other weathering effects.
Slightly weathered	W II	Rock may be slightly discolored, particularly adjacent to discontinuities, which may be open and will have a slightly discolored surface, the intact rock is not noticeably weaker than the fresh rock.
Moderately weathered	W III	Rock is discolored, discontinuities may be open, and will have discolored surfaces with alteration starting to penetrate inwards. intact rock is noticeably weaker, as determined in the field, than fresh rock.
Highly weathered	W IV	Rock is discolored, discontinuities may be open and have discolored surfaces, and the original fabric of the rock near the discontinuities may be altered. Alteration penetrates deeply inwards, but corestones are still present.
Completely weathered	W V	Rock is discolored and changed to soil but the original fabric is mainly preserved. There may be occasional small corestones. The properties of the soil depend in part on the nature of the parent rock.
Residual soil	W VI	Rock is discolored and completely changed to soil in which the original rock fabric is completely destroyed. There is a large change in volume.

7- Strength

The estimation of the mechanical strength of rock materials can, generally, require some laboratory or in-situ tests involving the determination of unconfined compression strength by the Schmidt hammer test or point load

test (Anon,1977). In this study, The description of rock mechanical strength is based on the compressive strength measured by the point load test which operated for rock samples of measured stations (Tables 4.7 and 4.8) show the scales and terms of rock strength based on (Anon, 1972: and Hawkins, 1986).

Table 4.7: Scales of rock strength (after Anon,1972 & 1977).

Term	**Compressive strength MN/mm^2 (MPa)**
Extremely strong	>200
Very strong	100-200
strong	50-100
Moderately strong	12.5-50
Moderately weak	5-12.5
weak	1.25-5
Very weak	<1.25

Table 4.8: Description of rock strength (after Hawkins,1986).

Term	**Unconfined compressive strength (Mpa)**	**Field Estimation of Hardness**
Extremely strong	>200	
Very strong	100-200	Rock samples can be brake by more than one hit of the hammer

strong	50-100	Rock sample can be brake by one hit of the hammer
Moderately strong	12.5-50	The sharp edge of the hammer leaves a 5mm impression on the rock body
Moderately Weak	5-12.5	Rock sample cannot be brake by hand into fragments
Weak	1.25-5	Rock is fragmented by stable hits by the sharp edge of a hammer
Very Weak	<1.25	Rock can be brake by hand

4-2 Classification of Rock Slopes

Many classifications were proposed for slope analysis; in this study, a classification of (Al–Saadi, 1981) has been performed. This classification depends on three parameters :

1- **Divergence angle (d)**: It is the angle between the strike of rock beds and the trend of the slope, three types of slopes could be recognized :
   - Parallel slope , when $0° \leq d \leq 20°$
   - Oblique lateral slope, when $20° < d \leq 70°$
   - Orthogonal slope , when $70° < d \leq 90°$

2- **Laterality:** It is defined by the emergence of the rock bed strike to the lateral side (left / right) of the observer facing the slope. accordingly, two types of slopes could be recognized :
   - Right emergent, when the strike of the beds' emergences to the right of the observer.

- Left emergent, when the strike of the beds' emergences to the left of the observer.

3- **Concordance**: It depends on the direction of the slope inclination concerning the dip direction of the rock beds. Two types of slopes could be recognized :
   - Concordant slope, when the rock beds dip toward the same general direction of the slope inclination.
   - Discordant slope, when the rock beds dipped in opposite to the general slope direction.

4-3 Point Load Test

The point load test is very useful for measuring the mechanical strength of rock masses (Anon, 1972). The samples require no machining and can tacked as rock cores and irregular lumps (Broch & Franklin,1972). The testing device is light and usually portable (Chaut & Wongt, 1996). In this study, the seventeen stations were tested for this purpose (Table 4.9).

Table 4.9: Point load test results

Station No.	Formation	Lithology of samples	I_s 50	σc (Mpa) = I_s50 * 24	Classification of rock strength
St1	Injana	Silty Sandstone	1.7	41	Moderately strong
St2	Injana	Clayey Sandstone	1.9	45.6	Moderately strong
St3	Injana	Sandstone	1.8	43.2	Moderately strong
St4	Fatha	Gypsum	1.9	45.6	Moderately strong
St5	Fatha	Gypsum	1.7	41	Moderately strong
St6	Fatha	Gypsum	1.6	38.4	Moderately strong
St7	Fatha	Dolomitic Limestone	9	216	Extremely strong
St8	Injana	Sandstone	5.25	126	Very strong
St9	Fatha	Dolomitic Limestone	11.5	276	Extremely strong
St10	Injana	Sandstone	2.4	57.6	Strong

St11	Injana	Sandstone	2.8	67	Strong
St12	Injana	Calcareous Sandstone	2.7	64.8	Strong
St13	Injana	Sandstone	2.6	62.4	Strong
St14	Injana	Sandstone	0.9	22	Moderately strong
St15	Injana	Clayey Sandstone	0.85	20.4	Moderately strong
St16	Injana	Clayey Sandstone	---	---	failed
St17	Mukdaiya	Sandstone	0.35	8.4	Moderately weak

4-4 The Terms and Symbols Used to Represent the Data

4-4-1 Symbols Used for Discontinuities and Slope Face

The attitude (dip/inclination direction and angle) are represented by two numbers; the Azimuth (direction) to the left, and the angle (amount in degrees) to the right.

4-4-2 The Terms Used for Failure Surfaces

Release surfaces aid in rock masses detaching and movement (Al-Saadi, 1991), these surfaces are used and classified according to their position concerning the detached blocks. The following classification is according to (Al-Saadi, 1991):

1- Back Release surfaces (B.R.S).

2- Lateral Release surfaces (L.R.S).

3- Composite Back Release surfaces (C.B.R.S).

4- Upper Release surfaces (U.R.S).

5- Basal surfaces (B.S).

4-4-3 The Symbols Used in the Stereographic Projection

The symbols that are used to represent data in the stereographic projection were modified after (Al-Saadi,1991), (Tables 4.10 and 4.11).

Table 4.10: Symbols used to represent the data in stereographic projection (modified after Al-Saadi,1991)

Symbol	Description
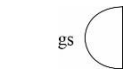	Cyclographic trace (great circle) of a general slope
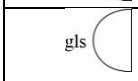	Cyclographic trace of a lateral slope
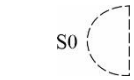	Cyclographic trace of the mean orientation of the bedding plane (S0)
	Cyclographic trace of a vertical slope
	Photo capture direction

Table 4.11: Symbols used to represent the failure types, used in stereographic projection

Symbol		**Failure Mode**
Present	**Potential**	
		Rockfall
		Toppling
		Rolling
		Sliding

4-5 Slope stability analysis in the study area

- **Station 1**

This station lies at the north bank of shurshirin valley, at latitude (33° 23′ 44″ N) and longitude (45° 57′ 07″ E), This station is located at the SW limb of the Himreen anticline, The Injana Formation beds are exposed and overlain by Alluvial fan sediments. The slope is discordant, oblique lateral (d=30°), right emergent slope, it inclined at (178/85), and the average height is 10.2m.

The rock properties are light brown, fine to medium grained, moderately spaced, moderately weathered, silty SANDSTONE.

The bedding plane dipping at (055/18) and segmented by two sets of joints (Plate 4.2) and (Figure 4.2). S1 (hol) 060/78, the spacing is (35cm) and it persists for (45cm). S2 (hkl) 145/75, the spacing is (45cm) and it persists for (30cm) some joints are closed, whereas others are in the range of (2mm-3cm), all opened joints are empty or filled by sandy and clayey materials.

Failure mode: The main failure type has occurred in the alluvial fan sediments is toppling, whereas rock fall is the main type of the Injana Formation beds where S1 acts as a (LRS) and S2 acts as (BRS), The potential failure mode for the Alluvial fan sediments is toppling.

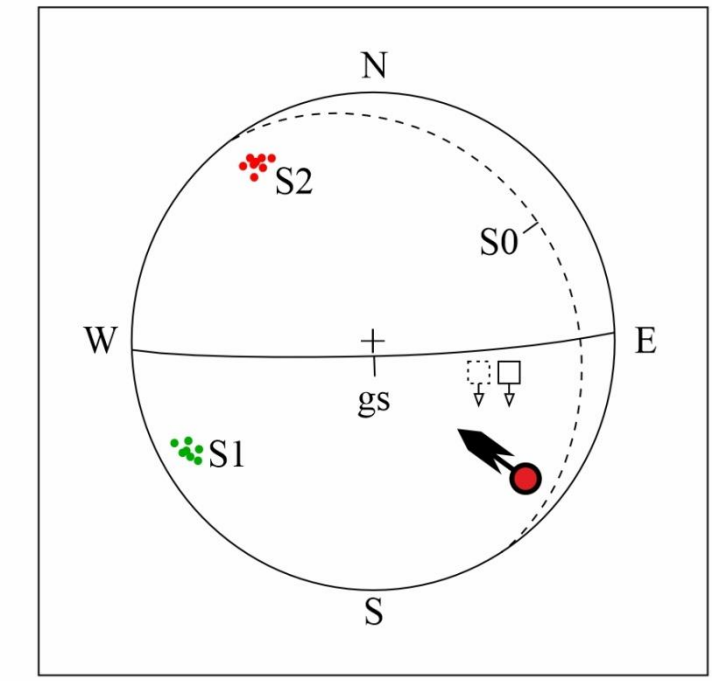

Figure 4.1: Lower hemisphere, equal area stereographic projection of station 1

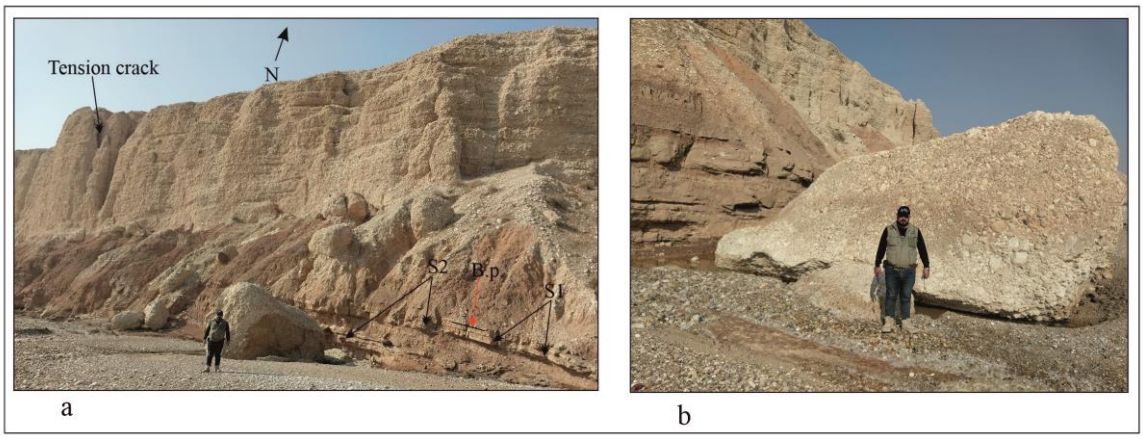

Plate 4.1: Station1, a) general view. b) detached block

- **Station 2**

This station lies at the north bank of shushirin valley within the SW limb of Himreen anticline at the latitude of (33° 24′ 10″ N) and longitude of (45° 57′ 19″ E). The Injana Formation beds are exposed in this station overlain by alluvial fan sediments. The main slope is discordant, oblique lateral (d=28°), right emergent slope inclining at (171/90). While the lateral slope is concordant, parallel (d=20°), left emergent slope inclines at (084/36). The average height is (9m).

The rock properties are light brown, fine grained, widely spaced, moderately weathered, clayey SANDSTONE.

The bedding plane is dipping at (064/25) segmented by two sets of joints (Plate 4.2) and (Figure 4.3). S1 (hko_1>a) 293/72, the spacing is (60cm) and it persists for range (0.8-1m). S2 (hko_2>a) 181/74, the spacing is (80cm) and it persists for range (o.55-0.9m). slightly of joints are closed, the dominants are opened in range (3mm-3cm), all opened joints are empty or filled by clayey and sandy materials.

Failure mode: The main failures that occurred along the main slope are rock fall and toppling, while the failure that occurred along the lateral slope is rock fall only. The potential failure in this station at the main slope is rock fall and toppling, while the possible failure at the lateral slope is rock fall and wedge sliding in case of removing the slope toe by weathering or by human

activity. In this station, S1 act as (LRS), S2 (BRS) and the bedding plane act as (BS).

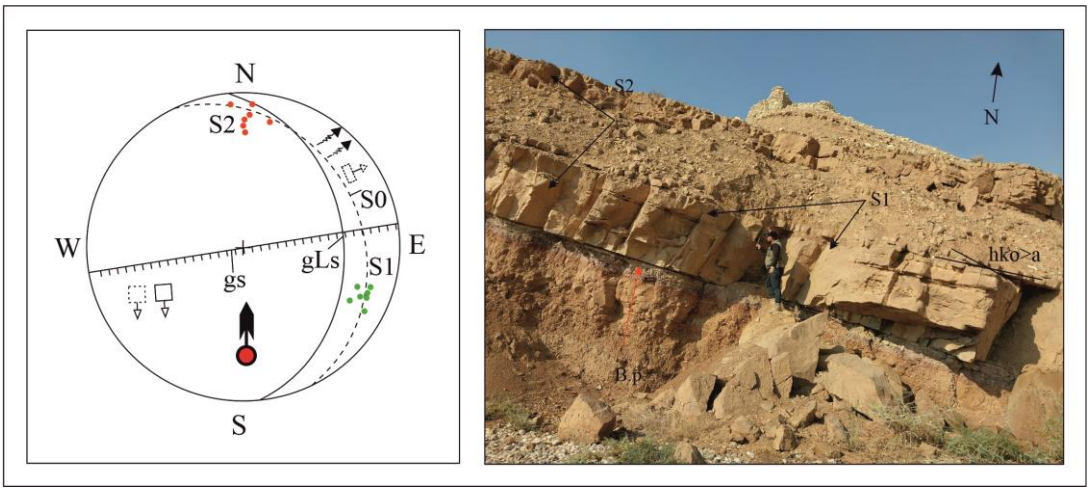

Figure 4.2: Lower hemisphere, equal area stereographic projection of station 2

Plate 4.2: General view of station 2

- **Station 3**

This station lies at the south bank of Shurshirin Valley within the SW limb of the Himreen anticline at the coordinates of (33° 24′ 10″ N) and (45° 58′ 02″ E).

The Injana Formation beds are exposed and overlain by Alluvial fan sediments. The slope is discordant, oblique lateral (d=50°), left emergent inclining at (016/78). The height is (9m). The rock properties are brownish grey, medium grained, moderately widely spaced, moderately weathered SANDSTONE.

The bedding plane is dipping at (251/46) segmented by two sets of joints (Figure 4.4) and (Plate 4.3). S1 (ac) 351/80, the spacing is (35-60cm) and persists at the range of (0.35-50cm). S2 (hko) 082/47, the spacing is (40-50cm) and persists at the range of (40-60cm). The aperture ranges from (2mm-5cm), some joints are empty and others are filled by sandy and clayey materials.

Failure mode: The main failure that has occurred is rock fall, the potential failure that may occur in the future is rock fall in the Injana rock beds, while the failure that may occur in the alluvial fan sediments is toppling at the side

of the slope and rock fall along the slope face. S1 acts as (BRS), S2 (LRS) and the bedding plane acts as (BS).

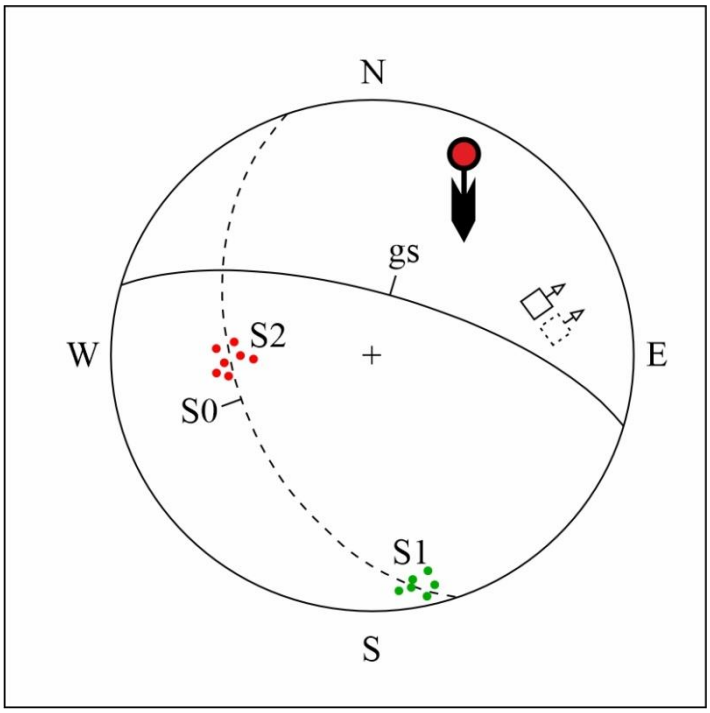

Figure 4.3: Lower hemisphere, equal area stereographic projection of station 3

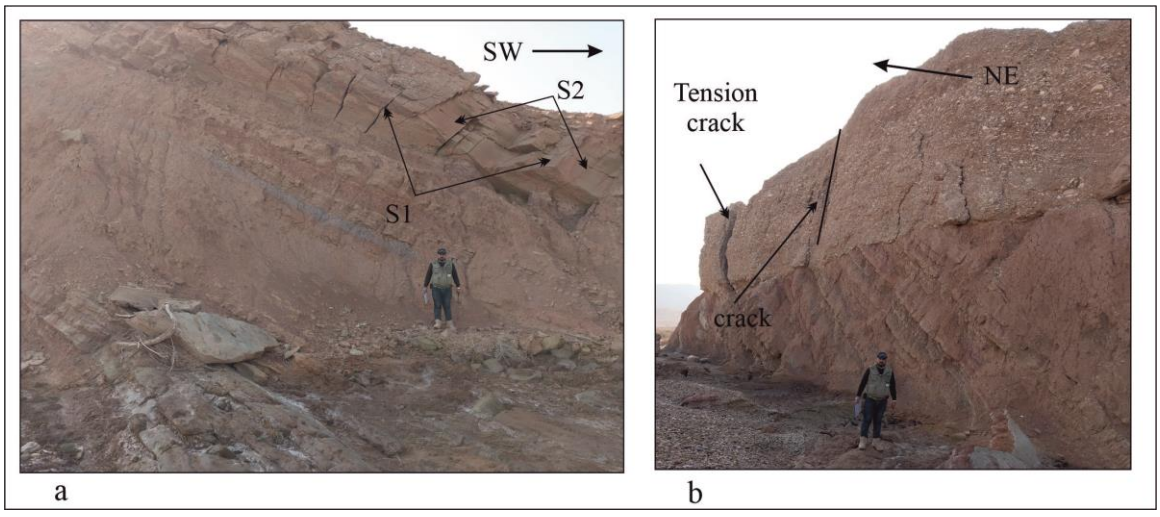

Plate 4.3: Station 3: a) general view. b) cracks of the alluvial fan sediments

- **Station 4**

This station lies at the north bank of shushirin valley within the SW limb of the Al-Faraee syncline the coordinates of (33° 24′ 10″ N) and (45° 58′ 43″ E). Fatha Formation rock beds are exposed in this station. The slope is discordant, oblique lateral (d=57°), right emergent slope inclining at (068/80). The height is (7m).

The rock properties are light brownish grey-whitish grey, very widely spaced, moderately weathered GYPSUM.

The bedding plane dipped at (011/28) and segmented by two sets of joints (Figure 4.5) and (Plate 4.4). S1 (hkl) 227/87, spacing is range from (200-300cm) and persists at the range of (110-120cm). S2 (ac) 340/89, the spacing is range from (100-130cm) and persists at the range of (190-220cm). some of the joints are closed and others have an aperture range from (2mm-5cm).

Failure mode: The main failure that has occurred as well as the potential failure in this station are toppling and rock fall, where S1 acts as (LRS) and S2 as (BRS).

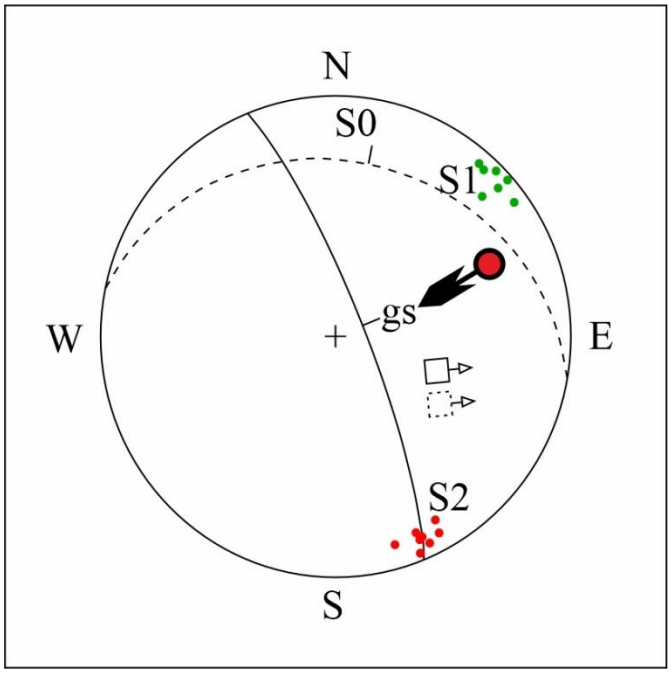

Figure 4.4: Lower hemisphere, equal area stereographic projection of station 4

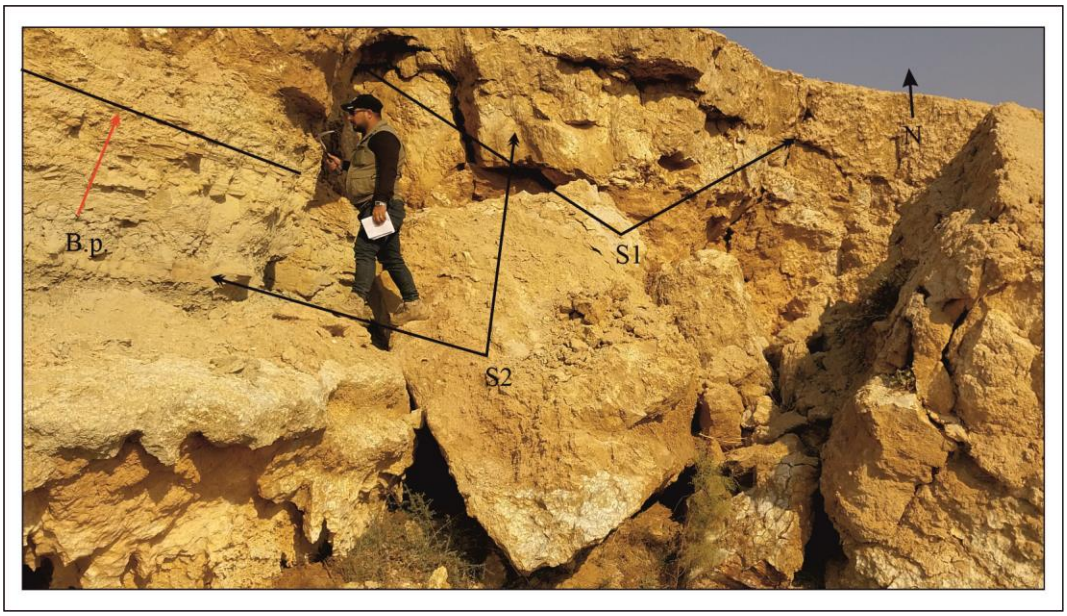

Plate 4.4: General view of station 4

- **Station 5**

This station lies on the south bank of shushirin valley within the eastern limb of Koolic 1 anticline at latitude (33° 24° 51° N) and longitude (45° 59° 51° E). Fatha Formation beds are exposed in this station. The slope is discordant, parallel (d=18°), left emergent slope inclining at (355/42). The height is about (30m).

The rock properties are light grey to whitish grey, widely spaced, highly weathered GYPSUM.

The bedding plane dipping at (170/40) and segmented by three sets (Figure 4.6) and (Plate 4.5). S1 (bc) 344/55, the spacing is (100cm) and persists up to (300cm). S2 (ac) 263/77, the spacing is (400cm) and persists up to (80cm). S3 (ab) 173/42, the spacing is (30cm) and persists up to (300cm). some of the joints are closed and others are opened with an aperture range from (3mm-5cm), the dominant opened joints are partially filled by sandy and gypseous materials.

Failure mode: The main failures have occurred as well as the potential failures are toppling and rock fall, where S1, S2, and S3 act as (BRS, LRS, and BS) respectively.

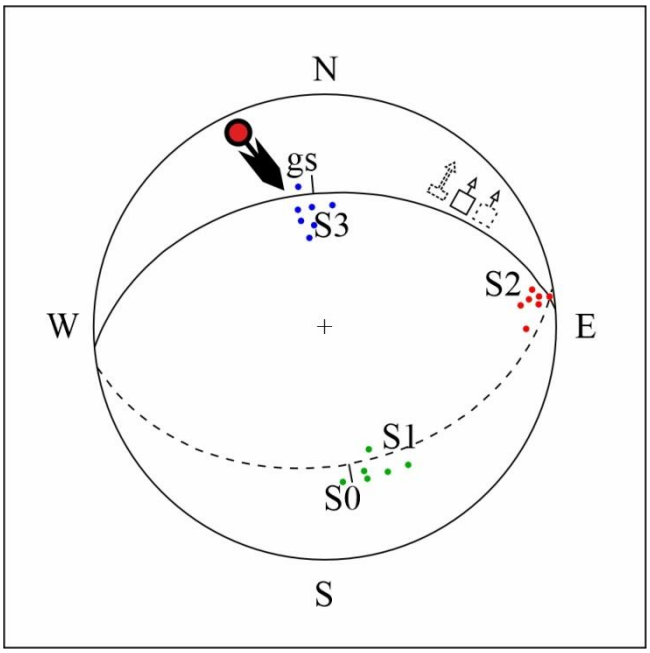

Figure 4.5: Lower hemisphere, equal area stereographic projection of station 5

Plate 4.5: general view of station 5

- **Station 6**

This station lies at the north bank of shushirin valley within the eastern limb of Koolic 1 anticline at the latitude of (33° 24′ 52″ N) and longitude of (45° 59′ 51″ E). The Fatha Formation beds are exposed in this outcrop. The slope is discordant, oblique lateral (d= 32), right emergent slope, inclining at (157/35). The height reaches (20m).

The rock properties are whitish grey, widely spaced, highly weathered GYPSUM.

The bedding plane is dipping at (014/40) segmented by three sets of joints (Figure 4.7) and (Plate 4.6). S1 (hkl_1) 179/71, the spacing is (75cm) and persists to (70cm). S2 (hkl_2) 226/73, the spacing is (73cm) and it persists up to (100cm). S3 (okl) 340/39, The spacing is (30cm) and it persists up to (25cm). The aperture ranges from (2mm to 5cm).

Failure mode: The main failures have occurred as well as the potential failures are toppling and rock fall, where S1, S2, and S3 act as (BRS, LRS, and BS) respectively.

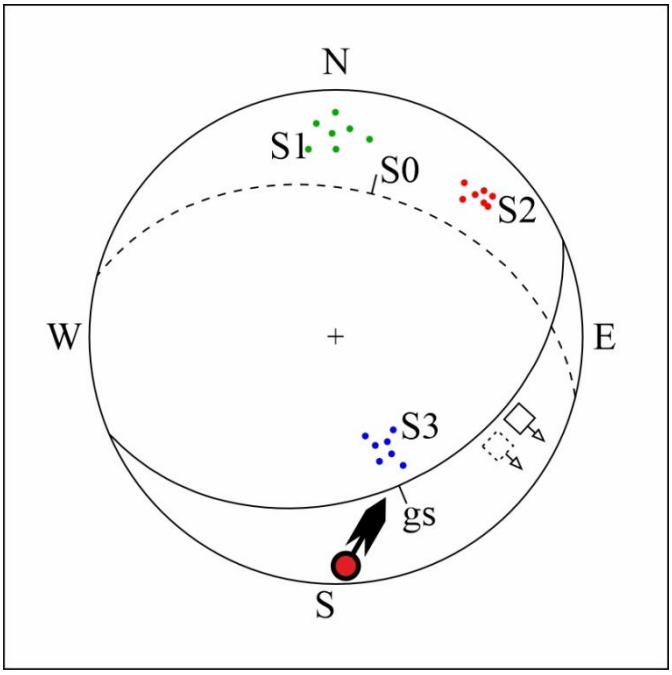

Figure 4.6: Lower hemisphere, equal area stereographic projection of station 6

Plate 4.6: General view of station 6

- **Station 7**

This station lies at the eastern limb of Himreen anticline at latitude of (33° 25° 53° N) and longitude of (45° 58° 38° E). The Fatha Formation beds are exposed in this station.

The slope is discordant, parallel (d=10°), right emergent slope, inclining at (290/40). The height is (20m).

The rock properties are brownish grey, moderately widely spaced, medium weathered, dolomitic LIMESTONE.

The bedding plane is dipping at (110/20) segmented by two sets of joints (Figure 4.8) and (Plate 4.7). S1 (ac) 011/80, the spacing is (30cm) and persists up to (50cm). S2 (hko) 265/66, the spacing is (45cm) and persists up to (30cm). Most of the joints are opened with an aperture range from (0.5-3cm).

Failure mode: The failure that has occurred in this station is toppling (at a small scale) and rock fall, the potential failures may occur is toppling and rock fall too, where S1 acts as (LRS) and S2 act as (BRS).

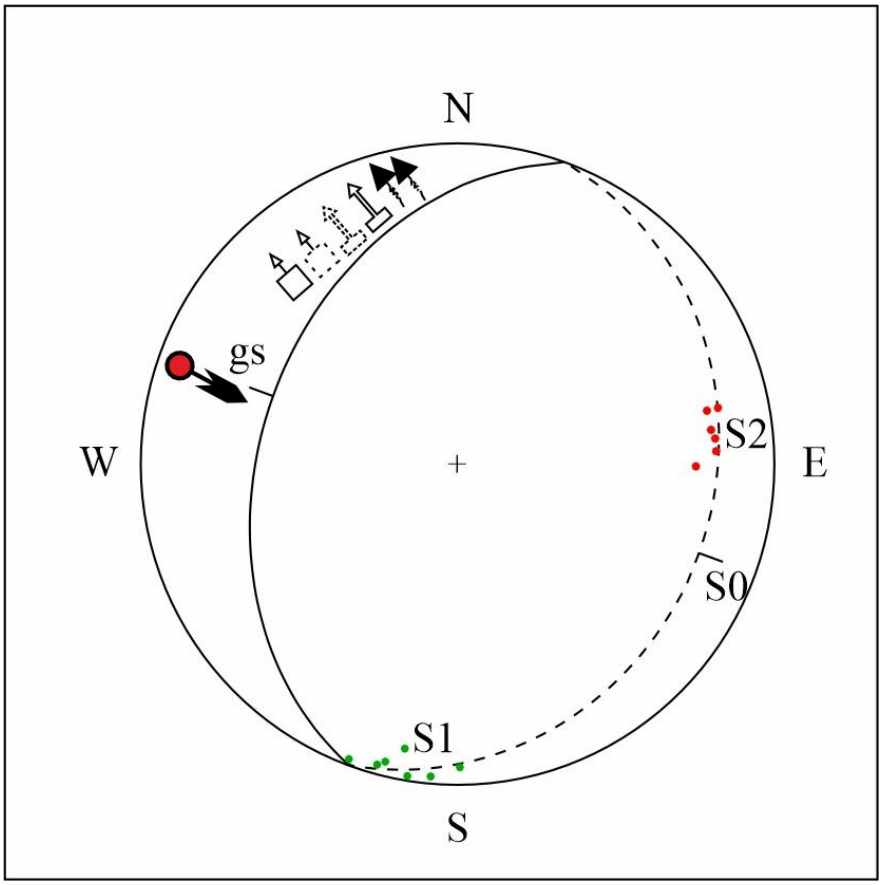

Figure 4.7: Lower hemisphere, equal area stereographic projection of station 7

Plate 4.7: Station 7. a) general view b) rock flow

- **Station 8**

This station lies at the western limb of the Himreen anticline at the coordinate latitude (33° 25° 56° N) and longitude (45° 58° 35° E). The Injana Formation beds are exposed in this station. The slope is concordant, parallel slope (d=2°) inclining at 272/70. The height is (13m).

The rock properties are brownish grey, fine grained, moderately widely spaced, highly weathered SANDSTONE.

The bedding plane is dipping at (272/78), segmented by two sets of joints (Figure 4.9) and (Plate 4.8). S1 (hko_1>a) 013/47, the spacing is (15cm) and it persists up to (35cm). S2 (hko_2>a) 176/64, the spacing is (35cm) and it persists up to (20cm). The aperture ranges from (2mm-3cm); opened joints are either empty or filled partially by sandy and clayey materials.

Failure mode: both existing and potential rock failure is rock fall, where S1&S2 acts as (LRS) and (BRS) while the bedding plane acts as (BS).

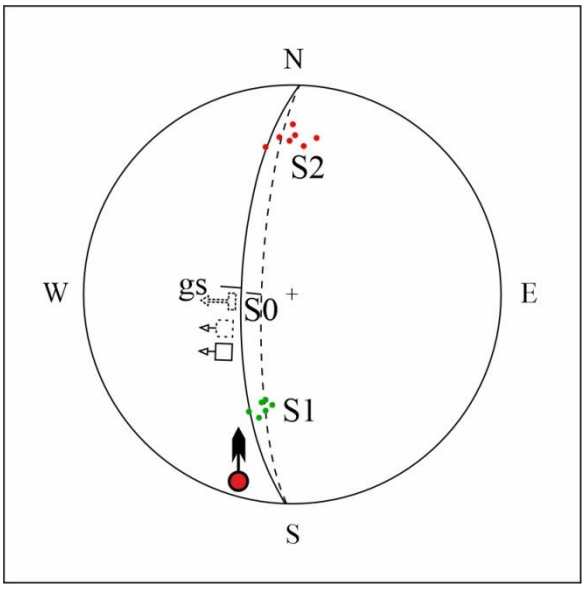

Figure 4.8: Lower hemisphere, equal area stereographic projection of station 8

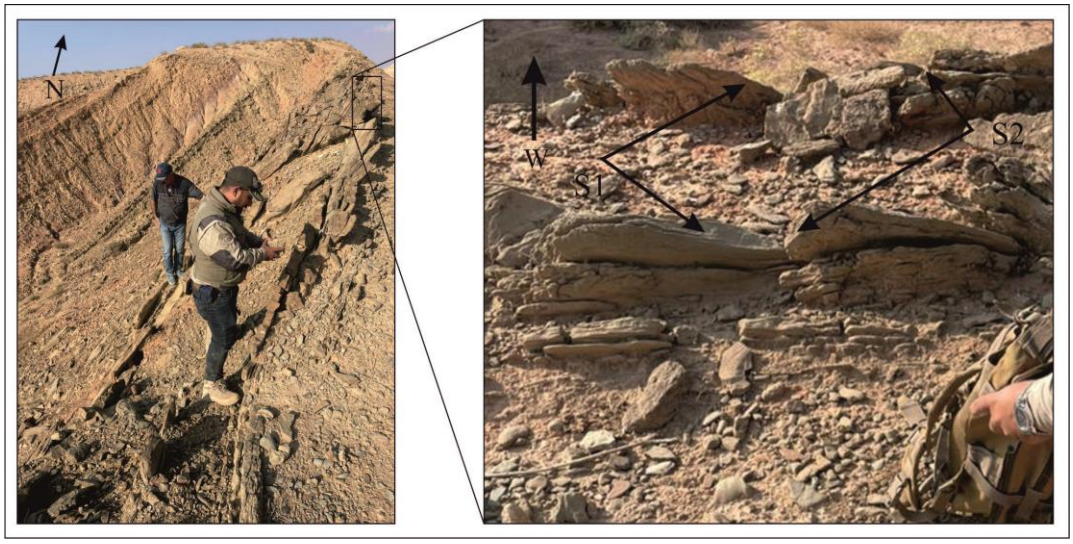

Plate 4.8: General view of station 8

- **Station 9**

This station lies at the western limb of the Himreen anticline. At the coordinate of (33° 26° 15° N) and (45° 58° 39° E). The Fatha Formation beds are exposed in this station. The slope is concordant, oblique lateral (d=41°), right emergent slope, inclining at (305/ 45). The height is (15m).

The rock properties are light grey, medium to coarse crystalline, moderately widely spaced, medium weathered, dolomitic LIMESTONE.

The bedding plane is dipping at (264/73) segmented by two sets of joints (Figure 4.10) and (Plate 4.9). S1 (ac) 358/86, the spacing is (80cm) and it persists up to (35cm). S2 (bc) 096/24, the spacing is (30cm) and it persists up to (80cm). The aperture ranges from (2mm-5cm).

Failure mode: The failure that occurred as well as the potential failure in this station is rockfall, where S1 acts as (LRS) and S2 acts as (BRS).

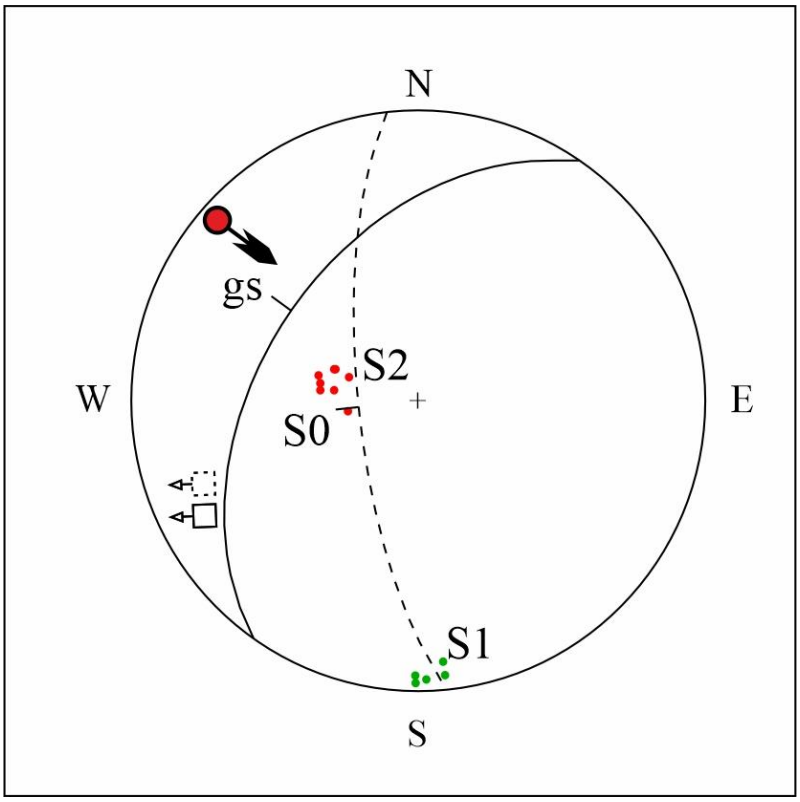

Figure 4.9: Lower hemisphere, equal area stereographic projection of station 9

Plate 4.9: General view of station 9

- **Station 10**

This station lies at the western limb of the Himreen anticline at the latitude of (33° 26° 27° N) and longitude of (45° 58° 27° E). The Injana Formation beds are exposed in this station. The slope is discordant, oblique lateral (d=50°), left emergent slope, inclining at (100/86). The height is (6m).

The rock properties are grey, medium to coarse grained, very closely spaced, highly weathered SANDSTONE.

The bedding plane is dipping at (275/78) segmented by two sets of joints (Figure 4.11) and (Plate 4.10). S1 (ac) 168/86, the spacing is (20cm) and it persists up to (30cm). S2 (bc) 076/12, the spacing is (15cm) and it persists up to (20cm). The aperture ranges from (2mm-6cm).

Failure mode: The failure that occurred as well as the potential failure is rockfall, where S1 acts as (L.R.S) and S2 acts as (B.R.S).

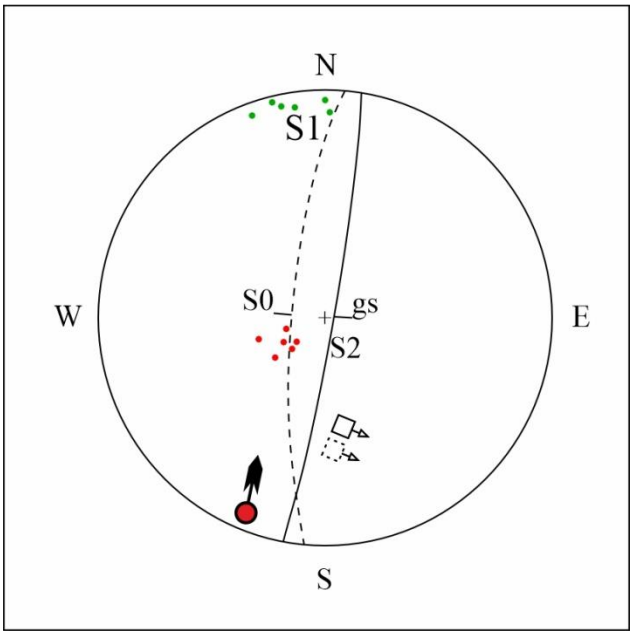

Figure 4.10: Lower hemisphere, equal area stereographic projection of station 10

Plate 4.10: General view of station 10

- **Station 11**

This station lies at the western limb of the Himreen anticline, at the latitude of (33° 27° 21° N) and longitude of (45° 58° 40° E). The Injana Formation beds are exposed in this station. The slope is concordant, parallel (d=3°), right emergent slope, inclining at (280/20). The height is (12m).

The rock properties are light grey, medium grained, moderately widely spaced, moderately weathered SANDSTONE.

The bedding plane is inclined at (283/89) segmented by three sets of joints (Figure 4.12) and (Plate 4.11). S1 (ac) 193/84, the spacing is (35cm) and it persists up to (40cm). S2 (hko_1>b) 197/30, the spacing is (40cm) and it persists up to (75cm). S3 (hko_2>b) 005/44, the spacing is (40cm) and it persists up to (75cm). The aperture ranges from (3mm-3cm).

Failure mode: The main failure that occurs as well as the potential failure is rockfall, where S1 acts as (LRS), S2 &S3 (BS), and the bedding plane acts as (BRS).

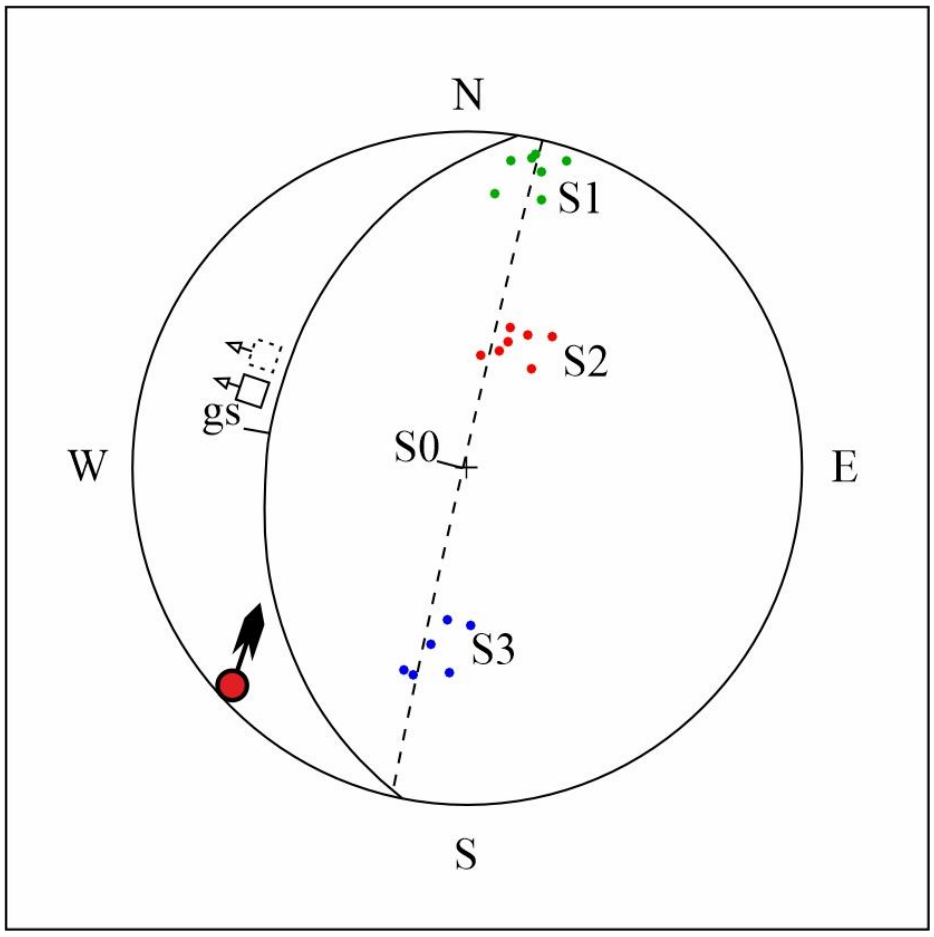

Figure 4.11: Lower hemisphere, equal area stereographic projection of station 11

Plate 4.11: General view of station 11

- **Station 12**

This station lies at the western limb of the Himreen anticline at the latitude of (33° 27° 48° N) and longitude of (45° 58° 48° E). The Injana Formation beds are exposed in this station. The slope is discordant, orthogonal (d=84°), right emergent slope, inclining at (196/45). The height is (12m).

The rock properties are brownish grey, medium to fine grained, very closely spaced, moderately weathered, calcareous SANDSTONE.

The bedding plane is dipping at (280/85) segmented by two sets of joints (Figure 4.13) and (Plate 4.12). S1 (hko_1>a) 189/42, the spacing is (20cm) and it persists up to (40cm). S2 (hko_2>a) 012/55, the spacing is (20cm) and it persists up to (30cm). The aperture ranges from (2mm-2cm).

Failure mode: The failures that occurred as well as the potential failure are toppling and rock fall, where S1, S2, and bedding plane act as (BRS, BS, and LRS) respectively.

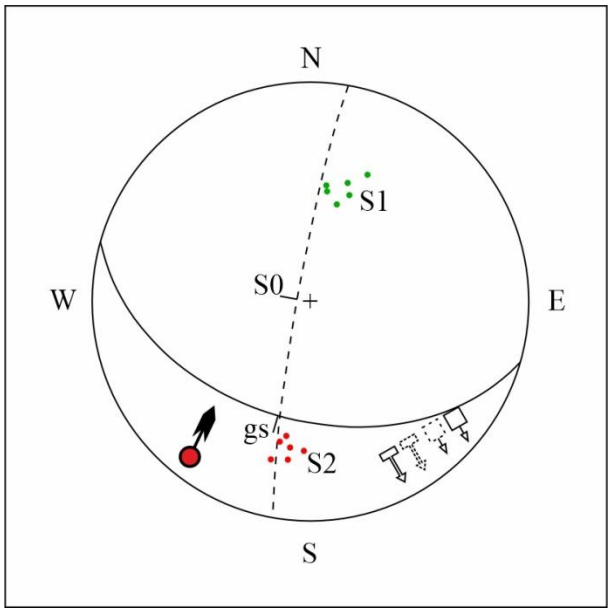

Figure 4.12: Lower hemisphere, equal area stereographic projection of station 12

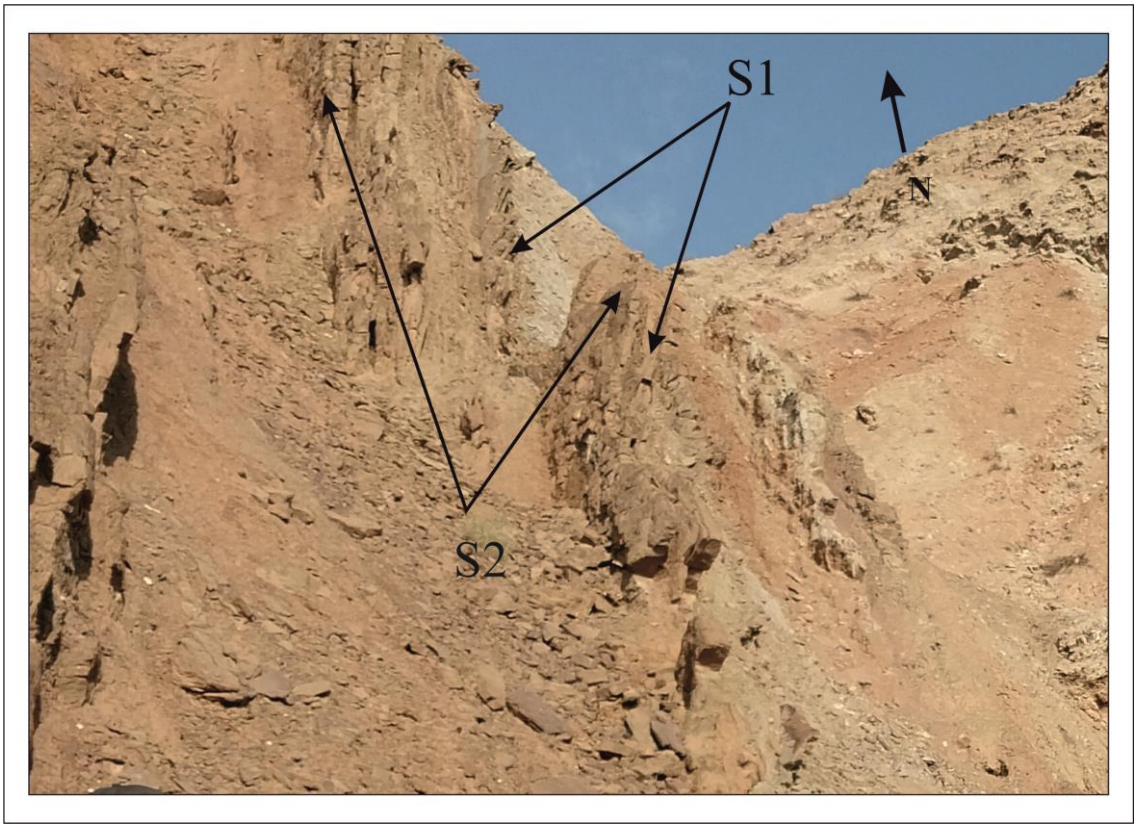

Plate 4.12: General view of station 12

- **Station 13**

This station lies at the western limb of the Himreen anticline at the latitude of (33° 27° 02° N) and longitude of (45° 58° 15° E). The Injana Formation beds are exposed in this station. The slope is discordant, oblique lateral (d=59°), right emergent slope, inclining at (105/35). The height is (35m).

The rock properties are greyish brown, medium grained, moderately widely to widely spaced, moderately weathered, SANDSTONE.

The bedding plane is dipping at (273/73) segmented by three sets of joints (Figure 4.14) and (Plate 4.13). S1(ab) 268/70, the spacing is (80cm) and it persists up to (100cm). S2 (bc) 090/24, the spacing is (30cm) and it persists up to (35cm). S3 (ac) 182/83, the spacing is (35cm) and it persists up to (30cm). The aperture ranges from (2mm-5cm).

Failure mode: The failures that occurred as well as the potential failure are toppling and rock fall, where S1 acts as (BRS). S2 acts as (BS), and S3 acts as (LRS).

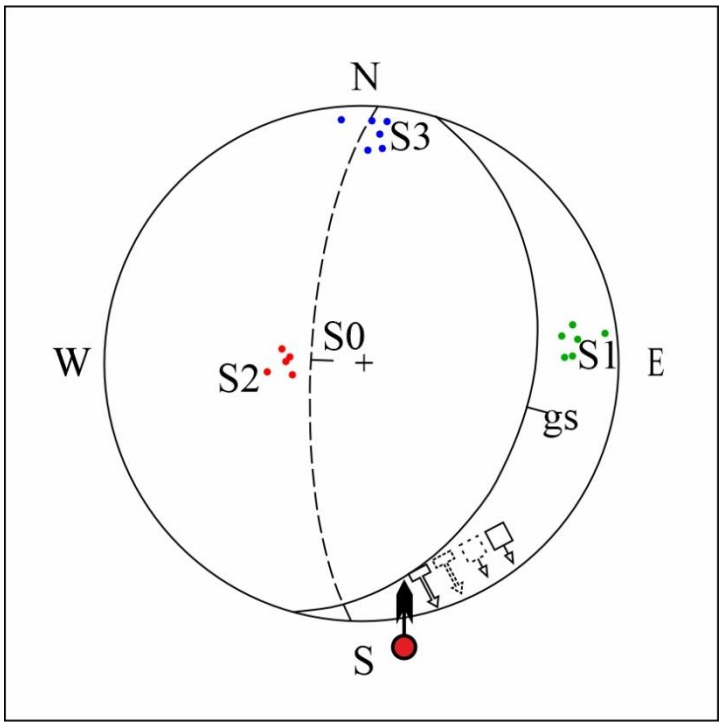

Figure 4.13: Lower hemisphere, equal area stereographic projection of station 13

Plate 4.13: General view of station 13

- **Station 14**

This station lies at the western limb of the Himreen anticline at the latitude of (33° 26° 59° N) and longitude of (45° 57° 20° E). The Injana Formation beds are exposed in this station. The slope is discordant, oblique lateral (d=68°), left emergent slope, inclining at (272/65). While the lateral

slope is discordant, orthogonal (d=80°), left emergent slope inclines at (010/63). The height is (20m).

The rock properties are grey-light grey, medium grained, moderately widely spaced, highly to moderately weathered, SANDSTONE.

The bedding plane is dipping at (268/72) segmented by two sets of joints (Figure 4.15) and (Plate 4.14). S1(ac) 357/75, the spacing is (40cm) and it persists up to (60cm). S2 (bc) 067/15, the spacing is (35cm) and it persists up to (35cm). The aperture ranges from (2mm-2cm).

Failure mode: The failures that occurred as well as the potential failure are toppling and rock fall, where S1 acts as (LRS). S2 acts as (BS).

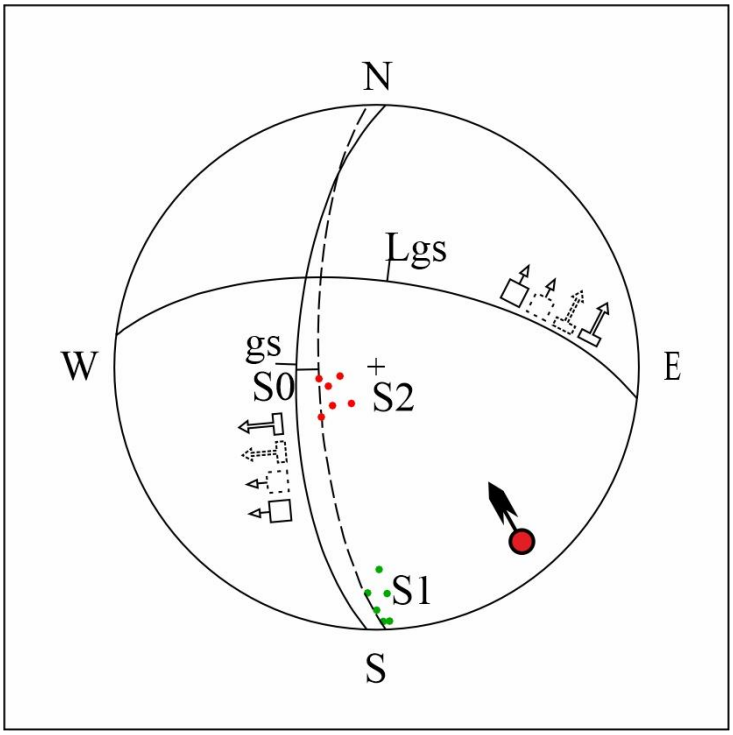

Figure 4.14: Lower hemisphere, equal area stereographic projection of station 14

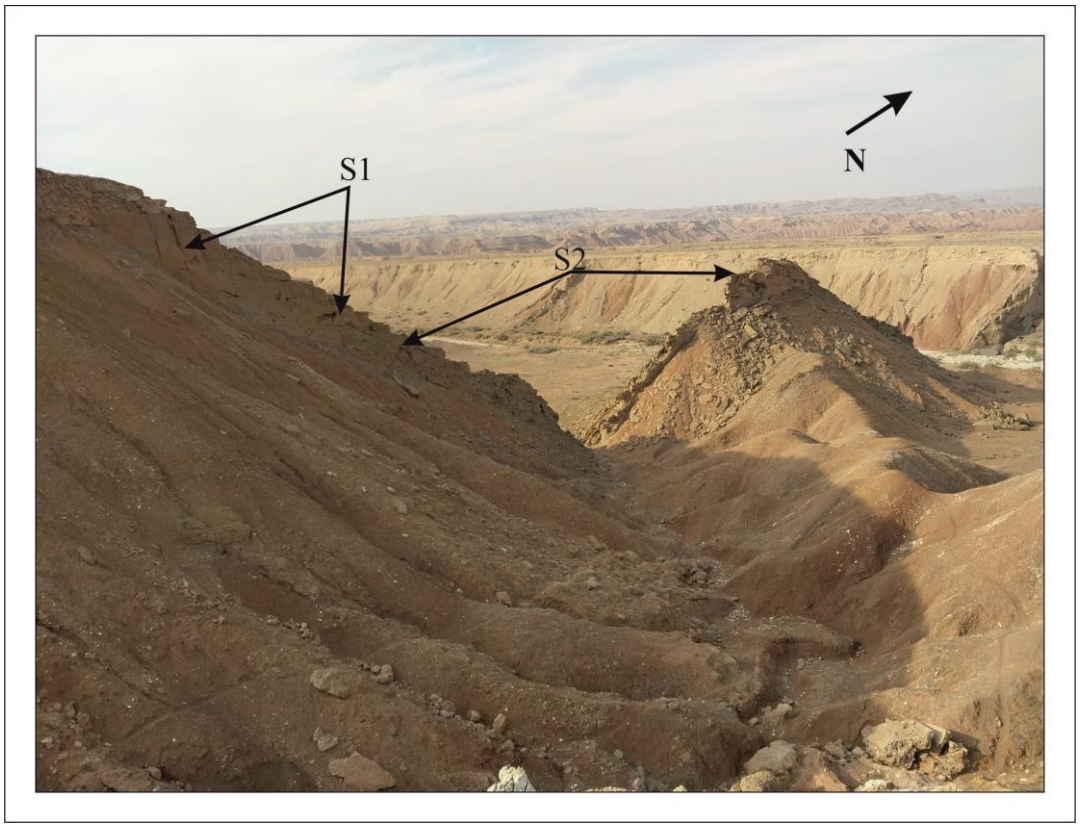

Plate 4.14: General view of station 14

- **Station 15**

This station lies at the western limb of the Himreen anticline at latitude of (33° 26° 25° N) and longitude of (45° 56° 57° E). The Injana Formation beds are exposed in this station. The slope is discordant, parallel (d=10°), left emergent slope, inclining at (110/85). The height is (35m).

The rock properties are greyish brown, fine grained, widely spaced moderately weathered, clayey SANDSTONE.

The bedding plane is dipping at (290/20) segmented by three sets of joints (Figure 4.16) and (Plate 4.15). S1 (okl_1>c) 012/62, the spacing is (80cm) and it persists up to (150cm). S2 (okl_2>c) 208/60, the spacing is (70cm) and it persists up to (160cm). S3 (bc) 113/71, the spacing is (50cm) and it persists up to (300cm). The aperture ranges from (3mm-5cm).

Failure mode: The failures that occurred as well as the potential failure are toppling and rock fall, where S1&S2 act as (LRS). S3 act as (BRS).

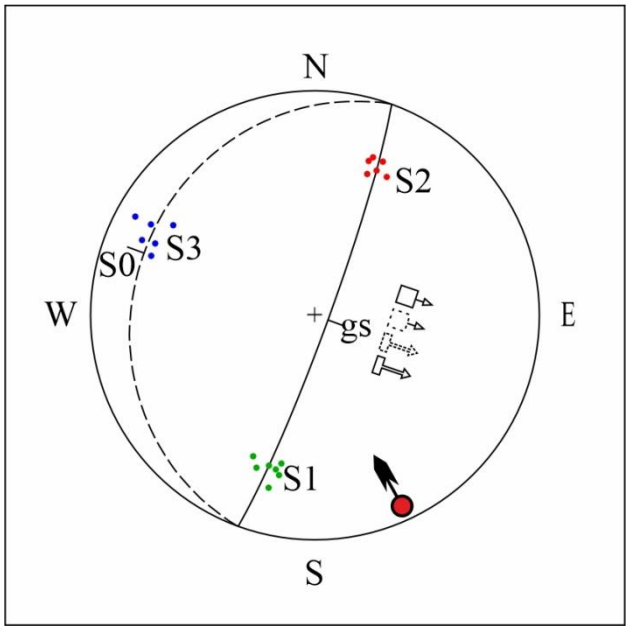

Figure 4.15: Lower hemisphere, equal area stereographic projection of station 15

Plate 4.15: General view of station 15

- **Station 16**

This station lies at the western limb of the Himreen anticline at latitude of (33° 25° 54° N) and longitude of (45° 56° 42° E). The Injana Formation beds are exposed in this station. The slope is discordant, parallel (d=8°), left emergent slope, inclining at (120/85). The height is (30m).

The rock properties are greyish brown, widely spaced moderately weathered, clayey SANDSTONE.

The bedding plane is dipping at (300/20) segmented by three sets of joints (Figure 4.17) and (Plate 4.16). S1 (hkl) 100/80, the spacing is (60cm) and it persists up to (350cm). S2 (hko_1>a) 050/75, the spacing is (60cm) and it persists up to (50cm). S3 (hko_2>a) 170/80, the spacing is (80cm) and it persists up to (70cm). The aperture ranges from (2mm-7cm).

Failure mode: The failures that occurred as well as the potential failure are toppling and rock fall, where S1 acts as (BRS). S2&S3 act as (LRS).

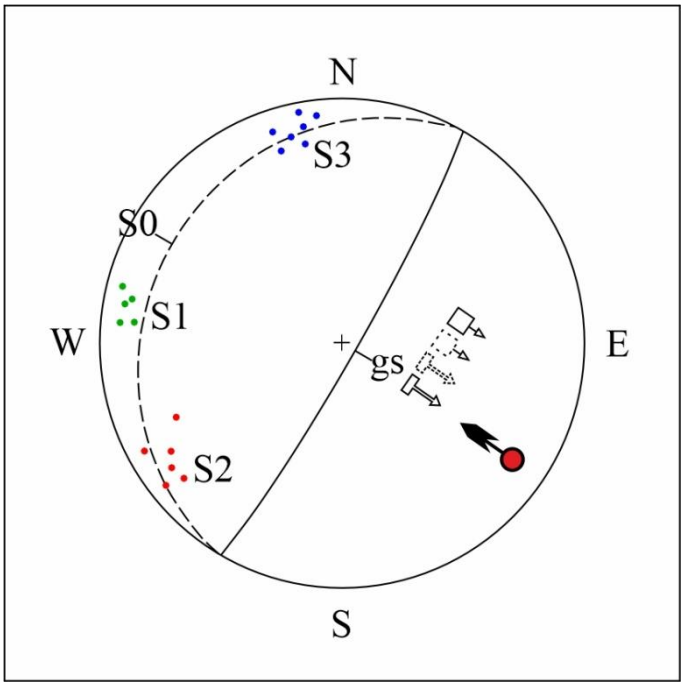

Figure 4.16: Lower hemisphere, equal area stereographic projection of station 16

Plate 4.16: General view of station 16

- **Station 17**

This station lies at the western limb of the Himreen anticline at latitude of (33° 25° 23° N) and longitude of (45° 56° 31° E). The Mukdaiya Formation beds are exposed in this station. The slope is discordant, parallel (d=17°), right emergent slope, inclining at (165/80). The height is (9m).

The rock properties are light brownish grey, fine to medium grained, moderately widely spaced, highly moderately weathered, clayey SANDSTONE.

The bedding plane is dipping at (343/13) segmented by three sets of joints (Figure 4.18) and (Plate 4.17). S1 (okl_1>c) 070/63, the spacing is (60cm) and it persists up to (70cm). S2 (bc) 163/75, the spacing is (20cm) and it persists up to (50cm). S3 (okl_2>c) 262/61, the spacing is (60cm) and it persists up to (65cm). The aperture ranges from (3mm-4cm).

Failure mode: The failures that occurred as well as the potential failure are toppling and rock fall, where S1&S3 acts as (LRS). S2 acts as (BRS).

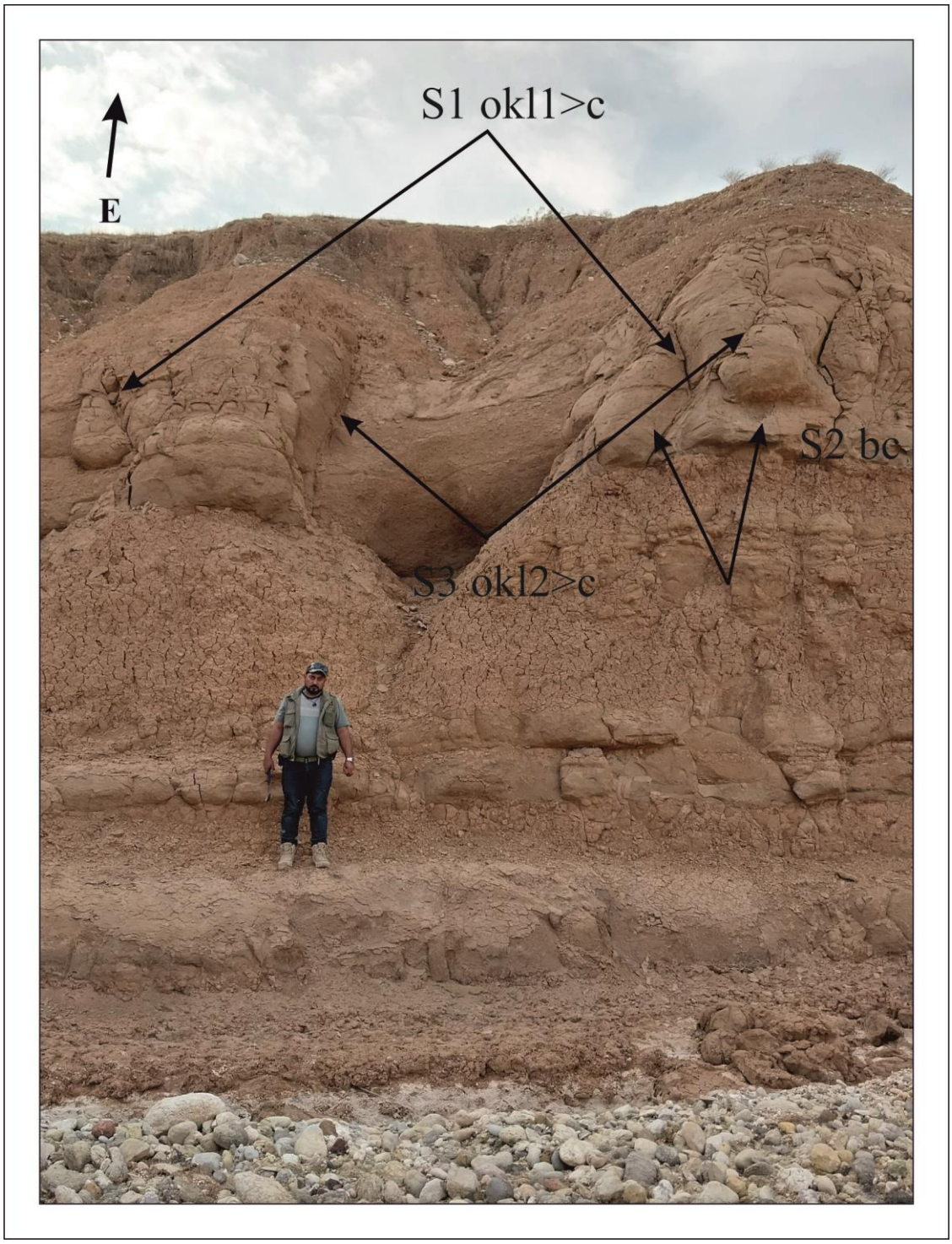

Plate 4.17: General view of station 17

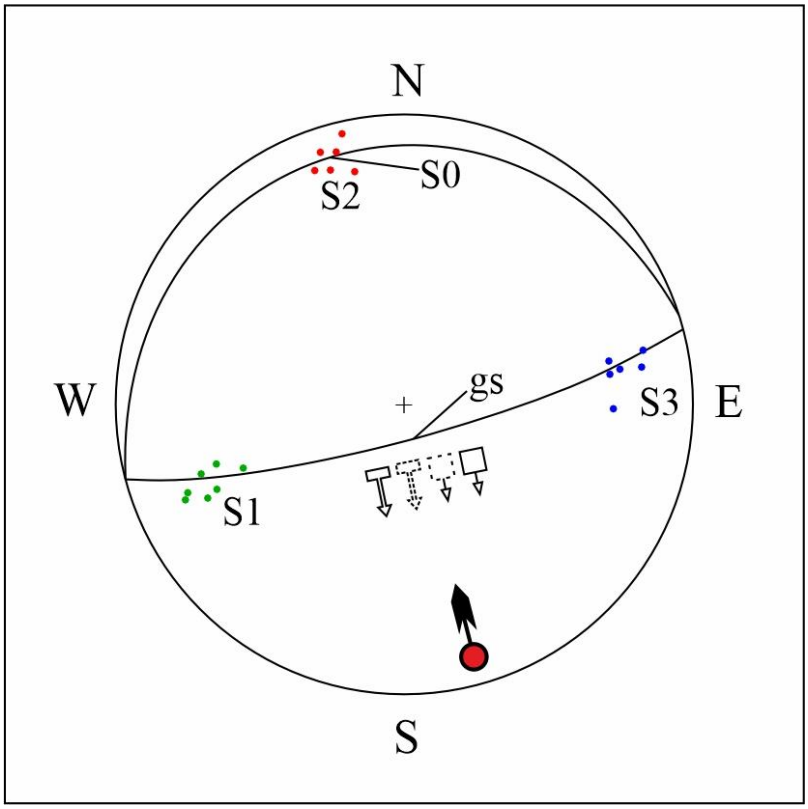

Figure 4.17: Lower hemisphere, equal area stereographic projection of station 17

4-6 Rock Failure Hazard Map

Landslide Possibility Index (Bejerman, 1994) was applied to assess the failure hazard grade and create a geological hazard map for the study area (Figure 4.19). The landslide possibility index (LPI) is based on ten parameters, the summation of these parameters is called the (LPI) value (Tables 4.12 and 4.13). All of these parameters were estimated for each slope of the seventeen stations (Table 4.15 and 4.16). the base map used to construct the failure hazard map was modified after (Mahmuod, *et. al.*, 2018). Only two stations were very highly hazardous (15 and 16), eleven stations (1, 2, 3, 4, 6, 7, 9, 10, 12, 13, and 14) have high hazard grades, while four stations (5, 8, 11 and 17) have moderate hazard grade.

Table 4.12: Parameters of (LPI) and their corresponding estimated values (modified after Bejerman, 1994)

Landslide Possilbiltiy Index					
Slope gradient estimation					
1-Slope Height	Estimat.	2-Slope Angle	Estimat.	3-Grade of Fracture	Estimat.
1-8m	1	<15°	0	Sound	0
9-15m	2	15-30	1	Moderately Frd.	1
16-25m	3	30-45	2	Highly Frad.	2
26-35m	4	45-60	3	Completely Frad.	3
>35m	5	>60	4		
4-Grade of Weathering	Estimat.	5-Gradient of Discontinuities	Estimat.	6-Spacing of Discontinuities	Estimat.
Fresh	0	<15°	0	>3m	0
Slightly	1	15-30	1	1-3m	1
Moderately	2	30-45	2	0.3-1m	2
Highly	3	45-60	3	0.05-0.3m	3
Completely	4	>60	4	<0.05m	4
Residual Soil	5				
7-Oreintation of The Discontinuities	Estimat.			8-Vegetation Cover	Estimat.
Favorable	0			Void <20%	0
Unfavorable	4			Scare 20-60%	1
				Abundent >60%	2
9-Water Infiltration	Estimat.			10-Previous Landslide	Estimat.
Inexist	0			Not Regestared	0
Scare	1			Registered (small volume)	1
Abundant:				Registered (high volume)	2
Perminant	2				
Sesonal	3				
1 + 2 + 3 + 4 + 5 + 6 + 7 + 8 + 9 + 10					
□ □ □ □ □ □ □ □ □ □ = □□					
I (small), (0-5)		III (low), (11-15)		V (high), (21-25)	
II (very low), (6-10)		IV (moderate), (16-20)		VI(very high), (>25)	
The LPI value is obtained by adding the estimation of attributes (1-10). The orientation of the discontinuities is Favorable, subtract the estimation of slope gradient.					

Table 4.13: Classification of hazard grades depending on (LPI) values (modified after Bejerman, 1994)

LPI Category	**LPI value**	**Hazard grade**
Nil	0	No Hazard
I	0-5	Small Hazard
II	6-10	Very Low Hazard
III	11-15	Low Hazard
IV	16-20	Moderate Hazard
V	21-25	High Hazard
VI	>25	Very High Hazard

The parameters of the LPI classification will be explained hereinafter:

1- Slope height: it is the vertical distance between the top of the slop face and the toe of the slope.
2- Slope angle: it is the inclination angle of the slope with the horizontal.
3- Grade of Fractures: this parameter has some categories which will be listed in (Table 4.14).

Tables 4.14: Categories of the grade of fracture (after Bejerman, 1994)

Term	Description	grade
Sound	The spacing between discontinuities is more than 3m	I
Moderately fractured	The spacing between discontinuities is between 1 and 3m	II
Highly fractured	The spacing between discontinuities is between 0.05 and 1m	III
Completely fractured	The spacing between discontinuities is less than 0.05m	IV

4- Grade of weathering: the categories of this parameter are listed in (Table 4.6).
5- The gradient of the discontinuities: it is the average of the dip amount of different sets of joints.
6- Spacing of discontinuities: it is the average distance between two adjacent discontinuities.
7- Orientation of the discontinuities: is the direction of the discontinuities corresponding to the slope face orientation.
8- Vegetation cover: it is the percentage of the slope surface that is covered by vegetation.
9- Water infiltration: it is the amount of water seepage into the rock mass, it is worth mentioning that the categories of this parameter correspond to the water accumulation near the studied site, the streams that contain water and the period of the rain precipitation. This parameter is very important in order of the study of slope stability because of the ability of the water to transport and sediment the clayey materials, the empty rupture discontinuity makes the rock mass containing this discontinuity more stable than the rock mass that contains clayey materials in between the surfaces of the discontinuities.
10- Previous landslide: the amount and the size of previously occurred rock failures.

Table 4.15: Classification of hazard grades for measured stations in the study area depending on (LPI) categories

Total No. of station	**No. of station**	**LPI Category**	**Hazard Category**
4	5, 8, 11 and 17	IV	Moderate
11	1, 2, 3, 4, 6, 7, 9, 10, 12, 13 and 14	V	High
2	15 and 16	VI	Very High

Table 4.16: Estimated parameters of LPI for each station in the study area

Station No.	Parameters										Total (LPI)
	One	Two	Three	Four	Five	Six	Seven	Eight	Nine	Ten	
1	2	4	2	2	4	2	4	0	3	2	25
2	2	4	2	2	4	2	4	0	3	1	24
3	2	4	2	2	4	2	4	0	3	1	24
4	1	4	1	2	4	1	4	0	3	2	22
5	4	2	1	3	3	1	4	0	3	2	23
6	3	2	2	3	4	2	4	0	3	1	24
7	3	2	2	2	4	2	4	0	3	1	23
8	2	4	1	3	3	2	0	0	3	1	19
9	2	3	2	2	3	2	4	0	3	1	22
10	1	4	2	3	3	3	4	0	3	1	24
11	2	1	2	2	3	2	4	0	3	1	20
12	2	2	2	2	3	3	4	0	3	1	22
13	4	2	2	2	3	2	4	0	3	2	24
14	3	4	2	2	3	2	4	0	3	1	24
15	4	4	2	2	4	2	4	0	3	2	27
16	4	4	2	2	4	2	4	0	3	1	26
17	2	4	2	2	4	2	0	0	3	1	20

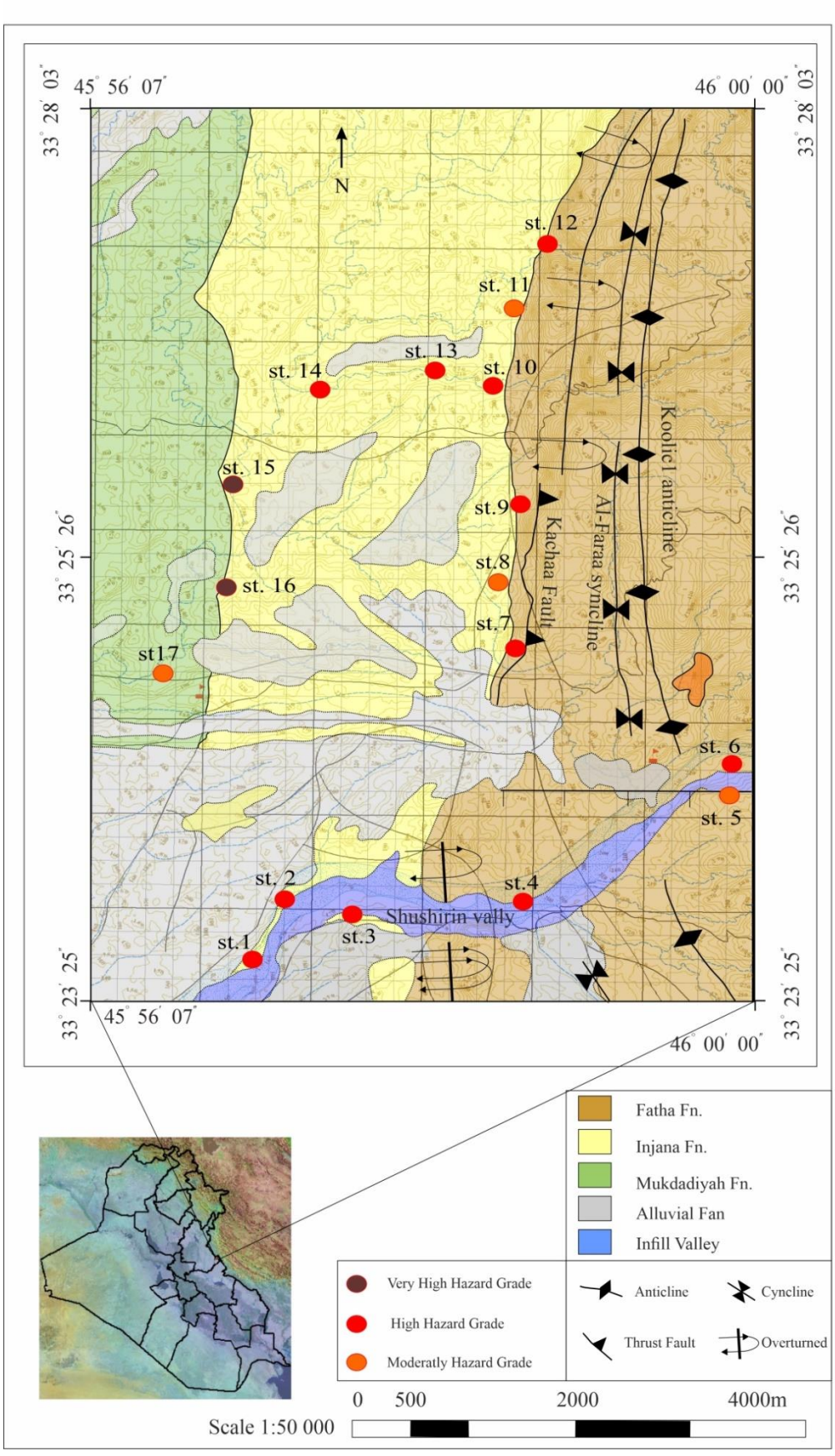

Figure 4.18: Geological hazard map of the study area

Chapter Five
Conclusions and Recommendations

5-1 Conclusions

This study can be concluded with the following explanations:

1- The dominant joint set was (bc), while the dominant conjugate join system was (hko>a).

2- The general direction of the paleo-tectonic movements was estimated by the estimation of the maximum principal stress (σ1), which indicates that the movement was in two trajectories, the first one is NW-SE at the eastern and southern parts of the study area, while the second orientation was NE-SW at the western parts.

3- The potential failure modes are toppling, rock fall, rolling, and sliding.

4- The vertical and semi-vertical discontinuities within the rock masses play an important role in rock failure (existing and potential failures), they act as lateral release surfaces or back release surfaces, while the horizontal discontinuities act as basal surfaces.

5- The water infiltration into the discontinuities within the rock masses plays an important role in slope stability by transporting and sedimentation of clayey materials between the discontinuities surfaces, these materials can act as lubricant materials and facilitate rock failures.

6- Failure hazard grade assessment indicated that the failure hazard ranges from moderately hazard to very highly hazardous.

7- A geological hazard map was constructed to illustrate the distribution of hazard categories in the study area.

5-2 Recommendations

1- Removing the unstable rock blocks that may fall or topple in the future to avoid their risks.

2- Installing warning signs to warn people passing the hazardous areas.

3- Study of seismic activity in and around the study area to determine its influences on slope stability.

4- The study area is tectonically and structurally complex, so it is important to perform many studies, about these subjects.

5- Installing warning signs near the area that contains mines.

References

Abramson, L. W., Lee, T. S., Sharma, S., and Boyce, G. M., (2002) Slope Stability and Stabilization Methods. John Wiley & Sons, Inc., New York. 701P.

Alavi, M., (2004) Regional stratigraphy of the Zagros Fold – Thrust Belt of Iran and its proforeland evolution. Amer. Jour. Sci., 304, p. 1–20.

Al-Hussainy, R. M. A., (2010) Slope Stability Study of Selected Sites From Tar Al – Sayyed Area (Karbala Governorate \ Middle of Iraq), Master Thesis, University of Baghdad, Unpubl., 120 p.

Ali, M. H., Hijab, S. R., and Aljassar, S. H., (1991) Engineering Geology. University of Mosul. 576p

Al-Mubarak, M.A. and Youkhanna, R.Y., (1976) Report on the regional geological mapping of Al-Fatha – Mosul Area. GEOSURV, int. rep. no. 753.

AL-MUSAWI, H. A., (2020) Geomorphological Analysis of Zurbatiyah Area, East Iraq Using GIS. Ph.D. thesis, College of Science, University of Baghdad, Iraq. 160p.

Al-Musawi, H. A., Abdallah, H. H., Azzawi, T. M., (2020) Neotectonic Activity of Segmented Alluvial Fans along Hemrin South Anticline, East Iraq. Iraqi Journal of Science, Vol. 61, No. 9, pp 2266-2276.

Al-Obaidi, L. D., (2005) Engineering-Geological Study of Rock Slope Stability for "Shiranish, Kolosh, Gercus and Pila spi " Fns. Around Shaqlawa area N-E of Iraq. Unpublished M. Sc. thesis, College of Science, University of Baghdad, Iraq, (in Arabic). 127p.

Al-Saadi, S. N., (1981) A method for Mapping Unstable Slopes with Reference to the Coastline of S.W. Dyfed, Wales, Unpub. PhD. Thesis, University of Bristol. 252 p.

Al-Saadi, S. N., (1991) Composite-Base Toppling of rock slopes south of Degala area NE- Iraq . J Sc. Nal, vol.1a pp.35-45 .

Al-Zubaydi, J. H., (1998) Engineering Geological Study of Selected Areas In Tar Al-Najaf -Middle of Iraq. Unpublished MSc Thesis, College of Science, University of Baghdad.126 p

Anon, (1972) The preparation of maps and plans in terms of engineering geology., Quarterly Journal of Engineering Geology, Vol. 5, 293- 382 p.

Anon, (1977) The Description of Rock Masses for Engineering Purposes. Quarterly Journal of Engineering Geology, Vol. 10, 355 – 388 p.

Barwary, A., Slaiwa, N., Yacoub, S., Hamza, N. and Dommas, J., (1993) Geological map of Mandali Quadrangle, scale 1:250000. 2nd edit., GEOSURV, Baghdad, Iraq.

Bejerman, N. J., (1994) Landslide Possibility Index System. Proceedings 7th Inter. IAEG Cong., Balkema, Rotterdam, III : 1303 1306 p.

Bell, F. G., (2007) Engineering Geology, Second Edition. Elsevier Ltd. USA. 581p.

Bellen R. C., Dunnington H. V., Wetzel R., and Morton D., (1959) Lexique Stratigraphique International, Asie, Iraq, Vol. 3C, 10a, 333p.

Blyth F. G. H. and de Freitas M. H., (1984) A Geology for Engineers,V.7, Elsevier, London, 365p.

Bolt, B. A. & Horn, W. L., Macdonald, G. A. and Scott, R. F., (1975) Geological Hazard, Tsunamis, Volcanoes, Avalanches, Landslide, Floods. Springer-Verlag Berlin Heidelberg, Germany. 328p.

Broch, E., and Franklin, J. A., (1972) The Point Load Strength Test. International Journal of Rock Mechanics and Mining Science & Geomechanics, Vol. 9, 669-679p.

Bromhead, E. N., (1992) Stability of Slopes, 2nd ed. Taylor & Francis Group. p.347

Buday, T., (1980) The Regional Geology of Iraq. Vol.1: Stratigraphy and Paleogeography. Edited by Kassab, M. I. and Jassim, S. Z. Publications of GEOSURV, Baghdad, 445p.

Chau, K. T., and Wong, R. H., (1996) Uniaxial compressive strength and point load strength. International Journal of Rock Mechanics and Mineral Sciences 33:183–188

Cheng, Y. M. and Lau, C. K., (2014) Slope Stability Analysis and Stabilization, New Method and Insight, Second Edition. CRC Press, Taylor and Francis Group. 397p.

Davis, G. H., and Reynolds, S. J., (1996) Structural Geology of rock and Regions, John Wiley & Sons, Inc., New York. 287 P.

Davis, G. H., Reynolds, S. J. and Kluth, C. F., (2011) Structural Geology of rock and Regions, third edition, John Wiley & Sons, Inc. 839 P.

Davis, W.M., (1903) The Mountain Ranges of the Great Basin. Harvard University Museum of Comparative Zoology Bulletin, v, 42, p, 129-177.

De Freitas, M. H. and Watter's, R. J., (1973) Some Field Examples of Toppling Failure Geotechnique. vol. 23 pp 495-514.

EdyTonnizam, M., Khairul, A. K. and Ibrahim, K. (2005) To Rip or To Blast: An Overview of Existing Excavation Assessment. Brunei International Conference on Engineering and Technology (BICET 2005): 27-36 p.

Emami, H. Vergés, J. Nalpas, T. Gillespie, P. Sharp, I. Karpuz, R. Blanc, E. P. and Goodarzi, M. G. H., (2010) Structure of the Mountain Front Flexure along the Anaran Anticline in the Pusht-e Kuh Arc (NW Zagros, Iran): insights from sand box models. Geological Society, London, Special Publications 2010; v. 330; p. 155-178

Evans, R. S., (1981) An Analysis of Secondary Toppling Rock Failures the Stress Redistribution Method , Qua. Jour. of Ing. Geol. ,V. 14 , pp; 77‑86 .

Fossen, H., (2010) Structural Geology, Published in the United States of America by Cambridge University Press, New York, 427 p.

Fossen, H., (2016) Structural Geology, second edition, Published in the United States of America by Cambridge University Press, New York, 1626p.

Fouad, S. F.A., (2012). Western Zagros Fold- Thrust Belt, Part I, The Low Folded Zone. Iraqi Bull. Geol. Min., Special Issue, No. 5, 39-62

Fouad, S. F.A., (2015) Tectonic Map of Iraq, scale 1:10000003rd edition. Iraqi Bull. Geol. Min., Vol. 1, No. 1, p. 1-7.

Freitas, M. H., (2009) Engineering Geology: Principles and Practice. Springer – verlag Berlin Heidelberg. 418p.

Ghazi, W., (2009) Structural Geology; Structural Analysis and Geotectonics. Basra University, College of Science. (in Arabic). 153p

Giani, G., P., (1992) Rock Slope Stability Analysis. Balkema, Rotterdam, Netherland. 344p.

Goodman, R. E., and Bray. J. W., (1976) Toppling of Rock Slopes. Proceedings of the Specialty Conference on Rock Engineering for Foundations and Slopes, 2, 201-234p.

Gudmundsson, A., (2011) Rock fractures in Geological Processes. Cambridge University Press. P566.

Gzar, A. M., (2020) Geotechnical Study of Marl Deposites and Validity for Cement Industry in Northeastern of Zurbatiyah District – Wasit Governorate– Iraq. MSc Thesis, College of Science, University of Babylon. 62p.

Hameed, A. A., (2019) Study of Structural Factors Effect on Rock Slope Stability of Bammo Anticline, Northeastern Iraq. MSc Thesis, College of Science, University of Baghdad.139 p.

Hamza, N. M., (1997) Geomorphological Map of Iraq, scale 1:1000 000, 1st edit., GEOSURV, Baghdad, Iraq.

Hancock, P., L., (1985) Brittle Microtectonics: Principles and Practice. Journal of Structural Geology, vol. 7. Pp. 437-457.

Hancock, P. L., (1991) Determining Contemporary Stress Directions from Neotectonic Joint Systems. Department of Geology, University of Bristol. 12p.

Hancock, P. L., Atiya, M. S., (1979) Tectonic Significant of Mesofracture System Associated with Lebanese Segment of the Dead Sea Transform Fault. Journal of Structural Geology, Vol.1, No.2, 143-153.

Hawkins, A. B., (1986) Rock Description and Classification for Engineering purposes. Geo. Soc. Eng. Geo. Special publication .No.2. 1186 p.

Hoek, H., and Bray, J. W., (1981) Rock Slope Engineering. 3rd Edition, Institution of Mining and Metallurgy, London, 358 p.

ISRM (International Society for Rock Mechanics), (1978) Suggested Methods for the Quantitative Description of Discontinuities in Rock Masses. International Journal of Rock Mechanics and Mining Sciences & Geomechanics Abstracts, Vol. 15, 319-368 pp.

ISRM (International Society for Rock Mechanics), (1981a) Suggested Methods for the Quantitative Description of Discontinuities in Rock Masses (ed. E. T. Brown). Pergamon Press, Oxford, UK, 211 pp.

ISRM (International Society for Rock Mechanics), (1981b) Basic geological description of rock masses. Int. J. Rock Mech. Min. Sci. & Geomech. 85–110pp.

Jassim, S. Z, and Goff, J. C., (2006) Geology of Iraq, First edition, Dolin, Prague and Moravian Museum, Brno, Czech Republic, 341 p

Kliche, C. A., (1999) Rock slope stability. Society for Mining, Metallurgy, and Exploration, Inc. 244p

Lateef, A. S., (1975) Report on the regional geological mapping of Himrin range from Al-Fatha to Ain-Layla. GEOSURV, int. rep. no. 7

Lisle, R. J . and Leyshon, P. R., (2004) Stereographic Projection Techniques for Geologists and Civil Engineers.

Ma`ala, Kh. A., Fouad, S. A., Lawa, F. A., Philip, W. and Al-Hassny, N., (1987). Report on the Geological Investigation for Northern sector of the Fatha-Mosul Sulfur District. GEOSURV,int. rep. no. 1935.

Meunier, P., Hovius, N., & Haines. J. A., (2008) Topographic Site Effects and the Location of Earthquake Induced Landslides. Earth and Planetary Science Letters Journal 275, University of Cambridge, 221- 232 p.

Mahmoud, A. A., Ali, M. A., Mohammed, A. J., AL-Mukhtar, L. E., AL-Kubaysi, K. N., Hussien, M. S., Al-Obaidy, R. A., Muhammad Ali, E. M., Tawfeeq, G., Jasim, M. K., Shnaen, S. R., and Kareem, A. Y., (2018) Detailed geological mapping of Iraq, Zurbatiyah region, east Iraq, scale 1:25000. GEOSURV, int.

Ogila, W. A., Abdeltawab, S., Abdelkader, A. M. and Yousef, M., (2022) Analysis of Slope Stability Hazards along Hilly Highways: Ain Sukhna-Zafarana highway, North Galala Plateau, Eastern Desert, Egypt. Egyptian Journal of Pure and Applied Science p 15-35

Peacock, D. C., Sanderson, D. J., and Rotevatn, A., (2017) Relationships Between Fractures. Journal of Structural Geology. 21p

Pollard, D. D., and Aydin, A., (1988) Progress in Understanding Jointing Over the Past Century. Geological Society of America Bulletin, 11 (8), 1181-1204 p.

Priest, S.D., and Hudson, J.A., (1976) Discontinuity Spacing in Rock: International Journal of Rock Mechanics, Mineral Science & Geomechanics Abstract, Vol. 13. 135-148 p.

Quinn, J. H., (1997) Escarpments. Encyclopedia of Geomorphology, pp 322-323.

Ragan, D. M., (2009) Structural Geology: An Introduction to Geometrical Techniques, Fourth edition, Published in the United States of America by Cambridge University Press, New York, 602 P.

Ramsay, J. G., (1967) Folding and Fracturing of Rocks. McGraw-Hill Book Company. 553p

Ramsay, J. G., and Huber, M. I., (1987) The Techniques of Modern Structural Geology. V.2, Folds and Fractures. Academic Press, London. p 700. rep. no. 3650.

Ritchie, A. M., (1963) The Evaluation of Rock Fall and its control. Highway Record, vol. 17 . p 13‑28 .

Rowland, S., M., Duebendorfer, E., M., and Schiefelbin I., M., (2007) Structural Analysis an Synthesis. A Laboratory Course in Structural Geology. Third edition. Black Wall Publishing. P 166.

Samarawickrama, M. N., Amarasinghe, U. V. and Bandara, K. N., (2021) Criteria to Assess Rock Quarry Slope Stability and Design in Landslide Vulnerable Areas of Sri Lanka: A Case Study at Thalathu Oya Rock Quarry. Engineer - Journal of the Institution of Engineers, Sri Lanka. p 49-58

Schultz, R., A., (2009) Introduction to Geologic Structural Discontinuities. Chapter in Geologic Fracture Mechanics. Cambridge University Press. Pp1-26.

Shakir, M. M. and Brano, J. M., (2020) Rock Joints Analysis to Determine the Main Stress Field in Bustana Structure Northeast of Iraq. Iraqi Geological Journal. Pp 56-67.

Singh, S., (2007) Geomorphology, Prayag Pustak Bahawan, Allahabad, India.

Sissakian, V. K., (1994) The Geology of Kirkuk Quadrangle. GEOSURV, int. rep. no. 2229.

Sissakian, V. K., and Al-Jibouri, B. S., (2012) Stratigraphy of the Low Folded Zone. Iraqi Bull. Geol. Min., Special Issue, No. 5, p. 63-131.

Sissakian, V. K., and Ibrahim, F., (2005) Geological Hazards of Mandali Quadrangle scale 1:250 000, sheet no. NI-38-11, GEOSURV, int. rep. no. 2918.

Sissakian, V. K., Jassim, H. M., Vanarelli, M. J. and Omer, H. O., (2021) Slope Stability Analysis of Haibat Sultan Road Cut, Kurdistan Region, Iraq Using a Field Method. Iraqi Geological Journal. P 98 – 109

Sissakian, V. K., Mustafa, H. I., Haris, G. H., Sadiq, S. A., Al-Ansari, N., and Knutsson, S., (2017) Landslides in Hareer Anticline, Central Northern Part of Iraq. Journal of Earth Sciences and Geotechnical Engineering, vol.7, no. 2, pp 25-43.

Sissakian, V. K., Omer, H. O., and Mustafa, Z. T., (2004) Slope Stability Assessment of Korre Village Landslide, SW of Shaqlawa Town, the Kurdistan Region.

Small, R. J. and Clarck, M. J., (1982) Slopes and Weathering. Cambridge University, Great British. 112 P.

Stein, RS., King, G.C.P., and Rundle, J. B., (1988) The growth of geological structure by repeated earthquakes. Field examples of continental dip-slip faults. Journal of Geophysical Research, Vol. 93, p. 13319-13331.

Tiwari, B. & Ajmera, B., (2017) Landslides Triggered by Earthquakes From 1920 to 2015. International Publishing, California State University. 5p.

Turner, F. J., Weiss, L. E., (1963) Structural analysis of metamorphic tectonites. McGraw-Hill Book, New York, cop., p 545.

Van der Pluijm, B. A., and Marshak, S., (2004) Earth Structure: An Introduction to Structural Geology and Tectonics, Second edition, WCB/ McGraw-Hill, USA, 656 p.

Ward, S., (1997) Hogback and Queasta. Encyclopedia of Geomorphology, pp 527.

Ward, S., and Roberts, N., (1997) Questa, Encyclopedia of Geomorphology pp 336–338.

Watts, C. F., Gilliam, D. R., Hrovatic, M. D., and Hong, H., (2003) Rock Slope Stability Computerized Analysis Package, Radford University, 32P.

WHO (World Health Organization), (2010) Regional Office for the Eastern Mediterranean, Seismic Hazard Map of Iraq.

Wyllie, D. C., (2018) Rock Slope Engineering, Civil Applications, Fifth Edition, Based on the Third Edition by E. Hoek and J. Bray. CRC Press, Taylor and Francis Group. 491p.

Wyllie, D. C., and Mah, C. W., (2004) Rock Slope Engineering Civile and Mining 4th ed., Based on the 3rd ed., by E. Hoek and J. Bray, spon press, Taylor and Francis Group, London and New York. 431p.

Yacoub, S.Y. Othman, A.A. and Kadhum, T.H., (2011) Geomorphology. In: Geology of the Low Folded Zone. Iraqi Bulletin of Geology and Mining, Special Issue 5, p. 7-38.

Zaini, M. T., (2005) Geological and Structural study for North Zakho area using Remote Sensing Techniques. Unpublished M. Sc. thesis, College of Science, University of Baghdad, Iraq, (in Arabic). 92p.

Zainy, M. T., (2020) Tectonic Evoluation of Zagros Suture-and Imbricate Zones in Iraq. PhD. Thesis, Lolea University of Technology, 100p.

Zhang, L., (2005) Engineering Properties of Rocks. Elsevier Geo-Engineering Book Series. 252p.

Zhang, L., (2016) Engineering Properties of Rocks. Butterworth-Heinemann. Second edition. University of Arizona Tucson, Arizona, United States. 366p.

المستخلص

تتضمن هذه الدراسة اجراء التحليل التركيبي الهندسي للانقطاعات المتواجدة ضمن الكتل الصخرية لبيان مدى تاثيرها على استقرارية المنحدرات الصخرية ضمن تكاوين الفتحة (المايوسن الأوسط)، انجانة (المايوسين المتاخر) والمقدادية (المايوسين المتاخر- البليستوسن) والمتكشفة في منطقة زرباطية التي تعد واحدة من اكثر المناطق المهمة في العراق. تقع منطقة الدراسة ضمن الإحداثيات التالية (″03 ′28 °33 و ″25 ′23 °33 شمالاً) و(″07 ′56 °45 و ″00 ′ 00°46 شرقاً) وتضم هذه المنطقة طيتي حمرين وكولك المحدبتين وطية الفارع المقعرة.

تم اجراء التحليل لسبعة عشرمحطة من المنحدرات الصخرية لتقييم إستقراريتها، تم اختيار محطتين ضمن طية كولك 1 المحدبة / تكوين الفتحة، محطة واحدة ضمن طية الفارع المقعرة / تكوين الفتحة، بينما كانت جميع المحطت الأخرى ضمن طية حمرين المحدبة وتوزعت ضمن جميع التكاوين المتكشفة في منطقة الدراسة.

اشتمل العمل الحقلي على تحصيل البيانات الحقلية، إيجاد زاوية الاحتكاك الداخلي لاسطح الانقطاعات المدروسة باجراء فحص الميل، ونمذجة الصخور واجراء فحص حمل النقطة لايجاد المقاومة الانضغاطية الغير مباشرة للصخور المدروسة. تم تمثيل وتحليل البيانات باستخدام تقنية الاسقاط الفراغي المجسم باستخدام برنامج (Stereonet V.11)، تم تعديل ورسم الخرائط المستخدمة في الدراسة باستخدام برنامج (Arc map GIS) ، بينماتم التعامل مع الصور والاشكال باستخدام برامج Adobe Illustrator، Corel Draw و Photo filter.

تم تحليل وتصنيف الفواصل المتواجدة ضمن الطبقات الصخرية بالنسبة للعلاقة بين أسطح هذه الفواصل والمحاور التكتونية الأساسية للتراكيب الجيولوجية التي تحتويها. تم استنباط الاتجاه العام للإجهاد الرئيسي الأعظم ($\sigma 1$) إعتماداً على تقاطع أنظمة الفواصل المقترنة وبالتالي قد وجد إتجاهين للحكات التكتونية القديمة: الإتجاه الأول (شمال غرب - جنوب شرق) وقد وجد هذا الأتجاه ضمن الأجزاء الجنوبية والشرقية من منطقة الدراسة، أما الإتجاه الثاني فهو (شمال شرق - جنوب غرب) وقد وجد في الأجزاء الغربية من منطقة الدراسة.

أظهرت المشاهدات الحقلية وتحليل البيانات ان جميع المحطات المدروسة غير مسقرة مع وجود عدة أنواع من الإنهيارات الصخرية (الحاصلة والمحتملة الحدوث) وهي السقوط الصخري، الإنقلاب و الإنزلاق. تم تحديد درجة المخاطر لكل محطة إعتماداً على مؤشرإحتمالية الإنهيارات الأرضية (LPI) والذي يعتمد على عشرة معايير. تم تصنيف المخاطر في منطقة الدراسة على ثلاثة أصناف (خطورة متوسطة، خطورة عالية، وخطورة عالية جداً). وقد تم إنشاء خارطة للمخاطر الجيولوجية لمنطقة الدراسة إعتماداً على هذه النتائج.

وزارة التعليم العالي والبحث العلمي
جامعة بابل
كلية العلوم
قسم علم الأرض التطبيقي

التحليل التركيبي و استقرارية المنحدرات الصخرية وتعيين المخاطر الجيولوجية لمناطق مختارة من زرباطية - شرق العراق

رسالة ماجستير مقدمة
الى مجلس كلية العلوم / جامعة بابل
كجزء من متطلبات نيل درجة الماجستير
في علم الأرض

من قبل

مصطفى باقر عبد الوهاب فتاح
بكالوريوس في علوم الأرض / كلية العلوم / جامعة بغداد
(2010)

باشراف

أ.د.
جعفر حسين علي الزبيدي

ر. جيولوجيين اقدم د.
ماهر تحسين حاتم زيني

1445هـ

2023 م